DEVELOPMENT OF TESTING SYSTEM FOR ANALYSIS OF TRANSVERSE CONTRACTION JOINTS IN PORTLAND CEMENT CONCRETE PAVEMENT

By

QIANG LI

A DISSERTATION PRESENTED TO THE GRADUATE SCHOOL
OF THE UNIVERSITY OF FLORIDA IN PARTIAL FULFILLMENT
OF THE REQUIREMENTS FOR THE DEGREE OF
DOCTOR OF PHILOSOPHY

UNIVERSITY OF FLORIDA

2011

To my parents, Wenjie Li and Fenghua Qi

ACKNOWLEDGMENTS

First of all, I would like to express appreciation to Dr David Bloomquist and Dr Reynaldo Roque. This dissertation would not have been possible without their insights, encouragement, guidance and support.

I would also like to thank other committee members, Dr. Mang Tia and Dr. John Mecholsky, for their support in accomplishing my work. They are all great mentors and advisors.

Thanks to George A. Lopp and Chuck Broward for their great help on my experiment. Thanks to Dr. Crowley for his great help. Thanks to all the students in materials group for their friendship.

Special thanks to my parents Fenghua Qi and Wenjie Li and other family members who gave me strength and confidence to conquer challenges that I faced along the way.

Finally, I would like to express my deepest love to my girlfriend, Xun Jia, for her selfless support and constant encouragement.

TABLE OF CONTENTS

page

LIST OF TABLES

LIST OF FIGURES

LIST OF ABBREVIATIONS

AASHTO	American Association of State Highway and Transportation Officials
ADHESTA	Adhesive Strength Testing Apparatus
ADOT	Arizona Department of Transportation
AIMS	Aggregate Imaging System
CDOT	Colorado Department of Transportation
CRCP	Continuous Reinforced Concrete Pavement
CRETA	Creep Testing Apparatus
FDOT	Florida Department of Transportation
FHWA	Federal Highway Administration
GDOT	Georgia Department of Transportation
IDOT	Illinois Department of Transportation
JOPEM	Joint Performance Evaluation Model
JPCP	Jointed Plain Concrete Pavement
JPQCD	Joint Preparation Quality Control Device
JRCP	Jointed Reinforce Concrete Pavement
KDOT	Kansas Department of Transportation
LTRC	Louisiana Transportation Research Center
LVDT	Linear Variable Differential Transformer
MEPDG	Mechanistic-Empirical Pavement Design Guide
NDOT	Nevada Department of Transportation
NS	Non-Self-Leveling
ODOT	Ohio Department of Transportation
PCP	Pre-Stressed Concrete Pavement
SL	Self-Leveling

SPS	Specific Pavement Study
UDOT	Utah Department of Transportation
WDOT	Wisconsin Department of Transportation

Abstract of Dissertation Presented to the Graduate School
of the University of Florida in Partial Fulfillment of the
Requirements for the Degree of Doctor of Philosophy

DEVELOPMENT OF TESTING SYSTEM FOR ANALYSIS OF TRANSVERSE CONTRACTION JOINTS IN PORTLAND CEMENT CONCRETE PAVEMENT

By

Qiang Li

August 2011

Chair: David Bloomquist
Cochair: Reynaldo Roque
Major: Civil Engineering

The joints of Portland cement concrete pavement are cracks intentionally built in pavement to accommodate expansion and contraction due to shrinkage of concrete and temperature changes. Joints minimize and control random cracks due to temperature and moisture changes. Sealant is the material for sealing the joint. In recent years, the Florida Department of Transportation (FDOT) has been asked to approve narrower 1/8 in. concrete joints as opposed to traditional joints specified at 3/8 in. Thus, a series of new testing procedures were developed and executed to evaluate the differences between 1/8 in. and 3/8 in. joints. A new creep test (CRETA) was developed and conducted on joint sealant to determine its viscoelastic properties. Results indicated that the sealant is a linear viscoelastic material and that its creep response does not appear to be significantly affected by temperature fluctuations. Further creep tests were conducted under artificial aging conditions. Hot water aging appears to cause both self-leveling and non-self-leveling sealant to become softer and more ductile. Freeze thaw aging had no significant effect on properties. Oven aging had no significant effect on the self-leveling sealant, but it did cause non-self-leveling sealant to become more

brittle. A new adhesive test (ADHESTA) was developed and conducted on joint sealant to determine its adhesive strength. Results indicated that the non-self-leveling sealant is stronger, but less ductile than the self-leveling sealant. A series of debris tests were conducted; they indicated that a “critical roughness” may be found for concrete joints. A series of adhesive strength aging tests was conducted; the results were similar to the creep test aging results. Moisture tests were conducted to evaluate the differences between 1/8 in. and 3/8 in. joints. Results indicated that the 1/8 in. joint dries significantly more slowly than the 3/8 in. joint, and that moisture significantly affects sealant adhesive strength. A new device (JPQCD) for evaluating joints in the field was developed to evaluate concrete joint adhesive strength. Results indicate that the 1/8 in. joint typically performs poorly when compared with the 3/8 in. joint. Further, data suggests that the 3/8 in. joint will perform closer to a joint’s average strength when compared with a 1/8 in. joint. CRETA, ADHESTA, JPQCD, and a theoretical model were used to develop a finite element model for evaluating long-term performance of 3/8 in. joints compared with long-term performance of 1/8 in. joints. Results suggest that for both self-leveling and non-self-leveling field-poured sealant, the 1/8 in. joint is significantly less effective than the 3/8 in. joint. Based on all results, the 1/8 in. joint is not recommended.

CHAPTER 1
INTRODUCTION

Problem

Joints are installed in concrete pavement so that cracks due to temperature or moisture changes can be minimized and controlled. Four types of joints are fairly common along roadways: transverse contraction joints, longitudinal joints, construction joints, and expansion joints. The Florida Department of Transportation (FDOT) currently requires transverse joints in concrete pavement to be 3/8 inches wide. According to FDOT, this width allows for adequate expansion and contraction of the joints. (FDOT 2007). Recently, however, FDOT has been asked to approve a narrower (1/8 inch) joint width.

There are two advantages to narrower joint. First, narrower joints require less sealant. Secondly, narrower joints should require less installation time, which in turn should translate to lower construction cost and shorter construction time. Despite these advantages, narrower expansion joints have several drawbacks which may affect their long term performance. First, the movement of the concrete slab in which the joint is cut is determined by the length of slab, not the width of the joint. For a given slab then, there is a fear that, the 1/8 inch joint may not provide adequate distance for expansion. Secondly, because a 1/8 inch joint is narrower than the more traditional joint, less sealant can be injected into it. Because there is less sealant, stress within the sealant, which is induced by slab expansion and contraction, may be greater than similar stresses associated with a 3/8 inch joint.

The topic of sealant stress and associated failure requires some elaboration. Two types of sealant failures are possible in concrete expansion joints: (1) cohesive failure

and (2) adhesive failure. With cohesive failure, local portions of sealant are broken within the sealant matrix itself. On the other hand, with adhesive failure, the interface between the concrete surface and sealant fails such that the sealant does not adhere properly to the concrete. Field observations appear to show that most sealant failures are adhesive, not cohesive. Therefore, the adhesive strength of the sealant is the critical factor.

Adhesive strength is determined by concrete surface conditions, particularly roughness and cleanliness. A rougher surface implies a larger surface area on which the sealant can adhere, as compared to a smoother surface. Empirical evidence suggests that because of this increase in surface area, sealant adhesion may increase significantly. An additional factor is dust, dirt, or debris in the expansion joint, which may prevent the sealant from adhering to the entire available surface area – thereby reducing adhesive strength. Generally, water blasting, sandblasting, wire brushing or other methods are used to remove the debris and to roughen the surface during joint installation. All of these surface preparation methods require a minimum joint width to function properly. Employing any of these methods to roughen the surface of a 1/8-inch joint is significantly more difficult than for a wider joint. In practice, this implies that when 1/8 inch joints are used, surface quality suffers. Low quality surface preparation may result in lower adhesive strength and poor field performance – which, in turn, may lead to adhesive joint failure.

Objectives

The purpose of this study is to develop a testing system for transverse joints in concrete pavement. The proposed system can be used to predict the field performance

of joints and to evaluate the constructability and service life of the narrower joint design.

The detailed objectives are as follows:

- Develop a laboratory testing method which accurately measures the adhesive strength between concrete surfaces and sealant.
- Develop a laboratory creep test to investigate the viscoelastic properties of the sealant.
- Develop a laboratory method to quantify the roughness of the concrete joint surface after sandblasting or wire brushing and evaluate the effect of roughness on adhesive strength.
- Design a laboratory approach to identify the quantity of debris on the concrete cutting joint surface after cleaning and evaluate the effect of cleanliness on adhesive strength.
- Build a relationship between field results and laboratory results by comparing data from the first Objective through fourth Objective with field data.
- Identify the effect of aging on sealant and adhesive strength.
- Develop an approach to predict temperature and shrinkage-induced concrete pavement slab movement.
- Develop a model to evaluate the long-term field performance of sealant at different joint widths.
- Develop equipment suited for narrow joint surface preparation.
- Develop a joint preparation quality control device to evaluate the surface preparation in field.
- Determine if narrower joint width allows for adequate slab movement.
- Using all the results above, determine the overall effects of narrow joints on constructability and service life.

Scope

Because of the scope of the problem, this study will look at a representative joint, a representative concrete type, and representative sealant type for testing. The goal is

to develop testing methods and apparatus that are robust enough to be used with other systems not tested here.

Joint Types

The four most common expansion joints used today are:

- Transverse contraction joints
- Longitudinal joints
- Construction joints
- Expansion joints

This study will focus on the first joint mentioned here – transverse joints. A testing system will be developed for analysis of this system. In principle, joint slab movement and joint performance for the four types of joints listed here are related to similar variables:

- Traffic load
- Temperature change
- Concrete shrinkage

The significant difference between these different joint types is their location, orientation, and purpose. In practice, similar sealant materials and installation methods are used for all of these joints. Therefore, investigators believe that results from a transverse system should be indicative of results from other systems.

Concrete Types

Limestone is the most commonly used aggregate in Florida; therefore, limestone concrete will be used during all tests. However, the testing method presented in this study should be applicable to any type of concrete.

Sealant Types

Several types of sealant are used in expansion joints. Sealants may be characterized by a combination of the following parameters:

- Leveling system – Self-leveling vs. non-self-leveling
- Base material – Silicone vs. asphalt
- Temperature – hot-poured vs. cold-poured

This study will focus on self-leveling, cold-poured silicone sealant and non-self-leveling, cold-poured silicone sealant. As previously indicated, this testing system should also be applicable to other types of sealant.

Testing Method

To meet the objectives, a number of tasks were completed:

- An algorithm for transverse joint analysis was developed to evaluate joint movement, sealant viscoelastic properties, and sealant tensile properties, both in the field and in the laboratory (Figure 1-1).
- Joint analysis was conducted analytically to determine strain load information on the sealant.
- A new creep test device was developed to obtain viscoelastic properties of the sealant.
- A creep test was conducted on new sealant at four different temperatures. The test was repeated with aged sealant to investigate aging effects.
- A new adhesive strength test was developed.
- Using the new adhesive strength testing device, the effects of aging, surface roughness, surface cleanliness, and moisture content were investigated.
- A joint sealant performance model was developed using all the results above.

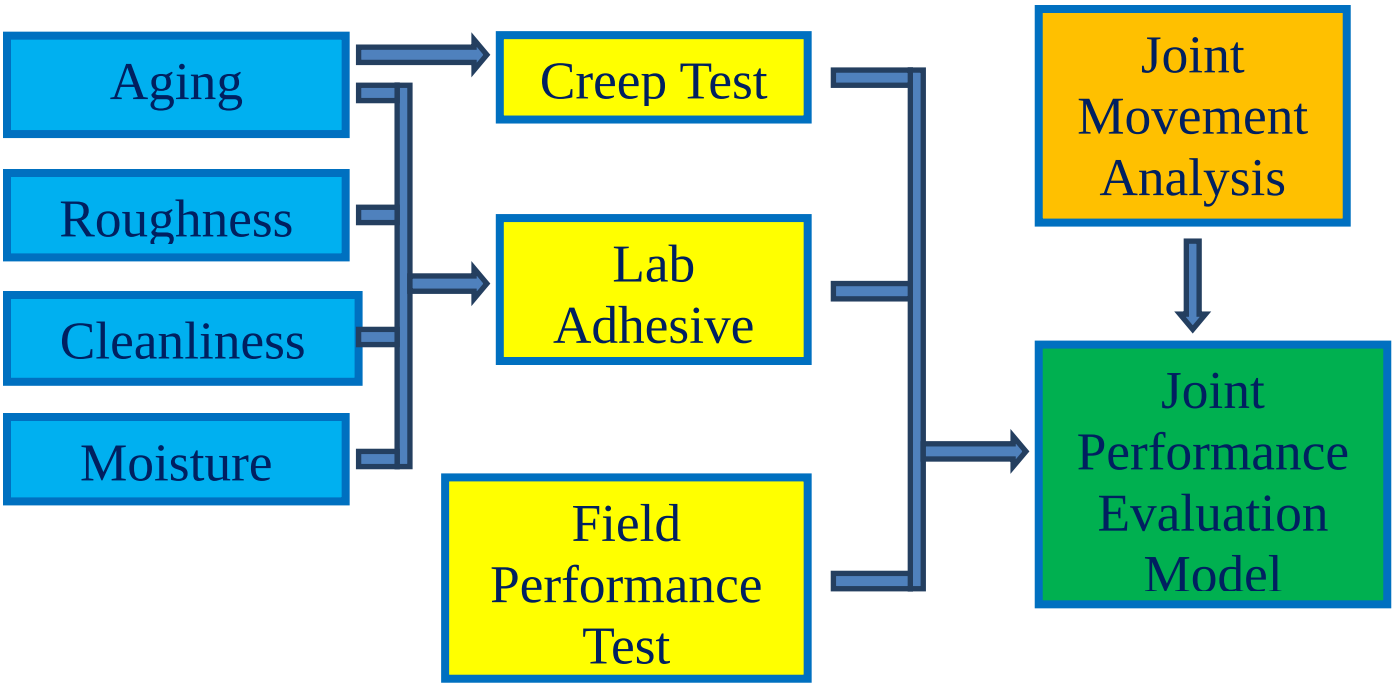

Figure 1-1. Flow chart of concrete pavement sealant testing system.

CHAPTER 2
BACKGROUND

Concrete Pavement Joints

Relevant background regarding the different types of concrete joints is discussed in this section. As mentioned briefly in Chapter 1, four types of joints are fairly common in roadways – transverse joints, longitudinal joints, construction joints, and expansion joints (Odum-Ewuakye, et al 2006).

Transverse Contraction Joints

Consider a rigid concrete slab with infinite length in the longitudinal direction. Over its service-life, the volume of the slab's concrete changes because of shrinkage during curing and seasonal temperature change. These volume changes can result in random cracking of the concrete which can reduce the service life of the pavement. Transverse contraction joints (Figure 2-1) are artificial cracks that are cut into the slab to accommodate expansion and contraction resulting from this volume change. Typical contraction joint spacing is approximately 3/8 inches. Because of the close spacing between joints relative to the overall longitudinal length of the slab, there will be thousands of joints within a given pavement. Therefore, joint performance significantly affects pavement performance.

A compromised transverse joint typically exhibits faulting or spalling. Faulting is the process by which a difference in elevation develops across a joint or crack. Spalling is cracking, breaking, chipping, or fraying of slab edges near the front-face of the transverse joint. Faulting and spalling result in a rough ride. In addition to faulting or spalling, poor joint performance may also lead to corner breaks, blowups, and mid-panel cracks. A corner break occurs when a crack develops across the slab's corner –

from the transverse face to the outer edge for example, while a blowup is a localized upward movement of the pavement surface at the transverse joint, or near cracks. Shattering of nearby concrete is common when a blowup occurs. Mid-panel cracks are transverse cracks in the middle of the concrete slab.

Longitudinal Joints

Longitudinal joints (also Figure 2-1) are usually used to relieve warping stresses when the slab width exceeds 4.57 m (15 ft.). The warping stresses are caused by temperature gradients between the top and bottom of a concrete slab. For example, when the sun shines on an elevated roadway, the road's surface may be much warmer than its underside.

Construction Joint

Although this type of joint is not a true movement joint, construction joints are commonly installed during construction. Construction joints can be horizontal or vertical and are formed when placement of the concrete is interrupted. For example, a construction joint may be included because the work-day ended; or perhaps because another task needed to be completed before concrete placement was finished. Regardless of the reason that a construction joint was created, the result is the same; a surface is formed as the already poured concrete cures, and then fresh, plastic concrete is poured against this surface later. The three types of commonly used construction joints are: simple vertical construction joints, joggle joints, and dowel bar construction joints (Figure 2-2).

Expansion Joint

Expansion joints are used to allow expansion and contraction of a concrete slab without generating potentially damaging forces within the slab itself or the surrounding

structure. If adjacent slabs are tied together by means of dowel bars, these dowels are sleeved in a “concrete bay” to allow expansion to take place without generating stresses within the slab (Figure 2-3).

Joint Sealant

When joints are added to a concrete slab, the joint must be injected with sealant. The sealant serves two major purposes. First, it reduces the amount water that infiltrates into the pavement. This is important because water infiltration may corrode a pavement’s concrete rebar. If sealant is not used, water may also penetrate into the sub-grade below the slab. The fines in the sub-grade aggregate matrix may be removed by the percolating water. This may in turn lead to a loss of support at the joint.

The second reason that sealant is important is that it prevents debris from entering the joint. When this happens, it may obstruct a slab’s ability to expand or contract as designed. If slabs cannot expand or contract freely, adjacent slabs may rub against one another, thus leading to spalling.

Sealant Classification

A number of different sealant materials are used with concrete joints:

- Polysulfide
- Silicone
- Polyurethane
- Rubberized asphalt
- Preformed compression sealant

Within this material-specific breakdown, sealant classification can be broken down further with respect to its installation method:

- Field poured sealants. As implied by its name, field poured sealants are applied to the joint in the field. When used on roads, this type of sealant requires time to cure before a roadway opens to the traffic.

- Pre-formed sealants. These sealants consist of pre-molded strips of styrene, urethane, poly-chloroprene, neoprene, or other synthetic rubbers. The material is pre-compressed and inserted into the joint with a special tool (Figure 2-4).

As discussed briefly in Chapter 1, sealants may be further classified as self-leveling (SL) or non-self-leveling (NS). Self-leveling sealants are viscous liquids with low viscosity before curing. After curing, these sealants are relatively flexible (low modulus of elasticity). Non-self-leveling sealants, on the other hand, have a very high viscosity before curing and are relatively stiff (high modulus of elasticity) after curing.

Finally, field poured sealants can also be classified as either hot-poured or cold-poured. Typically, hot-poured sealants consist of asphalt mastics filled with latex, butyl, or reclaimed rubbers. When overheated, these sealants tend to lose elasticity. Typical cold-poured sealants include polyurethanes, polysulfide, silicone, and modified epoxies. Generally, cold-poured sealants are more expensive. However, these sealants are generally less rigid and are less temperature-sensitive than their hot-poured counterparts. Therefore, a loss of viscoelastic properties is a non-issue with these materials. Typically, cold-poured sealants exhibit, relatively high adhesive and cohesive strengths.

In Florida, field-installed, cold-poured sealants are the most common for both self-leveling and non-self-leveling varieties. While the specific material used in practice varies somewhat, this project will focus on one material – silicone – and use data obtained from silicone sealants as an approximate representation of sealant properties on Florida roadways.

Factors Affecting Sealant Performance

Sealant performance is affected by a number of factors:

- Joint movement. Sealant width must be greater than or equal to joint width so that adequate adhesion can be maintained during concrete expansion or contraction.

- Bonding effectiveness. A solid bond between sealant and concrete limits water filtration into a joint. Conversely, poor bonding will allow more water to enter the joint.

- Durability. Sealants, especially on roadways, are often exposed to harsh environments. Under such conditions, the sealant must be resistant to sunlight, ozone, rain, snow, extreme temperature, and age-hardening.

Existing Method for Installing Concrete Joints

There are four steps for installing joints in concrete pavement:

- Sawing the joint
- Surface preparation
- Installing backer rod
- Sealant application

Joint Sawing

The first step in concrete joint installation is to saw the joint. The installer must take a number of precautions during this step. First, he or she must ensure that the sawing equipment does not damage pavement near the joint. Secondly, timing is an issue. The installer must be sure to saw the joints as soon as the pavement has hardened enough to prevent tearing and raveling from the saw blade. However, if the installer waits too long, he or she risks uncontrolled shrinkage and cracking within the concrete slab (FDOT 2007b)(FDOT 2007a)(FDOT 2007)(FDOT 2007).

The current standard for joint implementation advises joint installers to cut the joint in two steps. First, an initial 1/8 inch wide by 1/3 inch deep section is cut no more than twelve hours after the concrete is placed. Next, a second saw cut, conforming to specified joint dimensions as determined by the design drawings, is executed (Figure 2-5). Once the joint has been installed, uncontrolled cracks in the concrete must be

repaired. In the case of roadways, this means that pavement must be placed across the full width of all affected lanes (and shoulders). This repair pavement must extend longitudinally to the nearest transverse joint in either direction along the roadway.

Surface Preparation

Once the joints are cut, the surface along the joint-face is prepared to receive sealant. During surface preparation, the goal is to remove any debris including dust, grime, dirt, curing compounds, form oil, etc. by water blasting (Figure 2-6), light sandblasting (Figure 2-7), wire brushing, or other methods acceptable to the Engineer.

Backer Rod

A backer rod (Figure 2-8) is a round open-cell or closed-cell foam rod used to fill joints between adjacent concrete pavement slabs (Figure 2-9). The dimensions of backer-rods are such that they usually fill most of a joint's void-space. The backer rod must be compatible with joint sealant that is being used such that bonding or reactions between the rod and the sealant material do not occur.

Sealant Application

Sealant should be applied immediately after backer-rod installation so that debris does not have a chance to enter the pavement joint. Sealant should be recessed a minimum of 1/8 inch to 1/4 inch (3.18 mm to 6.35 mm) below pavement surface. Figure 2-10 illustrates proper sealant-placement procedures.

Sealant Failure Mechanisms

There are two major joint sealant failure mechanisms in concrete joints: cohesive failure and adhesive failure.

Cohesive Failure

Cohesive failure is defined as the failure of the sealant material itself when stresses within the sealant exceed the sealant's tolerance. Sealant stress is caused by two factors. Joint movement causes horizontal stress while traffic load produces shear stress. In both conditions, the strain rate (and subsequently loading rate) is relatively low. For this reason, properly installed sealant tends not to suffer from cohesive failure very frequently. Over time however, the combination of horizontal and vertical stresses coupled with the aging of the sealant may cause internal micro-cracking. Once micro-cracking has begun, the problem often grows in scale. Smaller micro-cracks lead to larger and larger micro-cracks and so on until eventually macro-cracks develop. Eventually, such a macro-crack may form along the entire sealant depth, allowing water and debris to infiltrate the joint. Once water or debris has entered the joint, the joint is said to have failed.

Adhesive Failure

Adhesive failure is defined as a failure at the sealant-concrete interface. Adhesive strength is affected by the adhesive properties of both the sealant and the joint surface. A rougher concrete surface will increase the contact area between concrete and sealant – thus increasing overall adhesive strength. If there is debris in the joint, sealant will adhere to the debris instead of the concrete slab, thereby decreasing the amount of contact area between slab and sealant. Generally, a "cleaner, rougher" joint surface implies better adhesive strength.

Like a cohesive failure condition, adhesive failure should take some time to develop in properly installed joints. Aging of the sealant material generally weakens the bond between concrete and sealant such that cracks develop along the sealant-

concrete interface. As with cohesive failure, this may eventually lead to water and debris infiltration.

When the sealant is too thin, a special type of failure may occur (Figure 2-11) (T.D. Biel 1997). If temperature is very high, and a concrete slab expands significantly, a thin sealant may “buckle” up or down instead of compressing. Under “buckle-up” conditions on a roadway, traffic may run over the sealant. Gradually, tires will peel small strips of sealant from the joint. Eventually, most of the sealant is removed from the joint, and the joint is said to have failed.

Summary

Ultimately, cohesive versus adhesive failure mode is determined by the magnitude of concrete compression and the adhesive strength between concrete and sealant. If the adhesive strength between sealant and concrete is great, aging may affect sealant cohesion first. Conversely, if adhesive strength is low, aging may instead lead to an adhesive failure. Biel, et al. suggests that cohesive failure is more common when PVC coal tar and rubberized asphalt are used. Adhesive failure on the other hand appears to be more common with silicone sealant (Biel, T.D. 1997).

Both of these failure mechanisms ultimately will lead to the same set of problems for a concrete slab. With either mechanism, water infiltration into the joint will increase. With added water comes added debris – as dust and extraneous particulates are also introduced to the joint-slab interface. Water in particular implies a common problem for roadways. Because water expands when it freezes, pooled water in concrete joints may lead to spalling, faulting, and blowups (e.g., potholes) along the joint-line. This in turn may lead to unsafe roadway conditions. Thus, it is essential to understand joint

failure mechanisms to improve road quality when transverse joints are installed in a roadway.

Standard Specifications for Joint Sealant

The American Society for Testing and Materials (ASTM) has developed a series of standards for testing joint sealants. For silicone sealants, cure evaluation, rheological properties, tack free time, bond, rubber properties in tension, effect of accelerated weathering, and resilience are tested specifically (ASTM 2006b).

Cure Evaluation

Cure evaluation tests whether or not the sealant has completely cured in a specified amount of time. According to ASTM, a 12.7 by 12.7 mm (0.5 by 0.5 in) cross section of sealant must cure within 21 days (American Society for Testing and Materials 2006b). A series of tests are used to verify curing; some of these tests will be discussed here.

Rheological Properties

Rheological testing is designed to determine a material's flow properties when the material is still a liquid. For uncured NS silicone sealant, slumping by more than 7.6 mm (0.30 in) must not be observed.(ASTM 2006a). ASTM C639 is used to test the rheological properties of SL silicone sealant (ASTM 2007). This test measures the amount of horizontal or vertical flow when sealant is applied to a set joint configuration at two pre-determined temperatures. Only samples conditioned at the same temperature may be directly compared. SL sealant must exhibit a smooth, level surface with no indication of bubbling during this test.

Tack Free Time

Tack-free time is a measure of the surface cure time. The goal of this test is to determine when the sealant can (1) resist damage by touch or light surface contact; (2) resist job-site or airborne dirt pick-up; and (3) resist impinging rainfall (ASTM 2009a).The test for tack-free time can be used at any temperature and humidity. When performing this test, it is important to simulate field conditions as accurately as possible. For example, if the sealant is to be used in a humid environment, the tack-free test should be conducted in a similarly humid environment. According to ASTM, The sealant shall be tack free, with no transfer of the sealant to the polyethylene, after five hours and ten minutes.

Bond

Due to the wide range of conditions affecting a road surface's roughness and cleanliness adhesive strength is the most important factor that impacts the performance of the joint(ASTM 2005a).

During this test of adhesive strength, a 0.5 in. x 0.5 in. x 2.0 in. sealant section is installed between two 1.0 in. x 1.0 in. x 3.0 in. mortar blocks. The sealant is tested at -29 degrees C (-20 degrees F). The sealant is stretched to 100% elongation, i.e. double its original length, five times. Three type of conditioning are applied to the specimens: non-immersed, water immersed and oven-aged. Each test is to be repeated three times. All specimens tested must not develop cracking, separation, or openings between the sealant and the mortar testing blocks. There is an apparent deficiency with this test: most sealants used in the field today do not fail in only five cycles. As such, this test merely identifies sealant material that egregiously fails to adhere to very elementary bonding standards.

Rubber Properties in Tension

Ultimate elongation tests and tensile strength tests are used to evaluate sealant tension properties (ASTM 2006c). During an ultimate elongation test, certain temperature specifications are given, and the sealant is stretched. Ultimate elongation achieved before breakage must not be less than 600% of the original length of the sealant bead. During the tensile stress test, a bead of sealant is stretched to 150% of its original length, and the force required to stretch the specimen is recorded. According to ASTM, no more than 45 psi (310 kPa) must be used to achieve 150% elongation.

Effect of Accelerated Weathering

Solar radiation contributes to the sealant cracking in concrete joints. The use of a laboratory accelerated weathering machine with actinic radiation, moisture, and heat appears to be a feasible method for predicting the likelihood of sealant cracking (ASTMs 2005b). According to ASTM, this test may actually produce more severe degradation than would be seen in the field. Therefore, this test appears to be a conservative barometer for evaluating weathering.

During this test, samples are made and cured for 72 hours. (ASTM 2005). Next, they are placed in the weathering device for 5000 hours. After testing, the sealant must not flow, show tackiness, show the presence of an oil-like film, or show reversion to a mastic-like substance. Additionally, the sample must not display surface blisters (either intact of broken) from internal voids, surface crazing, chalking, cracking, hardening, or loss of rubber-like properties. Finally, the sealant must not exhibit cracking or crazing when subjected to a C793 bend test.

Resilience

Resilience is an evaluation of the ability of a sealant to rebound when curing. During this test, a 7.0 cm diameter by 4.5 cm deep cylindrical sample is prepared by slightly overfilling a standard test tin with sealant and leveling the surface with a straight edge. The specimen is then cured for 21 days. Next, the sample is placed in a 70 degree C forced draft oven for 7 days. Finally, the sample is removed from the oven and tested according to the oven-aged resilience procedure (Method D 5329) (ASTM 2009b).

Summary

The failure of a sealant in an active joint is usually caused by cohesive failure in the sealant or adhesive failure between the sealant and the joint surface. In particular, adhesive failure is the most critical factor that affects the long term performance of the joint sealant. However, ASTM's standards do not directly measure the effects of aging on adhesive strength. Therefore development of a testing procedure for directly measuring adhesive strength under different aging scenarios appears to be appropriate.

Additionally, silicone sealant is a viscoelastic material that is capable of releasing stress as it accumulates. A viscoelastic material's modulus of elasticity is related to the rate at which it is loaded. Joint movement due to the temperature change or drying shrinkage is occurs very slowly. Under these conditions, the sealant may have time to release its stress. Conversely, shear stress caused by the traffic load occurs both quickly and frequently. Silicone sealant does not have time to reduce these stresses, and yet, it must accommodate high-frequency traffic loads along a roadway. This implies that traffic load may play a more important role than "slow" joint movement with respect to joint failure of silicone sealants. However, there is no standard test method to

identify the viscoelastic properties of silicone sealant. Therefore, it also seems necessary to develop a test method that can identify viscoelastic sealant properties with respect to shear stress performance.

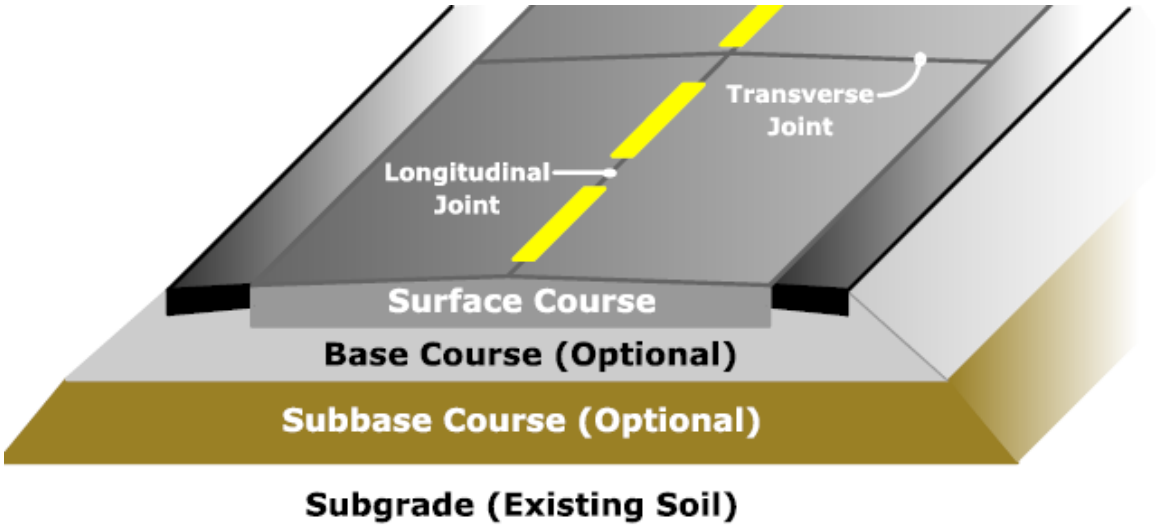

Figure 2-1. Transverse and longitudinal joints in concrete pavement (Photo courtesy of Steve Muench)

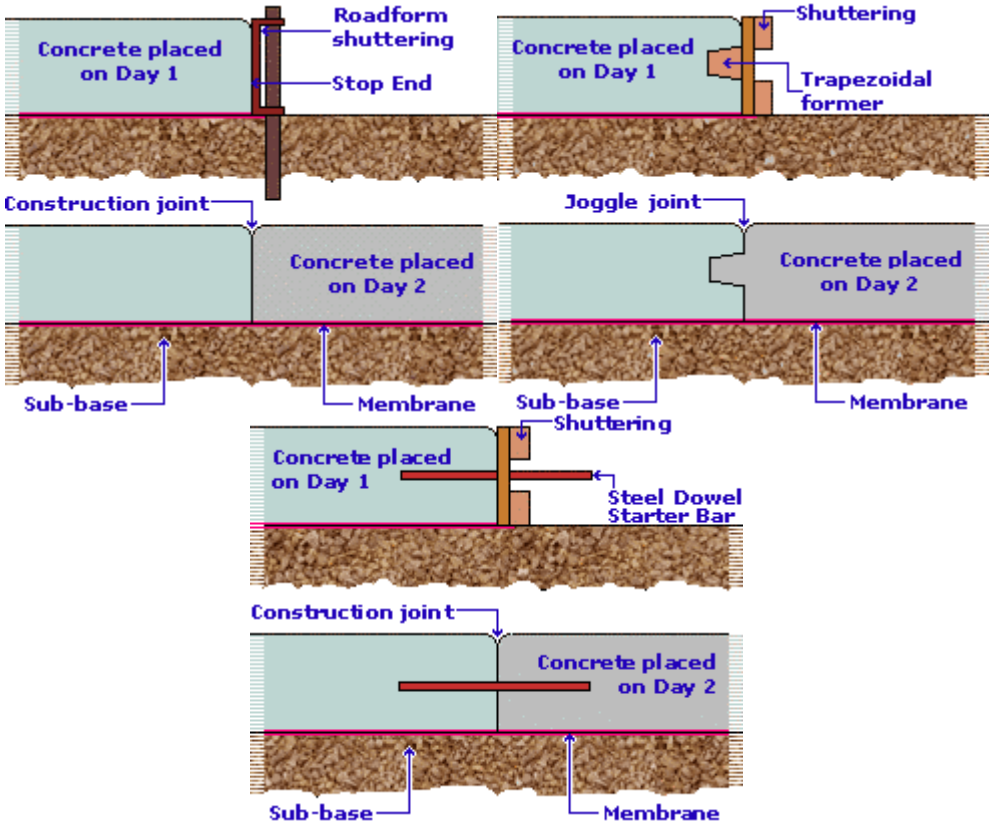

Figure 2-2. Construction joints (Source: www.zeallsoft.com, Last accessed December, 2010)

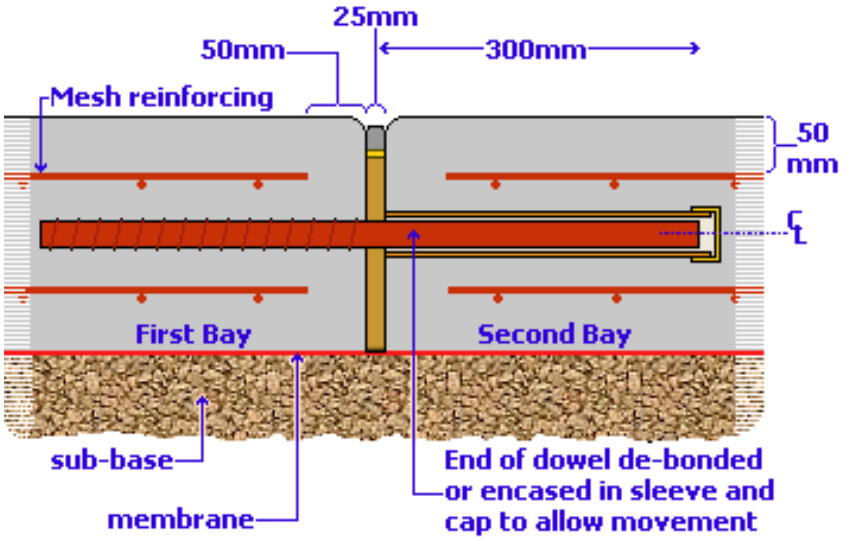

Figure 2-3. Doweled expansion joint (Source: www.zeallsoft.com, Last accessed December, 2010)

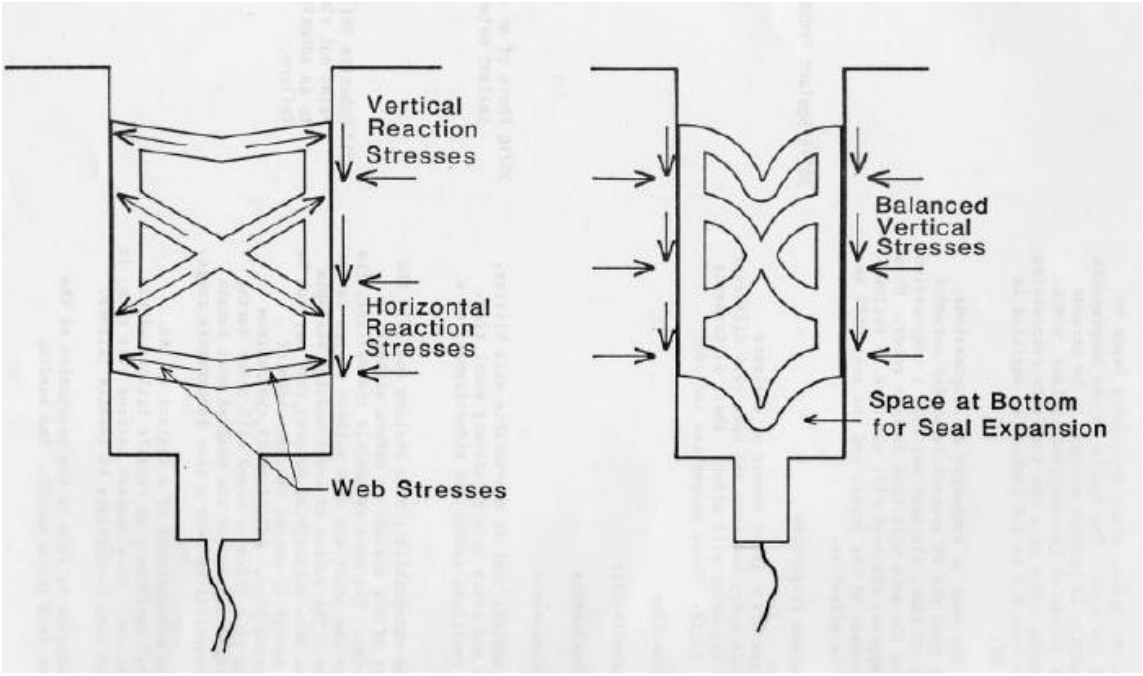

Figure 2-4. Mechanics of preformed sealants

Figure 2-5. Sawing a transverse contraction joint (Photo courtesy of Mang Tia)

Figure 2-6. Sandblasting in field (Photo courtesy of Robert Ferguson)

Figure 2-7. Water blasting in field (Photo courtesy of Robert Ferguson)

Figure 2-8. Backer rods (Photo courtesy of http://www.bestmaterials.com. Last accessed December, 2009)

Figure 2-9. Installation of backer rod (Photo courtesy of Mang Tia)

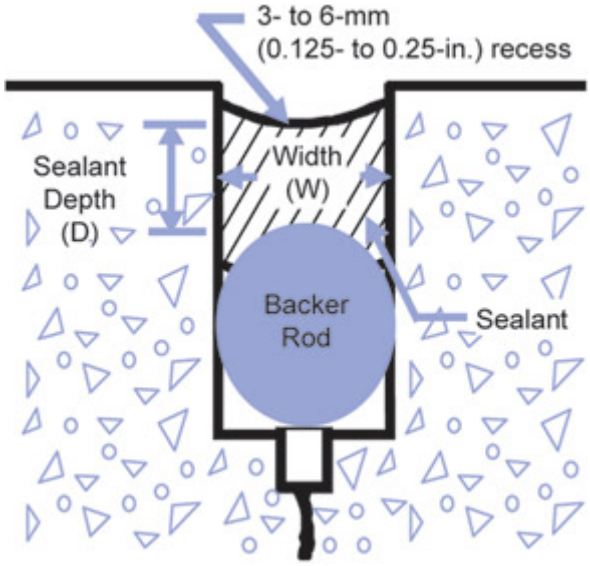

Figure 2-10. Field-poured joint sealant using a backer rod (Source: http://www.fhwa.dot.gov/pavement/pccp/pubs/06005/. Last accessed December, 2010)

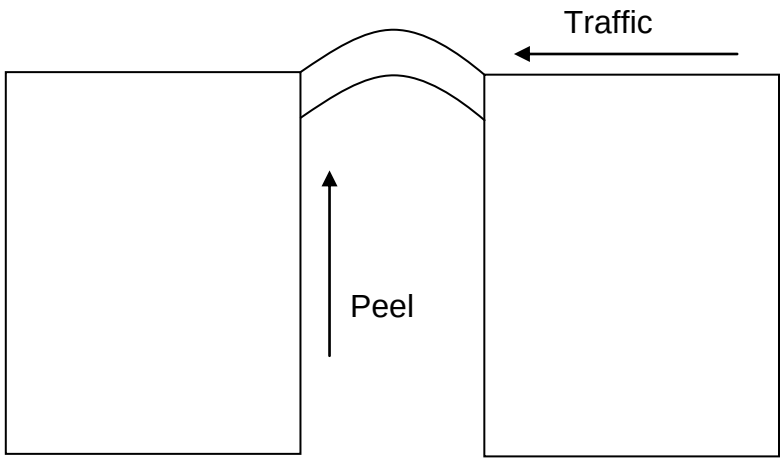

Figure 2-11. Buckling of thin sealant

CHAPTER 3
LITERATURE REVIEW

Federal and State Transportation Departments have studied modifications to transverse contraction joints. This section describes the testing and results of studies from:

- The Kansas Department of Transportation (KDOT)
- The Illinois Department of Transportation (IDOT)
- The Ohio Department of Transportation (ODOT)
- The Georgia Department of Transportation (GDOT)
- The Louisiana Transportation Research Center (LTRC)
- The Wisconsin Department of Transportation (WDOT)
- The North Dakota Department of Transportation (NDDOT)
- The Arizona Department of Transportation (ADOT)
- The Colorado Department of Transportation (CDOT)
- The Nevada Department of Transportation (NDOT)
- The Utah Department of Transportation (UDOT)

The first three of these Department of Transportation (DOT) projects were administered under the Federal Highway Administration (FHWA) High Performance Concrete Pavements Project. The final four projects were conducted under the FHWA Specific Pavement Study (PSP) 4-Joint Seal Test. The balance of these studies was independently conducted. Two important variables were analyzed in most of these projects: (1) cost; and (2) resiliency of different joint construction methods.

The FHWA High Performance Concrete Pavements Project

One of the goals of the High Performance Concrete Pavements Project was to identify joint sealing alternatives and construction techniques for analysis by individual state highway departments. Under this program, Kansas (K1), Illinois (IL 2 and IL 3), and Ohio (OH 1) participated in this joint research. Reviews of their projects are described here.

Kansas Department of Transportation

Under the High Performance Concrete Pavements Project, KDOT explored thirteen test sections, each approximately 0.6 mi. long, along Highway K-96 near Haven, Kansas(FHWA 2006c).

KDOT sought to improve pavement performance and evaluate potential cost benefits by testing recycled waste materials, untested aggregates, new load transfer devices, premium materials, and concrete mixes. In this study, 0.25 in. joints were evaluated; 31 without sealant and 79 with sealant.

The joints without sealant cost $0.67 less per joint than the joints with sealant. As of the 2003 report, the joints without sealant recorded an average spalling of 59 mm (2.3 in.) and 1 corner crack, while the joints with sealant recorded an average spalling of 50 mm (2.0 in.) and 6 corner cracks. This may imply that sealant induces corner cracking more frequently.

Illinois Department of Transportation (IL 2)

IDOT began its High Performance Concrete Pavements Project along State Route 59 near Naperville, Illinois (FHWA 2006a). The IL 2 project includes areas of Route 59 under reconstruction and areas where the road was widened.

Narrow joint widths and sealants were evaluated for transverse joints. Two sections contained a total of sixteen 0.62 in. joints with preformed seals. Five sections contained a total of seventy-nine 0.12 in. joints with sealant. One section contained thirty 0.12 in. joints without sealant.

After approximately seven years, the joints were continuing to perform without visible signs of spalling or faulting. However, it was observed that the preformed joint

sealant continued to perform well, while the field poured sealant began to lose adhesion with the concrete. Investigators reported that water and debris had entered these joints.

Illinois Department of Transportation (IL 3)

The IL 3 project is located on US Route 67 near Jacksonville, Illinois(FHWA 2006b).The primary focus of this project was to test dowel bar materials. A secondary focus was to continue testing with thin, unsealed joints. Sixteen sections were evaluated. One of the sections included 10 joints without sealant. The remaining six sections contained a total of 61 joints with sealant.

The joints were periodically observed for signs of deterioration. Improper sealant application caused overfilling and ride quality issues. Tests revealed bonding failures between sealant and concrete. Because of improper sealant application and the bonding failures, two failure modes were observed: (1) joint material began to wear away; and (2) joint material and some debris were pushed further into the joint. Joint-type was compared with load-transfer efficiency (to the dowel bar). Tests appeared to indicate that the unsealed joints performed as well as sealed joints.

Independent Tests

Several other states conducted independent research to evaluate new joint sealing alternatives. Their goals were similar to FHWA's goals: to evaluate long-term performance and cost efficiency. Reviews of their projects are described here.

Ohio Department of Transportation (OH 3)

ODOT performed a test for alternative joint sealing materials along 5 mi. of US 50 (FHWA 2006d).The purpose of this test was to examine the effectiveness of joint sealing practices, materials, and procedures with respect to cost and performance.

The tests revealed that the narrow joints performed poorly because the sealant lost adhesion and spilled over onto the surface of the concrete. Additionally, temperature, equipment, and installer experience impacted the performance of the joints. The latter point, installer experience, is very important. Tests suggest that inadvertent deviations from the manufacturer's instructions or user error during joint construction are critical factors that will ultimately govern joint performance. Adhesion loss due to inadequate cleaning may also impact sealant performance. This appears to indicate that proper joint cleaning is another crucial variable for evaluating a joint. The tests further appear to suggest that unsealed joints may be more prone than sealed joints to spalling and corner and mid-slab cracking failures. This contradicts data presented in research did by KDOT – an important inconsistency to note.

Georgia Department of Transportation (GDOT)

The GDOT conducted a study over a three-year period on a 1500 ft. stretch of roadway on Jimmy Dyess Parkway in May, 2001(Cown 2001).The purpose of this study was to compare sealant performance and the durability of three different test joint widths. Three joint types were tested: (1) 0.125 in. joints without sealant; (2) 0.125 in. joints with sealant; and (3) 0.25 in. joints with sealant. A standard 0.375 in. joint with sealant was also analyzed as a control for the tests. The joints were visually inspected and an average joint width and standard deviation were calculated for each test joint. Cleanliness, spalling, cracking, and sealant condition were also recorded and compared with construction method.

Joint manufacture method appeared to influence behavior significantly. After testing, the 0.125 in. joints without sealant filled with debris and expanded to a mean width of 0.268 in. The 0.125 in. joints with sealant remained clean. The sealant in one of

these joints failed, while the joints expanded to a mean width of 0.256 in. The 0.25 in. joints with sealant expanded to a mean joint width of 0.321 in. The 0.375 in. control joints remained clean, no sealant failures were observed, and they expanded to a mean joint width of 0.454 in.

The 0.25 in. joint experienced the smallest average widening. For the joints with sealant, one new spall and one sealant failure were observed. For the 0.125 in. joints without sealant, there were two new spalls that were continuously filled with debris.

Louisiana Transportation Research Center (LTRC)

Five test joints were installed on a 5400 foot section of Northline Road in Port Allen, Louisiana (Rasoulian et al. 2006). The LTRC's goal was to evaluate the performance difference between narrow joints and the standard joints. Tire noise for each of these joints was also evaluated.

The joint types tested were as follows: (1) 0.375 in. joints with sealant and backer rod, cut by the standard wet double cut method; (2) 0.125 in. joints without sealant, cut by the dry-cut method; (3) 0.125 in. joints without sealant, cut by the wet double-cut method; (4) 0.125 in. joints with sealant but without backer rod, cut using the standard wet double-cut method; and (5) 0.125 in. joints with sealant and backer rod, cut by the conventional wet double-cut method. The joints cut using the early dry saw-cutting method appeared to require a significantly shallower cut depth than those cut by the wet double-cut method.

Neither the saw-cut method nor the joint depth appeared to have any significance on the joints' performance. However, depth difference may cause difficulty when attempting to widen the joints. For these reasons the narrow joint cut using the wet-cut

method was recommended for use in Louisiana. However, to save time, labor, and money, further exploration of the narrow dry-cut method was also recommended.

Wisconsin Department of Transportation (WDOT)

Several studies that evaluated the relative merits of sealed versus unsealed pavements have led researchers to question whether sealing joints is really cost effective, or even if it actually increases performance. “The Great Unsealing” (Shober 1997), summarizes five specific studies:

- USH 51 in Marathon County, Wisconsin
- USH 18/151 in Iowa County, Wisconsin
- STH 16/190 in Waukesha County, Wisconsin
- STH 29 in Brown County, Wisconsin
- and STH 164 in Waukesha County, Wisconsin

Each of these studies was stimulated by the concept that customers drive highway management. Generally, customers are less concerned with failures and are more concerned with ride and pavement life. The goal of these studies was to determine whether joint sealing enhanced pavement performance, and if so, whether joint sealing is cost effective. Each of these studies analyzed a combination of sealed and unsealed sections, joint widths, and joint spacing.

With respect to failure, ride, and material integrity, sealed joints did not appear to perform significantly better than the unsealed joints. On the contrary, often the unsealed joints performed equal to, if not better, than the sealed joints in terms of concrete failure and ride quality.

WDOT concluded that there was no difference in pavement performance due to joint sealing. In 1990 WDOT discontinued sealing joints and specified a joint thickness of 3 – 6 mm (0.12 – 0.24 in.). Shober estimates that costs for constructing and

maintaining sealed joints in Wisconsin are $6,000,000 per year more than unsealed joints (Shober 1997). This implies that using unsealed joints may be beneficial from both a cost and a maintenance perspective.

Conclusions from the WDOT study have been met with some criticism. Two studies by Martin Burke (Burke 1998, Burke 2002) imply that these conclusions may not adequately describe sealed versus unsealed concrete joint behavior because WDOT data was taken over a relatively small (ten years) time period. Burke argues that extrapolating ten-year data to a roadway's service life, which is usually thirty years or more, may not adequately describe joint behavior from year eleven onward. Secondly, Burke argues that transportation agencies with the most long-term experience using unsealed joints, CalDOT and Western European DOT equivalents, have abandoned unsealed joints and instead have moved back to using the sealed joint. Therefore, Burke does not recommend using unsealed joints.

North Dakota Department of Transportation (NDDOT)

The objective of the project (Dunn 2009) was to determine if joint sealants are necessary for the performance and longevity of the pavement structure. Since 1997 the NDDOT have installed the unsealed joint in several PCC projects. Four items were monitored and evaluated. They are as follows;

- Distress at the joints.
- Ride.
- The amount of non-compressible material in the joints.
- Incompressible material filtered through the joint into the drainage system.

The locations of PCC project test sections with unsealed joints are:

- IM-6-029(027)161 - I-29 from ND 54 north to near Jct 17 (SB)
- IM-2-094(007)256 - I-94 near the City of Jamestown (WB)
- IM-5-094(008)071 - I-94 from Gladstone to Taylor (EB)

- IM-8-029(025)053 - I-29 from the Wild Rice River to 32nd Avenue (SB)

Several test sections with unsealed joints were installed along these roadways, and the number of spalled joints was recorded every other year in both the test section and a sealed control section of each roadway. Every test section studied shows a higher number of spalled joints in the unsealed test section when compared with a roadway's corresponding sealed control section. Based on these results, NDOT did not recommend using unsealed joints.

FHWA Strategic Highway Research Program

The FHWA ran a series of tests at six sites where a total of 125 test sections were evaluated. Both newly constructed and expanded roads were examined under the initiative (Smith et al. 1999). These sites include:

- US 60 in Mesa, Arizona
- US 287 in Campo, Colorado
- I-80 in Wells, Nevada
- I-15 in Tremonton, Utah
- UT 154 in Salt Lake City, Utah
- US 40 in Heber City, Utah

These studies sought to determine the most effective materials and construction methods for sealed joints in concrete pavement. Joint configurations included a:

- 3 mm (0.12 in.) joint
- 3 mm (0.12 in.) joint cut to a shallow depth
- 6 mm (0.24 in.) joint
- 9 mm (0.35 in.) joint
- 9 mm (0.35 in.) joint with a beveled edge
- 13 mm (0.51 in.) joint

The first five joints were cut with a standard riding saw; the last was cut using the Soff-Cut method. A total of 29 distinct joint types were tested. In total, over 2000 joints were tested. The study recommends 9 mm (0.35 in.) joints using self-leveling silicone

sealant. However, some sealants proved effective in 3 – 6 mm (0.12 – 0.24 in.) joints. Reduced material associated with these narrower joints may result in more cost effective strategies. The tests revealed no significant difference in the performance of the joints with respect to the sawing methods.

Summary

A series of studies was conducted to evaluate the long-term performance of different concrete joints along roadways. While smaller joints or unsealed joints may be more cost effective, overall, results from these studies are inconclusive with regard to reliability and performance. Some studies concluded that non-sealed joints or narrower joints had minimal effects on performance while other studies concluded that the effects of these variables were significant. This discrepancy appears to suggest that further research should be conducted to evaluate the effects of joint size and sealant on concrete joints.

CHAPTER 4
ANALYTICAL APPROACH TO COMPUTING SLAB MOVEMENT IN CONCRETE PAVEMENT

Background

Concrete slab movement is caused by three factors: (1) drying shrinkage; (2) thermal expansion or contraction; and (3) slab curling. As implied by its name, drying shrinkage occurs when a freshly cured slab dries and contracts. Thermal strain is caused by temperature fluctuations. These temperature changes may occur at high frequency (for example, from day to night) or low frequency (for example, from winter to summer). Generally, higher-frequency temperature fluctuations are associated with lesser temperature change magnitudes. Seasonal temperature variations tend to exhibit greater magnitude temperature variations.

In 1993, AASHTO developed an expression for predicting maximum joint expansion:

$$\Delta L = CL(\alpha \cdot \Delta T + \varepsilon) \tag{4-1}$$

where ΔL is magnitude of the change in joint width due to temperature and moisture changes in the concrete; L is slab length; α is the linear thermal coefficient of expansion/contraction; ε is the drying shrinkage coefficient; and C is an adjustment coefficient to account for the slab-base frictional restraint (0.65 for stabilized bases and 0.8 for granular bases).

Equation 4-1 is only applicable for computing maximum joint expansion or contraction reached for a given temperature, assuming that the material is allowed time to achieve this value. In reality, joint opening is dynamic in the sense that over time, a joint's gap periodically expands and contracts. Therefore an analytical method to

characterize these dynamic features may be more appropriate. To develop an expression to describe the adiabatic evolution of the concrete, the three components that cause expansion and contraction (thermal strain, shrinkage, curling) are isolated, analyzed separately, and their net-effect on expansion/contraction are added together.

Thermal Strain

A simple temperature-strain relationship can be developed to determine a slab's thermal expansion:

$$\varepsilon_t(t) = \alpha \cdot \Delta T(t) = \alpha \cdot (T_c(t) - T_{ref}) \tag{4-2}$$

where $\Delta T(t)$ is now the instantaneous magnitude of the slab's temperature change; $T_c(t)$ is the slab's temperature; T_{ref} is a reference temperature; and t is time. A positive value of $\varepsilon_t(t)$, or the strain, implies expansion; a negative value implies contraction.

Figure 4-1 shows the coordinate system used in Equation 4-2. Note that Equation 4-2 requires a slab's temperature. Concrete slabs generally do not have a uniform temperature from top-to-bottom. Rather, the temperature often changes dramatically from one side to the other, typically with a non-linear profile. To account for this non-uniform slab temperature, Mechanistic-Empirical Pavement Design Guide (MEPDG) software can be used to compute representative temperature profiles for slabs based on temperature data. To calculate $T_c(t)$, an average is taken with respect to depth:

$$T_c(t) = \frac{1}{h}\int_{-h/2}^{h/2} T(z,t)dz \tag{4-3}$$

where $T_c(t)$ is average temperature; h is the slab thickness; and z is the height measured from the center of the concrete slab.

In order to compute $T_c(t)$ the real Florida climatic data downloaded from MEPDG website (http://onlinepubs.trb.org/onlinepubs/archive/mepdg/climatic_state.htm). Hourly temperature data from September, 1998 to November 2002 in Gainesville, FL was used as an input data, and MEPDG version 1.100 was used to compute the temperature profile of 10 inches concrete slab. Figure 4-2 shows a sample temperature profiles for January 1, 2001 while Figure 4-3 shows another sample temperature profiles for July 1, 2001. As demonstrated, temperature varies as a function of depth and time. $T_c(t)$ was computed from the hourly temperature profiles using equation 4-3. Representative concrete parameters (Table 4-1) were used with the ten inch dimension to compute the amount of thermal expansion using question 4-2.

Temperature Curling

A concrete slab's temperature profile causes slab curling. During the day, temperature at the top of the slab is greater than temperature at the bottom of the slab. This temperature gradient causes the top of the slab to expand more than the bottom of the slab. The net effect is a downward bend (Figure 4-4A). During the night, the top of the slab will be cooler than the slab's bottom. Thus, the bottom will contract less than the top, and the slab will bend upward (Figure 4-4B). In the former case, a compression zone exists along the slab's bottom while a tension zone exists along the slab's top. In the latter case, the compression and tension regions are reversed.

Although Figure 4-2 and Figure 4-3 show non-linear slab temperature profiles, a linear approximation will be made to simplify the concrete curling computation. An expression based on Westergaard's (1926) curling deflection theory can be developed to quantitatively describe curling based on this linear temperature profile:

$$Z(x,y) = f(y - \frac{B}{2}) + F(x - \frac{L}{2}) \tag{4-4}$$

where *y* is a slab's width coordinate (measured from the center); *x* is a slab's length coordinate; *Z(x, y)* is deflection; *f* is a deflection function for a slab with infinite length and width, *B*; and *F* is a deflection function for a slab with infinite width and length, *L*.

According to Westergaard *F* can be expressed explicitly as:

$$F(x) = -z_0 \frac{2\cos\lambda\cosh\lambda}{\sin 2\lambda + \sinh 2\lambda}[(-\tan\lambda + \tanh\lambda)\cos\frac{x}{l\sqrt{2}}\cosh\frac{x}{l\sqrt{2}} + (\tan\lambda + \tanh\lambda)\sin\frac{x}{l\sqrt{2}}\sinh\frac{x}{l\sqrt{2}}] \tag{4-5}$$

where *l* is a slab's relative stiffness radius; μ is Poisson's ratio for concrete; *k* is the modulus of subgrade reaction; λ is a constant decided by the shape of concrete slab; and ΔT is the temperature difference between top and bottom of the slab. To compute z_0, *l*, λ, and ΔT, the following expressions are used:

$$l = \sqrt[4]{\frac{Eh^3}{12(1-\mu^2)k}} \tag{4-6}$$

$$\lambda = \frac{L}{l\sqrt{8}} \tag{4-7}$$

$$z_0 = \frac{(1-\mu)l^2\alpha\Delta T}{h} \tag{4-8}$$

$$\Delta T = T(-\frac{h}{2}, t) - T(\frac{h}{2}, t) \tag{4-9}$$

where *E* is the concrete modulus of elasticity, and other terms have been previously defined. *Curl(t),* defined as the change in the joint opening due to the minute angular

rotation of the concrete surface, may be approximated by computing *F'*, the first derivative of *F* at *x* = *L/2*:

$$Curl(t) = h\left|F'(\frac{L}{2})\right| \text{ if TL(-(h/2),t)<TL((h/2),t)} \quad \text{(4-10a)}$$

$$Curl(t) = -h\left|F'(\frac{L}{2})\right| \text{ if TL((h/2),t)<TL(-(h/2),t)} \quad \text{(4-10b)}$$

Note that curling is only computed along the slab's length since we are interested in the effects on transverse joints. For longitudinal joints we would consider curling with respect to the slabs width.

The same climatic data for thermal strain was used for the calculation of the curling strain. The temperatures at top and bottom of the concrete slab temperature profile were used to establish a linear temperature profile. The curling strain were computed using this linear temperature profile and equations from 4-4 to 4-10b.

Drying Shrinkage

Shrinkage is influenced by a number of factors such as:

- Specifics of the concrete mix (water-cement ratio, aggregate size, etc.)
- The temperature and relative humidity of the environment during curing
- The age of the concrete when it is poured
- The size of the structure, member, or thickness of slab

When concrete cures, water is lost as the concrete hardens. According to the American Concrete Institute (ACI) Committee 209 (Mindess et al. 2003), shrinkage can be computed using the following expression:

$$\varepsilon_{dry}(t) = \frac{t}{35+t}\varepsilon_u \quad \text{(4-11)}$$

where *t* is time (days); ε_u is the concrete's ultimate drying shrinkage strain; and $\varepsilon_{dry}(t)$ is drying shrinkage strain. Figure 4-5 (Barr 2003) implies that shrinkage is most significant

during the early stages of curing. According to Barr's data, the most significant strain (shrinkage) occurred during the first 90 days of curing.

Prediction of Joint Opening Using Analytical Approach

As briefly discussed in the calculation of thermal strain, the parameters relevant to a typical slab computation were computed using data from a ten-inch slab from Gainesville, FL. In addition to the thermal strain computation, shrinkage (Eq. 4-12) and curling plus shrinkage (Eq. 4-13) effects on joint opening were computed using representative data (Table 4-1):

$$JO(t) = C \cdot L \cdot \left(\varepsilon_t(t) + \varepsilon_{dry}(t)\right) \tag{4-12}$$

$$JO(t) = C \cdot L \cdot \left(\varepsilon_t(t) + \varepsilon_{dry}(t)\right) + Curl(t) \tag{4-13}$$

A MathCAD code was written to execute this computation (Appendix A).

Results from MathCAD are plotted such that total slab movement is presented as a function of time. Results in Figure 4-6 are obtained using Eq. 4-13 while results presented in Figure 4-7 are obtained using Eq. 4-12. Figure 4-8 shows the difference between results from Eq. 4-12 and Eq. 4-13. As demonstrated, curling effects appear to be relatively minor when compared with shrinkage. Results appear to be similar to Barr's (2003) results – shrinkage is most significant during a slab's first three months. After the first 90 days, seasonal changes appear to have the most significant effect on concrete expansion and joint size.

Table 4-1. Parameters used in the model

Parameter name	Parameter value
Concrete setting temperature (°C)	35
Coefficient of concrete thermal expansion (1/°C)	10.35×10^{-6}
Concrete 28 days elastic modulus (MPa)	25900
Poisson's ratio	0.2
Ultimate drying shrinkage	7.8×10^{-4}
Composite modulus of sub-grade reaction (pci)	450
Length of concrete slab (mm)	4570
Thickness of concrete slab (mm)	254
Depth of water table (mm)	3048

Figure 4-1. Coordinate system schematic.

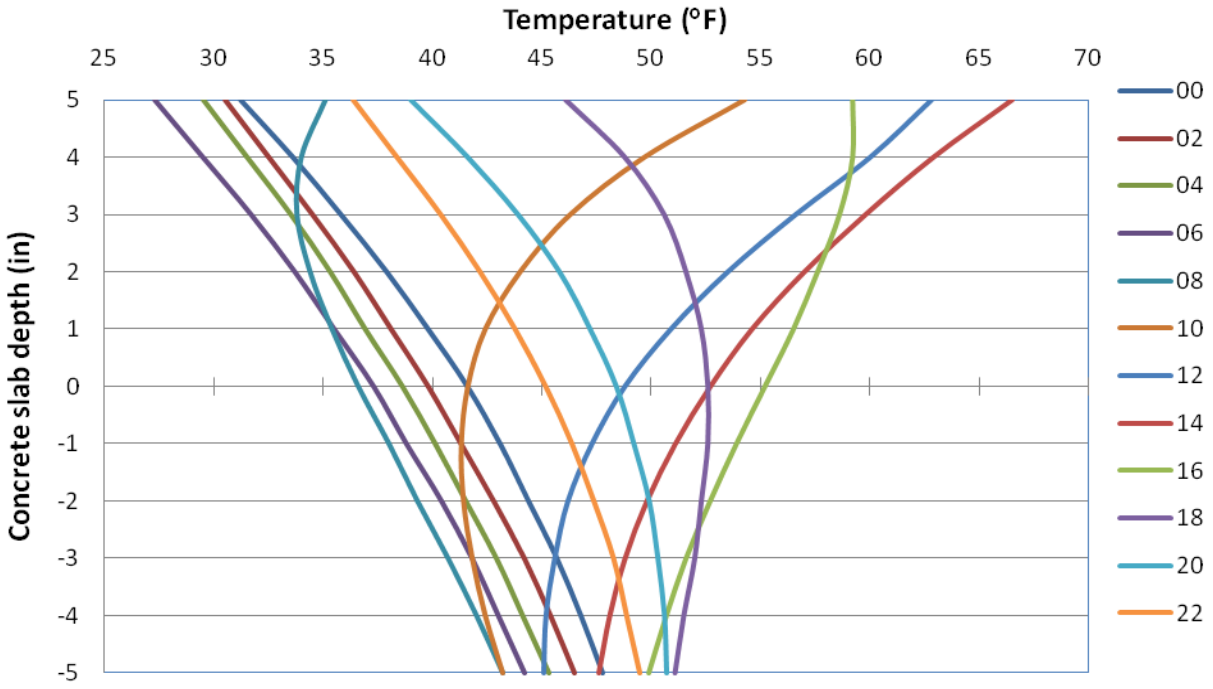

Figure 4-2. Representative slab temperature profiles on January 1st 2001. Each line corresponds to a different time (hrs.)

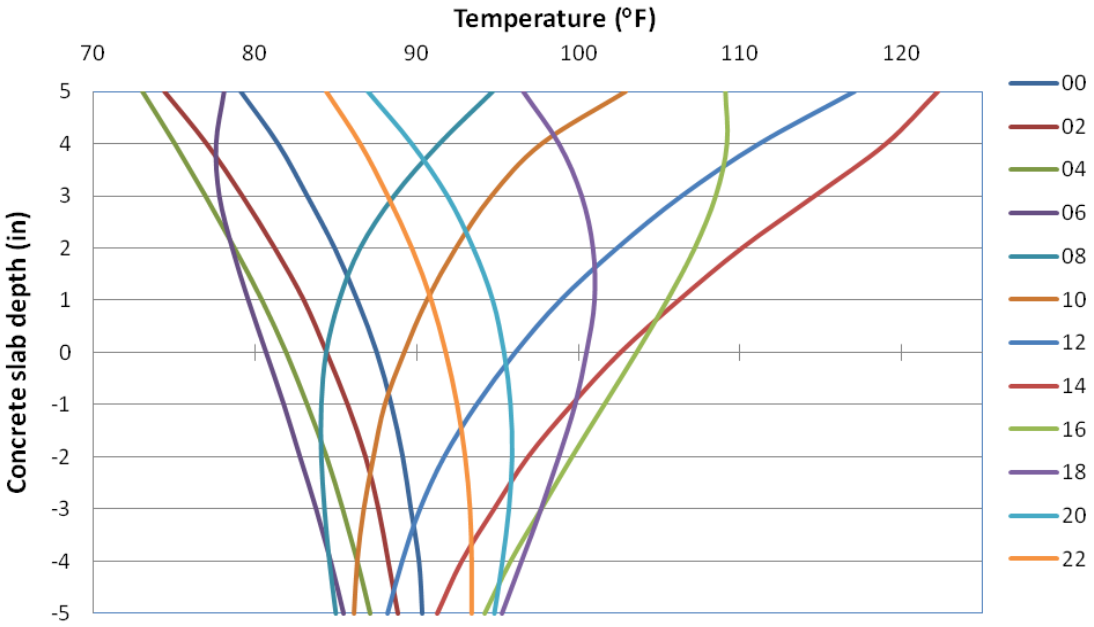

Figure 4-3. Representative slab temperature profiles on July 1st 2001. Each line corresponds to a different time (hrs).

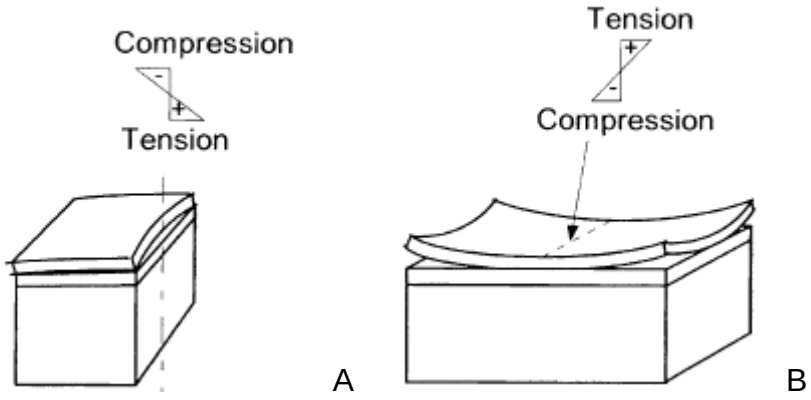

Figure 4-4. Curling schematic, (A) during the day, (B) during night.

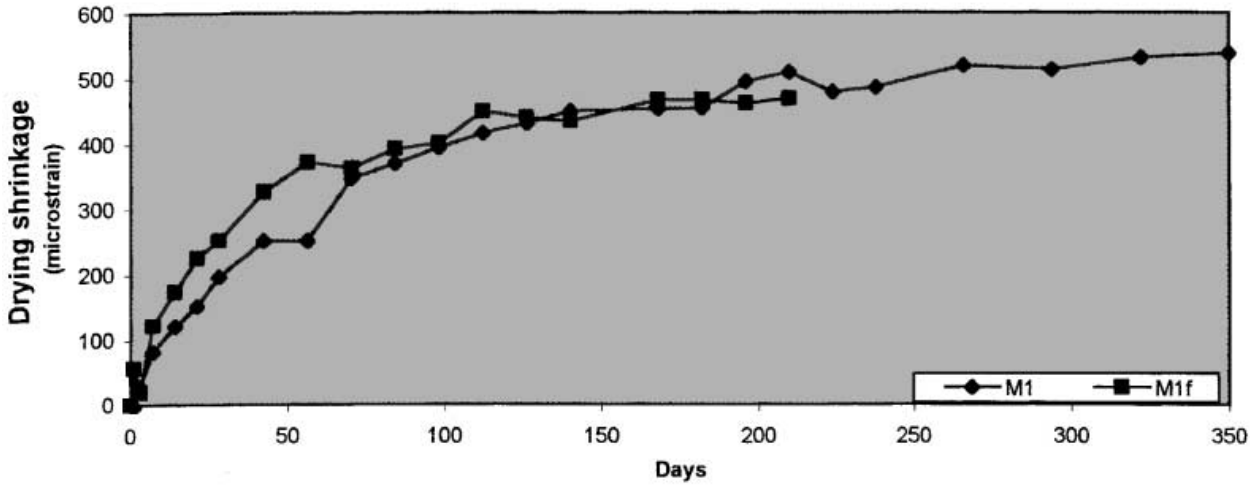

Figure 4-5. Drying shrinkage of the concrete (Barr 2003)

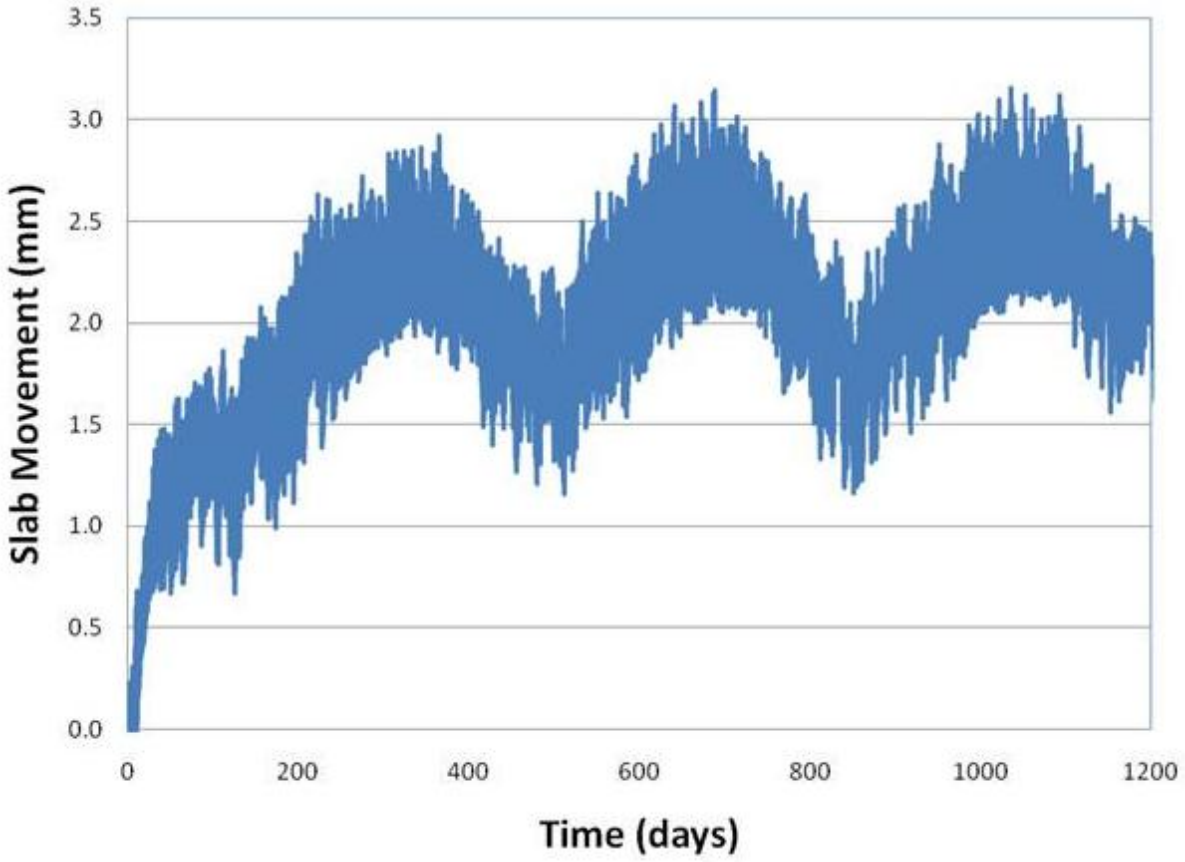

Figure 4-6. Slab movement (curling included).

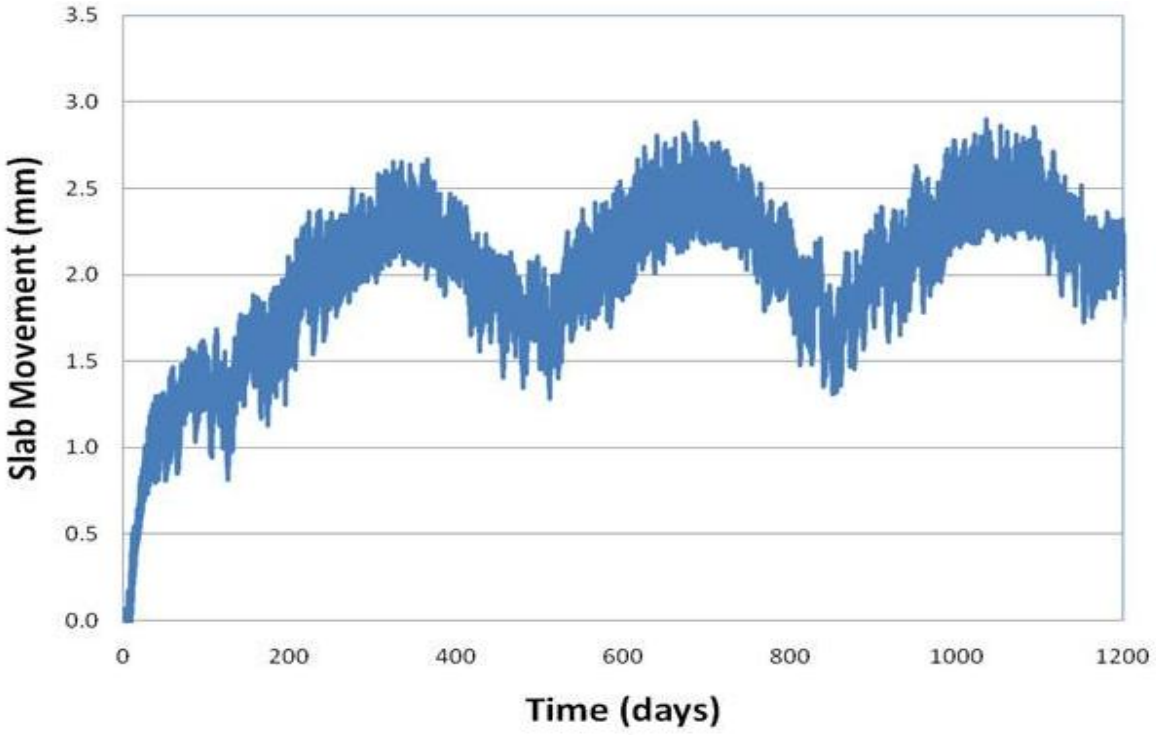

Figure 4-7. Slab movement (curling excluded).

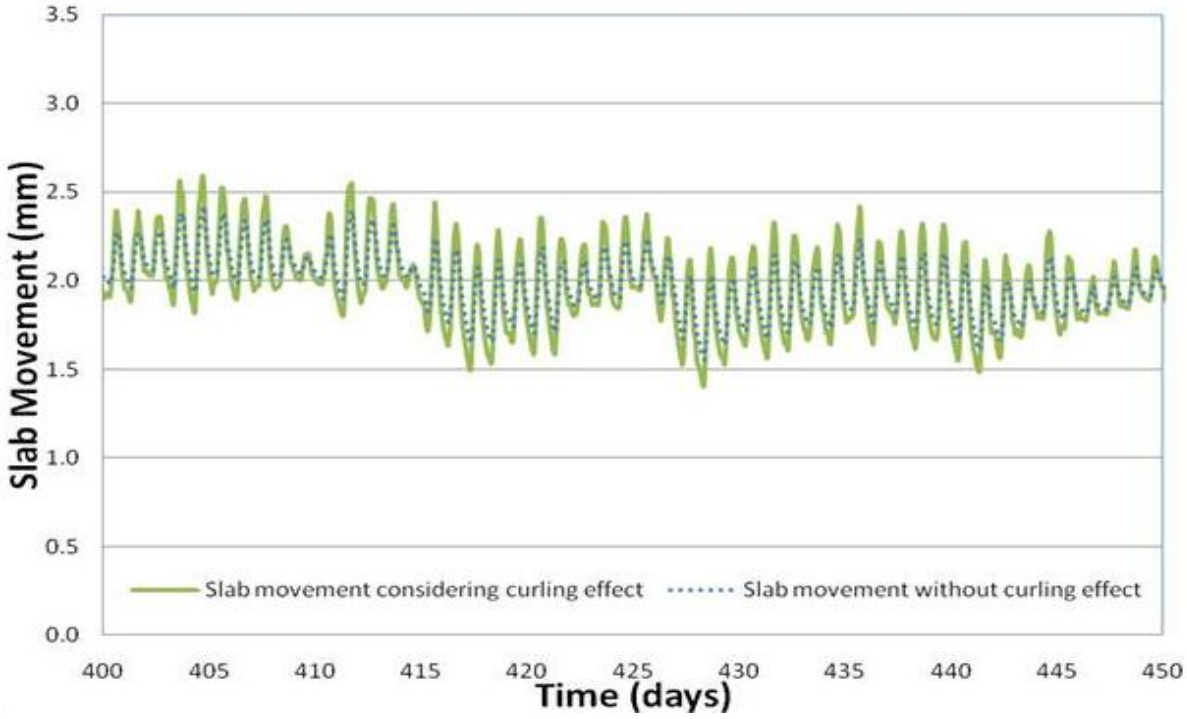

Figure 4-8. Curling's effect on slab movement.

CHAPTER 5
CREEP TEST FOR CONCRETE SEALANT

Background

Both self-leveling and non-self-leveling silicone sealant exhibit viscoelastic behavior. The following is a brief discussion of viscoelastic principles.

Elasticity, Plasticity, and Viscoelasticity

Most materials behave elastically under small stress. This means that they tend to return to their original shape after a minute deformation stress is removed from them. Generally, a kind of Hooke's Law is obeyed, meaning that deformation, or strain, depends linearly upon the stress.

Plasticity on the other hand describes deformation of a material when the material undergoes a non-reversible change of shape under an applied stress (J. Lubliner 2008). For example, a solid piece of metal or plastic may be permanently pounded or bent into a new shape. This permanent change in shape is said to be a plastic deformation.

When initially loaded at a constant stress, viscoelastic materials tend to exhibit classical elastic behavior. As the constant stress continues, eventually these materials will deform beyond their elastic threshold. When strained beyond this threshold, viscoelastic materials tend to display a slow, continuous increase of strain at a decreasing rate. When the stress is removed, a continuously decreasing strain follows an initial elastic recovery (Findley et al. 1976).

Figure 5-1 is an illustration of viscoelastic material deformation behavior. In this diagram, the material is stressed at an initial stress, σ_o , from t_0 to t_1 (Figure 5-1a). Figure 5-1b shows its strain behavior. From t_0 to t_1, strain increases – first elastically and then strain increases at a decreasing rate. When the stress is removed, the

material recovers elastically (ε_0), and then slowly back to its original position. Figure 5-2 (Findley et al. 1976) is an illustration of a similar viscoelastic curve. This viscoelastic curve is contrasted with a plastic material's strain curve and an elastic material's strain curve. Note that in all three cases, stress is held constant at σ_0.

Creep

In general, there are three stages that describe creep deformation when a material is subjected to a constant stress (Figure 5-3). In the primary stage, strain rate is initially relatively high. Over time, strain rate slows because increasing strain causes a material to harden. This hardening is known as "working hardening." In secondary stage, strain rate becomes nearly linear. This stage of creep strain is what most engineers refer to when they reference "creep rate." Beyond the secondary stage of creep deformation lies the tertiary phase. During this stage, strain rate rapidly increases. This increase in strain rate is usually the result of fractures that have developed in the material during the first two phases of creep deformation.

The time-scale in Figure 5-3 is relatively long – sometimes on the order of several years. Consider a roadway containing transverse joints filled with sealant with a design-life of 25 years. Under these conditions, a design engineer must account for the primary and secondary deformation so that the timing of the tertiary deformation can be predicted. Thus, understanding rate of creep for joint sealant is important.

Linear Viscoelastic Materials

A linear viscoelastic material is a special type of viscoelastic material whose induced stress is proportional to the associated strain at any given time. Under these

conditions, the material is said to be linearly viscoelastic and linear superposition principles apply. Stated mathematically, for a linearly viscoelastic material:

$$\varepsilon[C \cdot \sigma(t)] = C \cdot \varepsilon[\sigma(t)] \quad (5\text{-}1)$$

$$\varepsilon[\sigma_1(t) + \sigma_2(t - t_1)] = \varepsilon[\sigma_1(t)] + \varepsilon[\sigma_2(t - t_1)] \quad (5\text{-}2)$$

where σ is the applied stress to the material; ε is the associated strain; C is a material-dependent constant; and t is time.

Equation 5-1 means that strain output, ε, due to stress input, σ, equals the scalar C times the strain output, ε, due to the stress input σ. Equation 5-2 states that the strain output, ε, due to the combination of any two arbitrary, but different stress, σ_1 and σ_2 at different times, t and $t - t_1$, equals the sum of the stain outputs resulting from $\sigma_1(t)$ and $\sigma_2(t - t_1)$. Eq. 5-2 is usually called the "Boltzmann superposition principle." For a viscoelastic material to be called linear, both Eq. 5-1 and Eq. 5-2 must apply.

Objectives and Methods

As discussed briefly in Chapter 2, one of the primary goals of this study is to evaluate sealant viscoelastic behavior for concrete joint sealant. While several existing tests for sealant were described in Chapter 2, a creep test was not discussed because a reliable creep test does not yet exist. During this study, investigators designed a new creep test. The goals of this test are to:

- Determine viscoelastic behavior during a creep test under standard conditions.
- Identify the temperature sensitivity of the silicone sealant during creep.
- Determine whether or not a sealant may be classified as linearly viscoelastic.
- Determine the effects of aging on the material's viscoelastic properties.

To perform this new creep test, a new testing procedure was designed and executed. Testing required development of a new piece of equipment – the CRETA or Creep Testing Apparatus.

Specimen Preparation

Investigators made a series of "dog-bone-shaped samples" (Figure 5-5) to use during creep testing. The "dog-bone-shape" was found to be appropriate because the goal is to induce load into a narrow portion of the sample (Part 2 in Figure 5-5). The two heads of the dog-bone shown in Figure 5-5 connect to the CRETA during testing. Since the heads are much larger than the neck, which is only 10mm x 10mm x 30 mm, virtually all of the deformation should take place in the neck region.

Using a dog-bone-shape for testing materials similar to silicone sealant is fairly common. For example, dog-bone-samples are used during bituminous material ductility testing (ASTM 2009). In fact, the dog-bone-shaped specimens used in this study have the same dimensions as samples used for testing bituminous asphalt. The difference between the two tests is the addition of "backer-plates" to prevent Part 1 and Part 3 from sliding out of their respective loading dies during testing (Figure 5-6).

Traditionally, dog-bone-shaped samples are made by casting a material into dog-bone-shaped molds. While effective for bituminous ductility testing, this technique is time consuming when silicone sealant is to be tested. Silicone sealant requires three weeks to fully cure. Rather than use multiple dog-bone-molds, investigators instead decided that it would be more efficient to create a "silicone sealant sheet" (Figure 5-7 and Figure 5-8). Then, samples could be cut from the sheet using a die (Figure 5-9). A silicone sealant sheet is large enough (290mm x 140mm) to yield 14 to 15 samples

(Figure 5-10). Hence, several “silicone pours” could be reduced to one using this method.

Both self-leveling and non-self-leveling sealant were investigated in this study. For self-leveling sealant, cutting samples was easy; since the sheet self-leveled, all samples were about the same height (10mm). For non-self-leveling sealant, cutting was more difficult. Since the sheet did not self-level, samples had to be carefully trimmed after cutting to ensure a nearly-constant 10mm height.

Prototype Creep Test Apparatus (CRETA) Development

Because silicone sealant is a very soft material, testing was required to be run at relatively small stresses. Existing equipment is incapable of maintaining such a constant low-scale stress. Therefore a new piece of equipment, the CRETA, was developed for dog-bone-shape silicone sealant testing.

First, two prototype systems were developed (Figure 5-11). Both apparatuses use a Celesco SP1 string pot (Figure 5-12) to measure strain. A DATAQ DI-148U-SP USB data acquistion system (Figure 5-12) was used to collect data. For the inclined plane CRETA (Fig. 5-11a), the sample was inserted into its loading die with backer plates. The die-sample configuration was placed onto the inclined plane. One of the loading dies was attached to the string pot. The other loading die was attached to a string such that a mass could be added. Thus, a nearly constant stress was developed within the sample. As the sample deformed, extension was measured. For the perpendicular CRETA (Fig. 5-11b), the setup was similar except that the string pot was affixed to the base of the instrument and a series of pullies were used to apply the force. The advantage to the vertical test is that with this test, there are no friction forces between

the inclined plane and the sample's loading dies. Because of this, investigators eventually settled on the perpendicular apparatus.

An example of testing results is presented in Figure 5-14. Because the force on the sample is known (applied mass times gravity), and the cross-sectional area of the sample is known, stress can be computed and plotted as a function of computed strain. Compliance, the ordinate in Figure 5-14, is defined as computed strain divided by computed stress. As demonstrated in Figure 5-14, results appear to indicate that strain increases at a decreasing rate – thereby appearing to confirm that silicone sealant is viscoelastic.

Prototype Limitations and Final Version of the CRETA

The prototype CRETAs provided an excellent means of determining the general behavior of silicone sealant. However, the prototypes were not accurate enough to give conclusive results because of design limitations. A "proper" creep test should be performed under a constant stress. With the prototypes, although mass was constant, as the test was run the samples tended to stretch. As the samples stretched, their cross-sectional areas decreased, and therefore, the amount of stress resulting from the constant load increased. Therefore, these prototypes were only appropriate for measuring very small strains.

The string pot is excellent for measuring relatively large strains, but it struggles to measure the relatively small strains appropriate for this type of slow-loading creep test. Therefore, in the final version of the CRETA, the principles of the perpendicular CRETA prototype were preserved, but the string pot was replaced. Thus, smaller masses were added to the sample, and smaller strains were measured using a Linear Variable Differential Transformer (LVDT, Figure 5-15). While the string pot's resolution was

0.019in., the LVDT has much better resolution. The governing limitations of an LVDT are noise, DC stability, and detection circuitry. The LVDT was powered by a DC S7AC transducer amplifier (Figure 5-16a). The signal from the LVDT was amplified using a S7AC data acquisition amplifier and sent to a more precise DAQ system – a USB 1608FS DAQ device (Figure 5-16b). The timber frame shown used for the prototype (Fig. 5-11b) was replaced with an aluminum and steel frame (Fig. 5-17).

Creep Testing Results

Once the CRETA and the samples had been designed and built, a series of tests was run on self-leveling and non-self-leveling silicone samples. Temperature sensitivity, linearity, and aging effects were investigated.

Temperature Sensitivity

As previously discussed, prototype tests appeared to confirm that silicone sealant exhibits viscoelastic behavior.Generally, viscoelastic materials are sensitive to temperature fluctuations. Because of this, creep tests were run at four different temperatures (0°C, 20°C, 40°C, and 60°C) to determine the temperature sensitivity of the silicone sealant.

Methods

Since the creep test was run at four difference temperatures, and the LVDT is temperature sensitive, the LVDT needed to be calibrated at each temperature. A series of calibration tests was run at each of the four temperatures (Figure 5-18). Raw signals from the LVDT did not exhibit significant noise during testing (Figure 5-19). During temperature tests, both self-leveling and non-self-leveling samples were tested at each temperature. Thus, eight groups of tests were run – four temperatures times two types of samples per temperature. Each test was repeated three times for a total of 24 tests.

For the non-self-leveling sealant, a 100 g mass was used with the CRETA. Tests were conducted for thirty minutes. For the weaker, non-self-leveling sealant, a 1000 s (16.67 min.) test was run with a 20 g mass. During testing, the CRETA was placed into a temperature chamber (Figure 5-19) so that temperature was highly regulated.

Results

Averaged results are presented in Figure 5-21 (non-self-leveling sealant) and Figure 5-22 (self-leveling sealant). Figures are labeled according to sealant type ("NS" means non-self-leveling; "SL" means self-leveling) and temperature. For example, SL-0 is the curve for self-leveling sealant at 0 degrees Celsius. Results do not appear to indicate that there is any correlation between strain rate and temperature for self-leveling and non-self-leveling sealants from 0 to 60 degrees Celsius. This implies that the creep tests may be run at any temperature between 0 and 60 degree Celsius and results will be similar – an important conclusion.

Linear Viscoelasticity

The objective of this portion of the analysis was to identify whether or not silicone sealant is linearly viscoelastic. If a material behaves such that stress is proportional to strain (in accordance with Eq. 5-1), it will be said to obey proportionality. If a material behaves such that it behaves in accordance with Eq. 5-2, it will be said to obey superposition.

Proportionality

To identify whether or not sealant obeys proportionality, two different masses were successively applied to the same sample, and the corresponding strains were compared with one another. For the non-self-leveling sealant 400g and 200g masses were applied to a sample; for the self-leveling sealant, 20g and 50g masses were

applied. Figure 5-23 and Figure 5-24 show the results from these tests. As shown in these figures, results from the smaller mass were multiplied by the appropriate factor and plotted against results from the larger mass. For the non-self-leveling sealant, results from the 200g mass were multiplied by two. For a linearly viscoelastic material, one would expect that this should match the curve produced by the 400g mass. Similarly, for the self-leveling sealant, 20g results were multiplied by 2.5 and the results were compared with the 50g curve. A strain ratio was computed between the theoretical and measured strain, and results were plotted (Figure 5-25).

As shown in these figures, the curves are relatively close to one another. Or, put another way, the ratio between computed strain and measured strain is approximately 1.0. In one case, a proportionality assumption tended to slightly over-predict strain, while in the other case, a proportionality assumption tended to slightly under-predict strain. This appears to indicate that there is no bias in the proportionality assumption for these silicone sealants.

Superposition

Another creep test was designed to verify superposition for silicone sealants. For the non-self-leveling system, a 200g load was applied for 40 minutes. Then, an additional 200g load was applied to the sample for 20 minutes and afterwards a third 200g load was added (Figure 5-26). For the self-leveling system, loading was similar, but loads were reduced by a factor of ten (Figure 5-27). Figure 5-28 and Figure 5-29 are the results from these tests. Results are color-coordinated with corresponding loading from Figure 5-26 and Figure 5-27. For example, the “blue” line in Figure 5-26 corresponds to the “blue” result in Figure 5-28.

The “red” line in Figure 5-28 and Figure 5-29 corresponds to a superposition computation. For the first twenty minutes, the “red” line should be the similar to the “blue” line in both figures. Beyond 20 minutes, the “red” line should obey Eq. 5-2 such that strain is given by:

$$[\varepsilon(t) + \varepsilon(t - t_1)] \tag{5-3}$$

where t_1 is 20 minutes; $\varepsilon(t)$ represents the strain due to 200g load added in the second 20 minutes; and $\varepsilon(t - t_1)$ is due to 200g load added in the first 20 minutes.As demonstrated, results are extremely close to predictions; computational results were plotted against measured values to illustrate this (Figure 5-30 and 5-31). As shown, average deviation from y=x was 5.7% for self-leveling sealant and 6.5% for non-self-leveling sealant.

Summary

Because of the smallness of the differences between the results based on superposition and proportionality and actual measured data, investigators concluded that the silicone sealant used in these tests appeared to be linearly viscoelastic.

Aging Effects

Field tests appear to indicate that, over time, silicone sealant becomes stiffer because of aging (D. Oldfield 1996). The objective of this portion is to investigate the viscoelastic behavior of aged silicone sealant. Due to time constraints, samples were artificially aged using three acceleration procedures – hot water aging, oven aging, and freeze-thaw aging. Creep tests were conducted on samples both before and after artificial aging.

Hot water aging

Sealant in the field may come in contact with significant amounts of water. To investigate the effect of this water over time, sealant was "hot-water aged" and a series of tests were conducted on both self-leveling and non-self-leveling samples before and after hot-water aging. To age the samples, specimens were submersed in 90 degree Celsius water for ten days. As with the linear viscoelastic tests, loading for the self-leveling and non-self-leveling sealant was 20g and 200g, respectively. Results are presented in Figure 5-32 and Figure 5-33.

Both Figure 5-32 and Figure 5-33 appear to indicate that aging may have a significant effect on sealant strain. To further investigate, the strain for aged sealant versus strain for non-aged sealant was plotted in Figure 5-34. The strain of aged samples was found to be larger than non-aged ones. The slope of linear trend line for aged self-leveling sealant was 2.2; for the non-aged sealant, the slope of linear trend line was 2.0. These results appear to indicate that prolonged exposure to water causes sealant to soften by approximately 100%.

Oven aging

The purpose of this series of tests was to determine the effects of oxidation aging on silicone sealant. To accelerate oxidation aging, samples were placed into an oven at 150 degrees Celsius for 10 days. Creep tests were run on original and aged samples, and each test was repeated three times. Loading conditions were the same as they were during hot-water tests – 200 g for non-self-leveling sealant and 20 g for self-leveling sealant. Average results are presented in Figure 5-35 and Figure 5-36.

As shown in these figures, the self-leveling sealant does not appear to be affected significantly by oven aging. Results were non-dimensionalized and plotted against one

another to illustrate this (Figure 5-37). Average slope-error for self-leveling sealant was 11%. Research by Oldfield (Oldfield et al 1996) appears to indicate that long-term aging of self-leveling sealant may actually make the material stiffer. Non-self-leveling results appear to be in agreement with Oldfield's work. As illustrated in Figure 5-37, when strain is low, oven-aging does not appear to affect the sealant's performance significantly. As strain increases, non-self-leveling sealant appears to stiffen by a factor of approximately two. Further long-term aging tests should be conducted where samples are placed in an oven for longer than 10 days to quantify this effect.

Figure 5-35 appears to indicate that oven aging may be significant for non-self-leveling sealant because strain for aged samples is much lower than it was for non-aged samples. The slope of linear trend line for self-leveling sealant was 0.7 (Figure 5-37). This result is significant for engineers in the field. It implies that if a non-self-leveling sealant is used and subjected to prolonged heat, the sealant may become stiffer and more brittle. This could lead to an increase in joint stress as the slab moves and closes/opens the joint. If stress within the sealant becomes greater than the adhesive strength of the sealant, an adhesive failure may occur. As previously mentioned, adhesive failures will be discussed comprehensively in Chapter 6.

Freeze-thaw aging

The purpose of these tests was to investigate the effect of cyclic freeze-thaw action on silicone sealant. Samples were soaked with water, and subjected to five freeze-thaw cycles. During the "freeze phase," samples were placed in a freezer at -5 degrees Celsius for 24 hours. During the corresponding "thaw phase" samples were transferred to a refrigerator at 20 degrees Celsius for 24 hours. Creep tests were run both before and after cyclic freeze-thawing. Results are shown in Figure 5-38, Figure 5-

39, and Figure 5-40. As demonstrated in these figures, freeze-thaw aging over five cycles appeared to be insignificant. For self-leveling sealant, average deviation from non-aged results was 14.6%; for non-self-leveling sealant, the average deviation was 4.1%.

Summary and Conclusions

The following is a summary of creep testing including important conclusions:

A new device, the Creep Testing Apparatus (CRETA) was designed and constructed.

A series of tests were run with the CRETA to determine whether or not concrete joint silicone sealant behaves like a linear viscoelastic material. Results appear to indicate that proportionality and superposition are satisfied – thus sealant appears to be linearly viscoelastic.

A series of tests was conducted to quantify silicone sealant's response to temperature fluctuations. Results appear to indicate that temperature differences do not affect silicone sealant's viscoelastic properties significantly.

A series of tests was conducted to determine the effects of oven aging, hot water aging, and freeze-thaw aging on silicone sealant. Results appear to indicate that freeze-thaw aging does not affect performance significantly. Oven-aging appears to cause non-self-leveling sealant to become more brittle; it appears to have little effect on self-leveling sealant. Hot water aging appears to cause both types of sealant to become softer and more ductile.

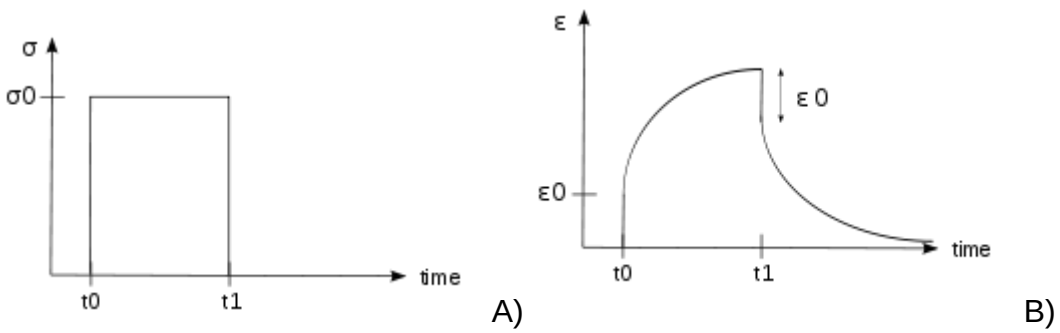

Figure 5-1. Viscoelastic behavior, (A) Applied stress and (B) induced strain.

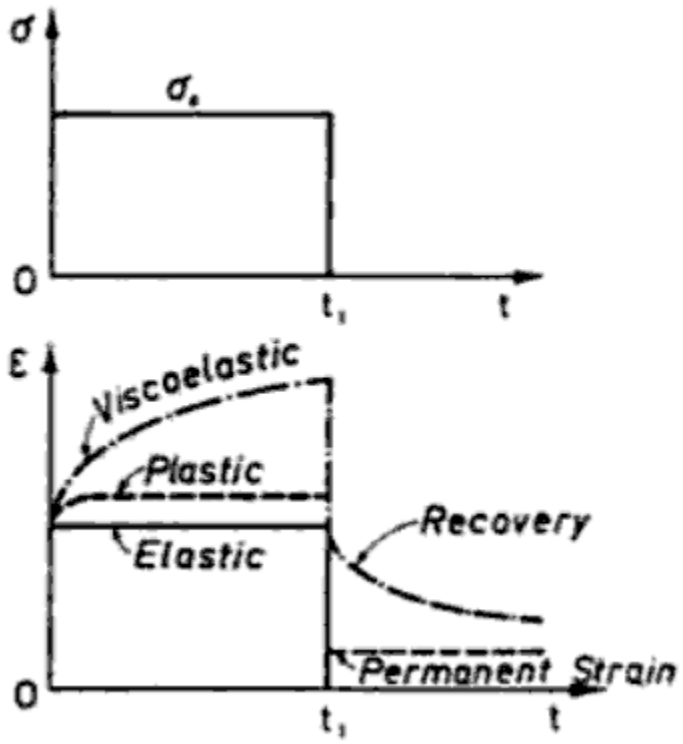

Figure 5-2. Viscoelastic, elastic, and plastic strain responses to a constant stress (Findley et al. 1976).

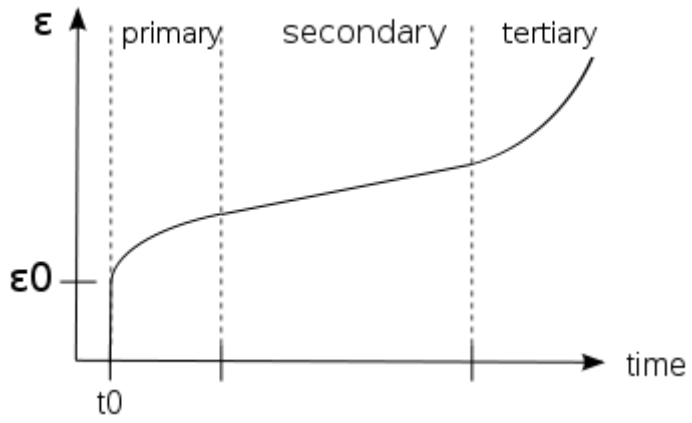

Figure 5-3. The three stages of material deformation

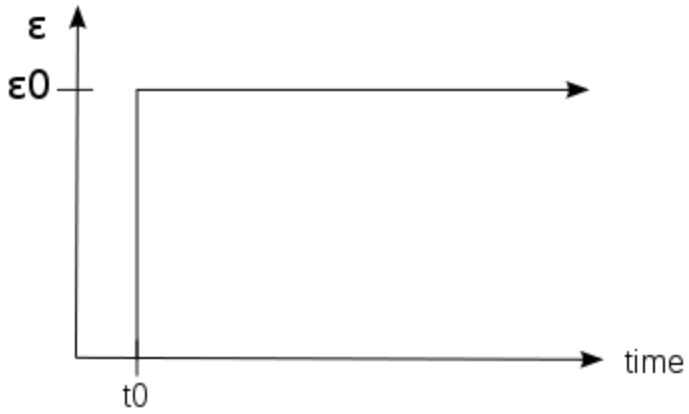

A)

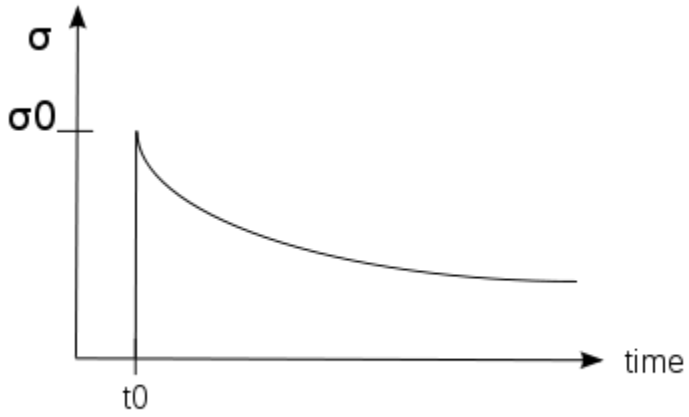

B)

Figure 5-4. (A) Applied strain and (B) induced stress as functions of time for a viscoelastic material

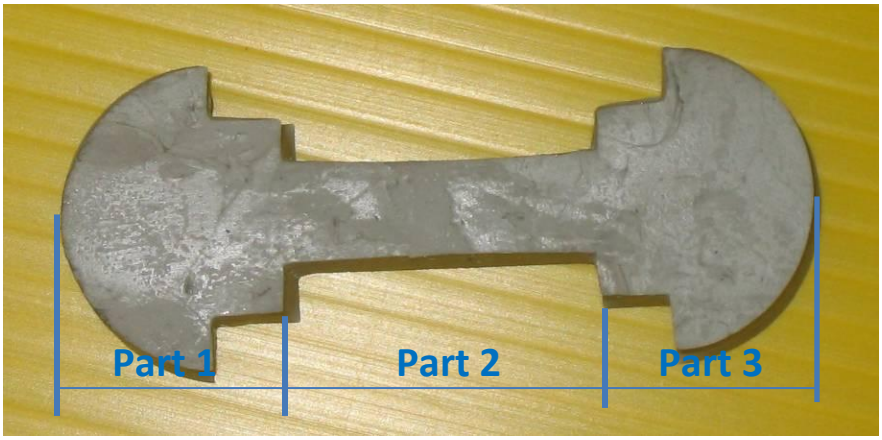

Figure 5-5. Example of a dog-bone-shaped sample (Photo courtesy of Qiang Li)


A)


B)

Figure 5-6. Dog-bone specimen in loading die, (A) traditional die, (B) New die with backer-plate (Photo courtesy of Qiang Li)

Figure 5-7. Silicone sheet mold (Photo courtesy of Qiang Li)

Figure 5-8. Self-leveling silicone sealant sheet (Photo courtesy of Qiang Li)

Figure 5-9. Silionce sealant dog-bone blade (Photo courtesy of Qiang Li)

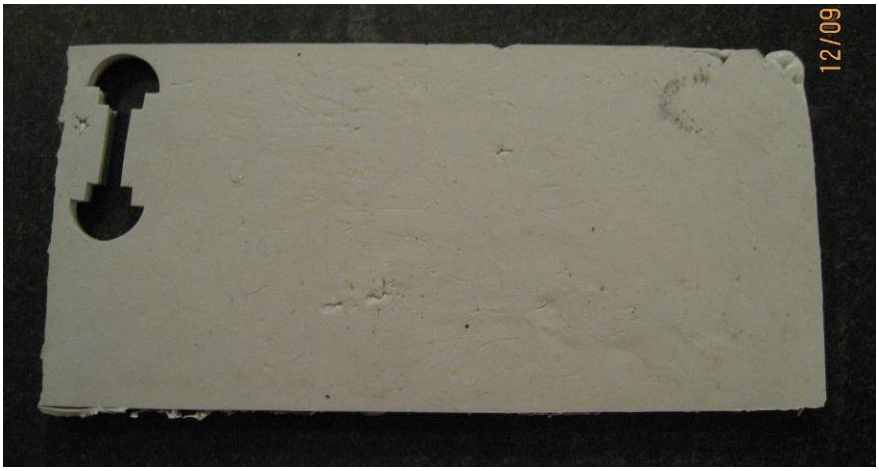

Figure 5-10. Non-self-leveling silicone sealant sheet with one dog-bone specimen cut from it (Photo courtesy of Qiang Li)

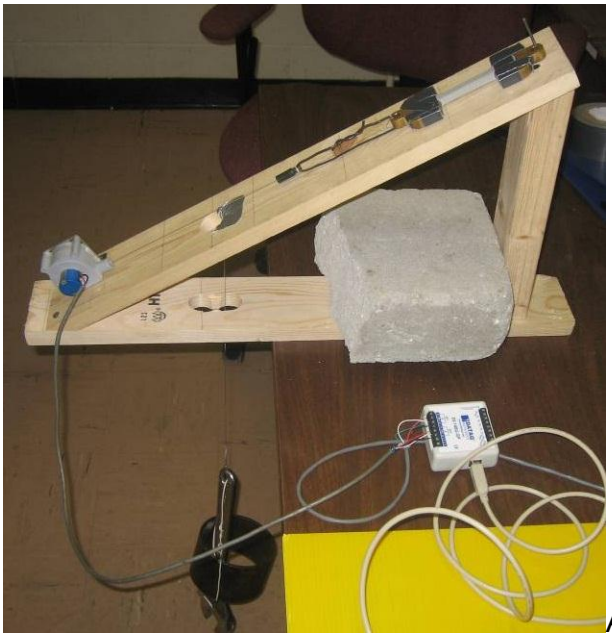
A)
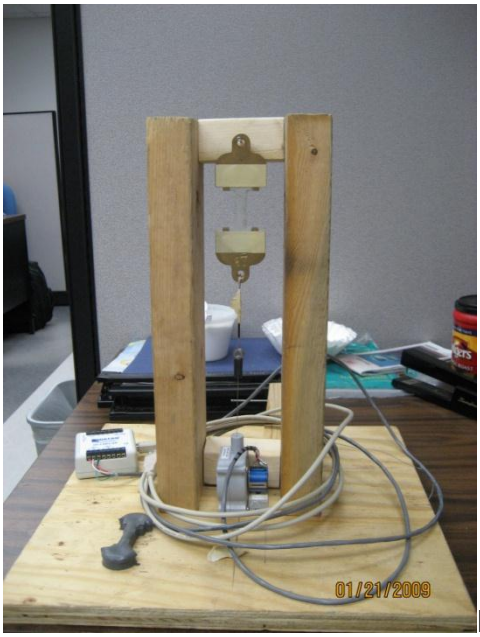

B)

Figure 5-11. Prototype Creep Test Apparatus (CRETA), (A) inclined plane tension version, (B) perpendicular tension version (Photo courtesy of Qiang Li)

Figure 5-12. Celesco SP1 string pot (Photo courtesy of Qiang Li)

Figure 5-13. DATAQ DI-148U-SP USB data acquistion system (Photo courtesy of Qiang Li)

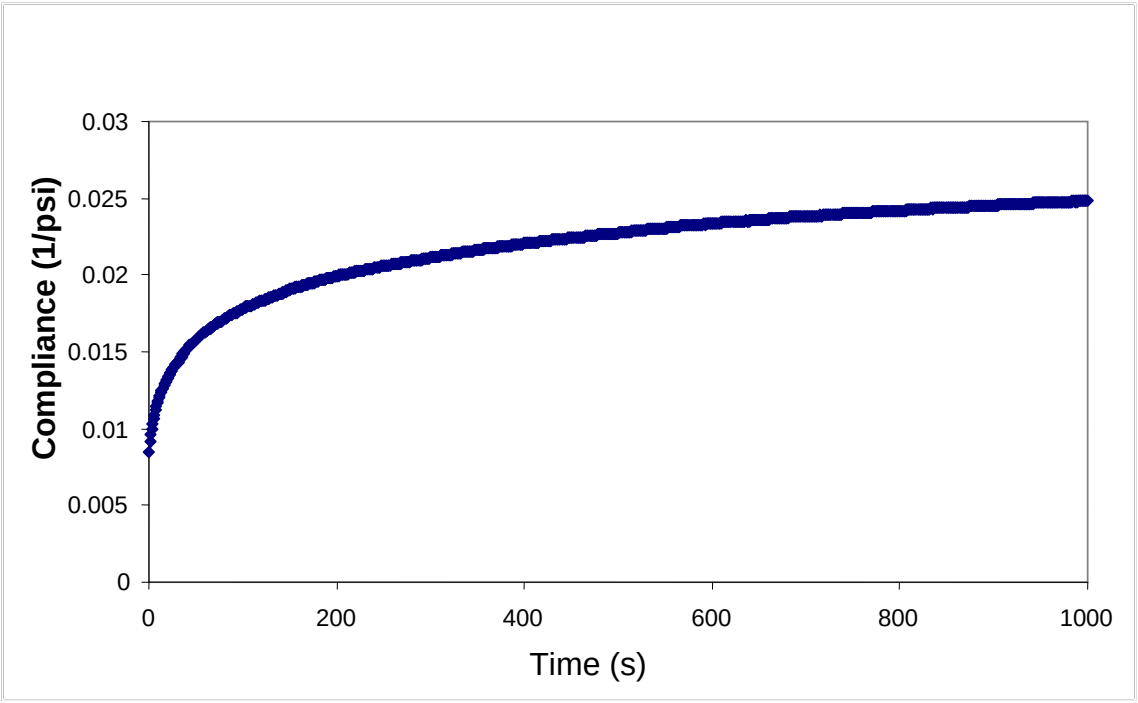

Figure 5-14. Trial test result using perpendicular CRETA

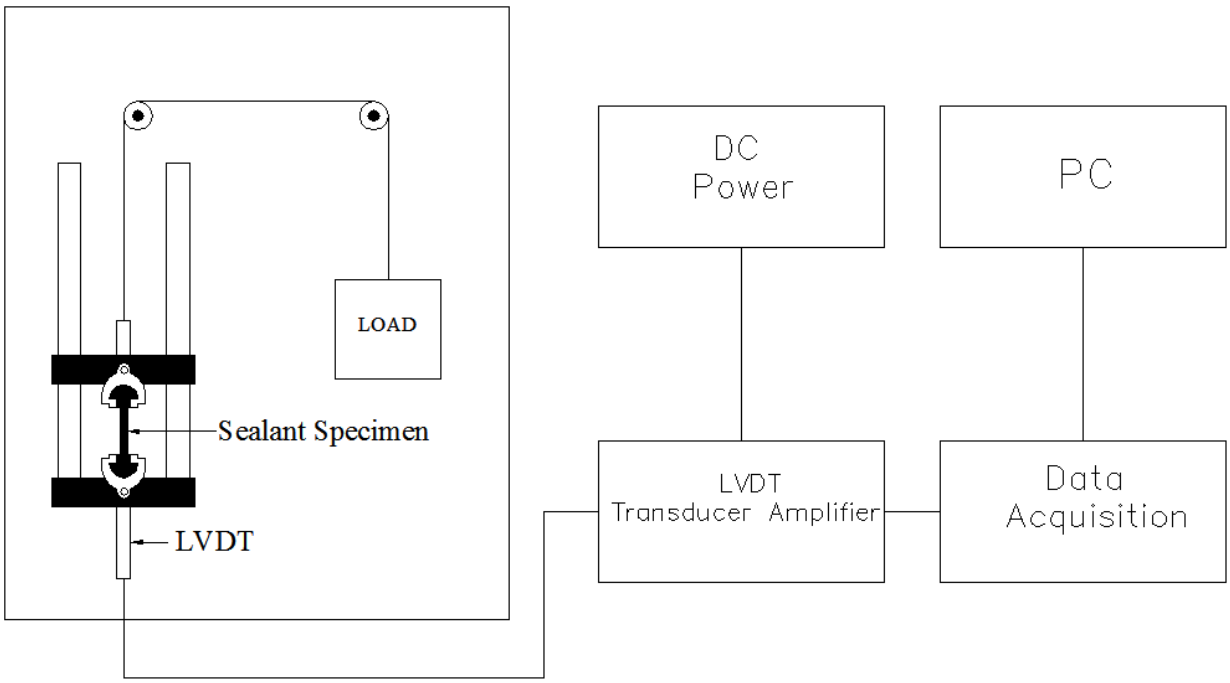

Figure 5-15. Perpendicular CRETA final version

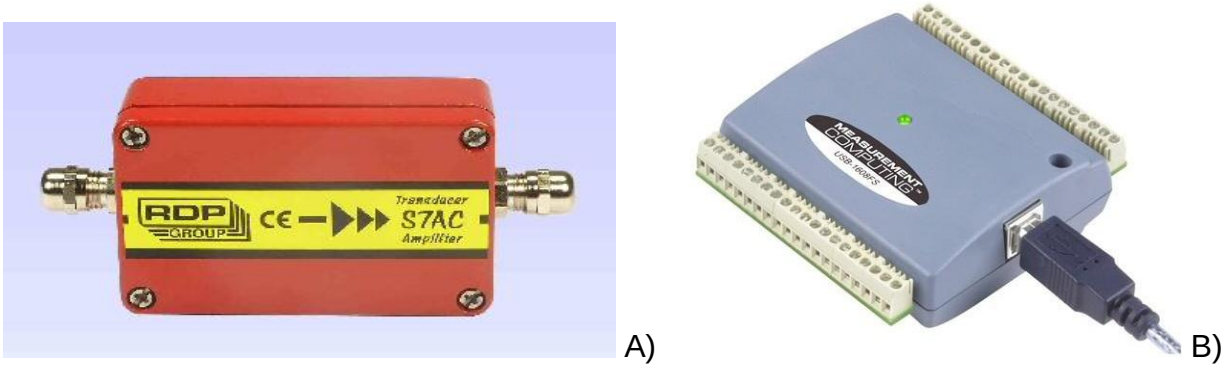

A) B)

Figure 5-16. (A) S7AC transducer amplifier; (B) USB-1608FS data acquisition (DAQ) device (Photo courtesy of Qiang Li)

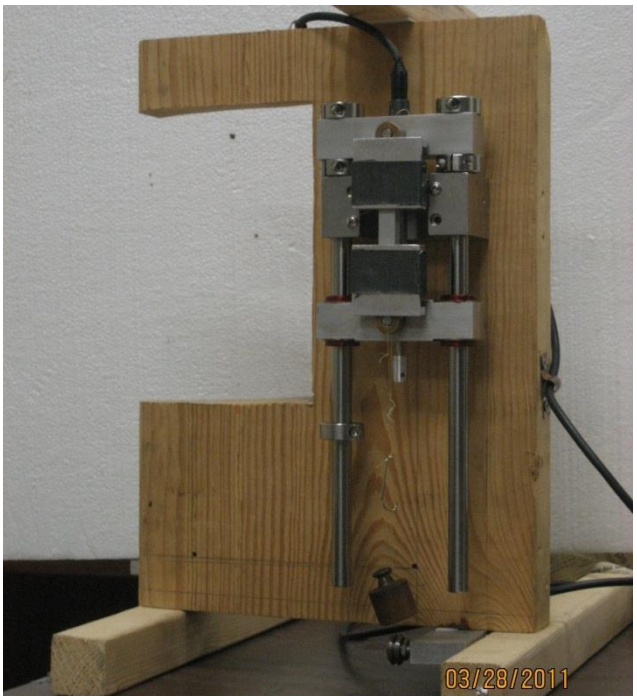

Figure 5-17. Creep test apparatus (Photo courtesy of Qiang Li)

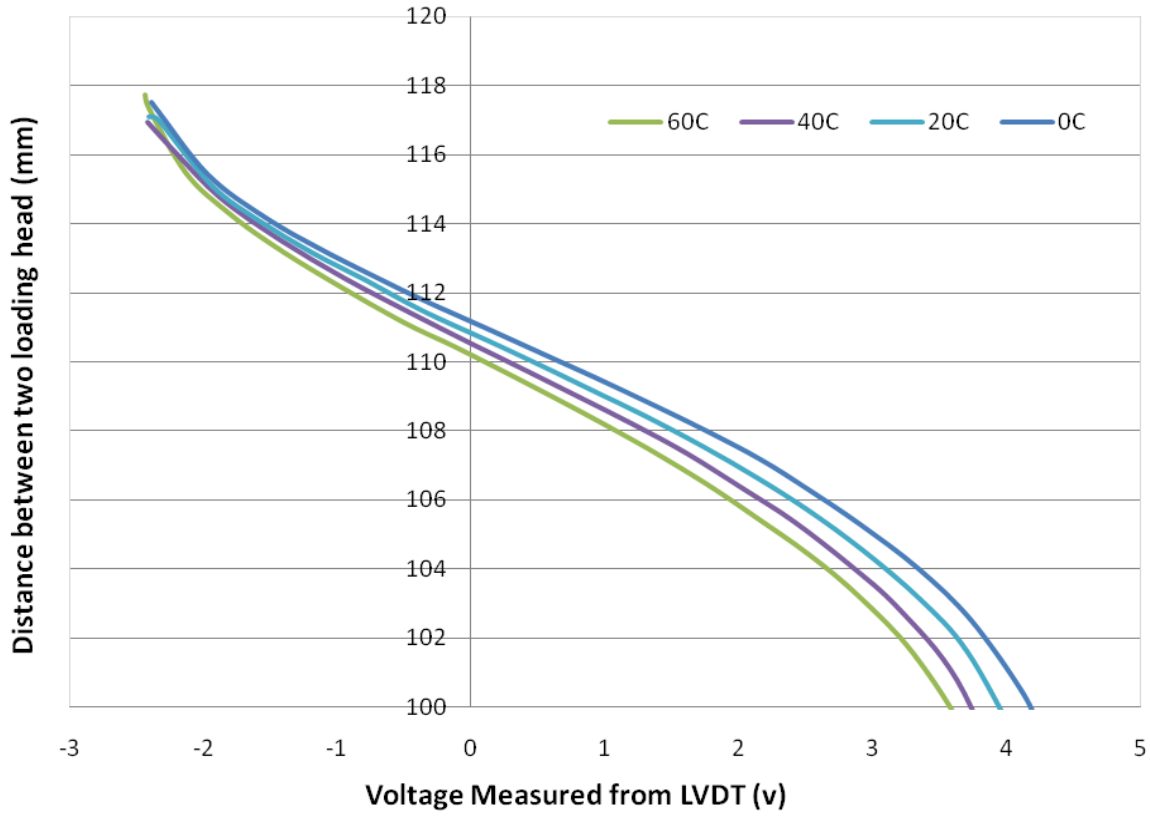

Figure 5-18. LVDT calibration curves

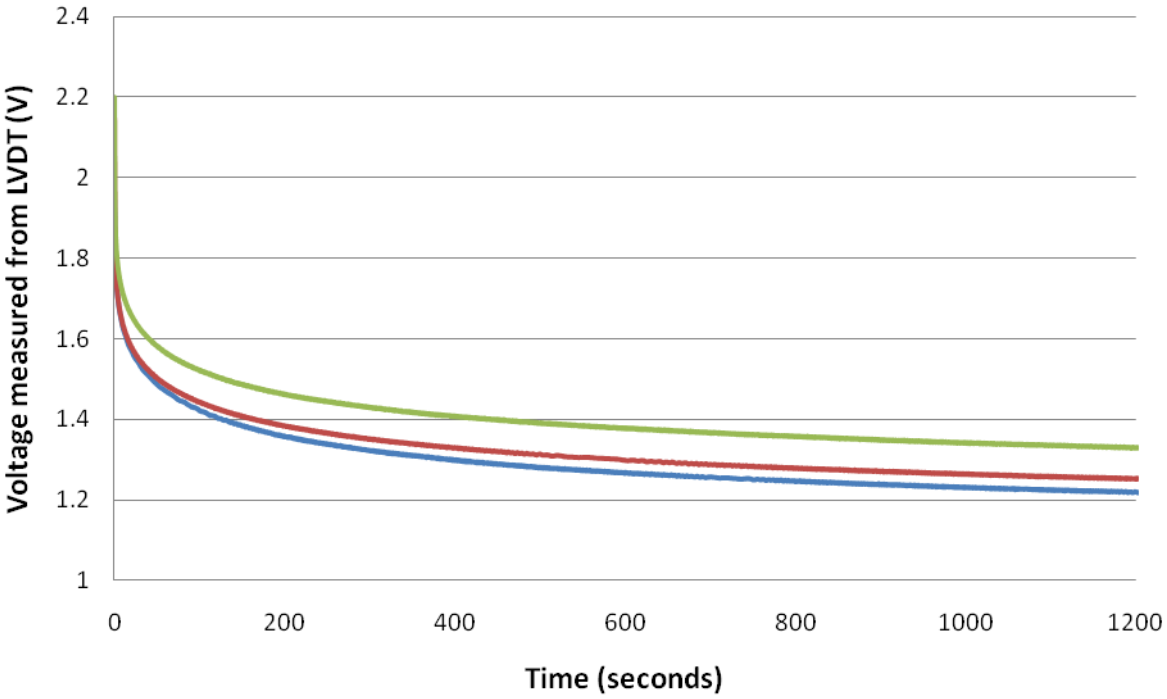

Figure 5-19. Example of LVDT raw signal

Figure 5-20. Temperature control chamber (Photo courtesy of Qiang Li)

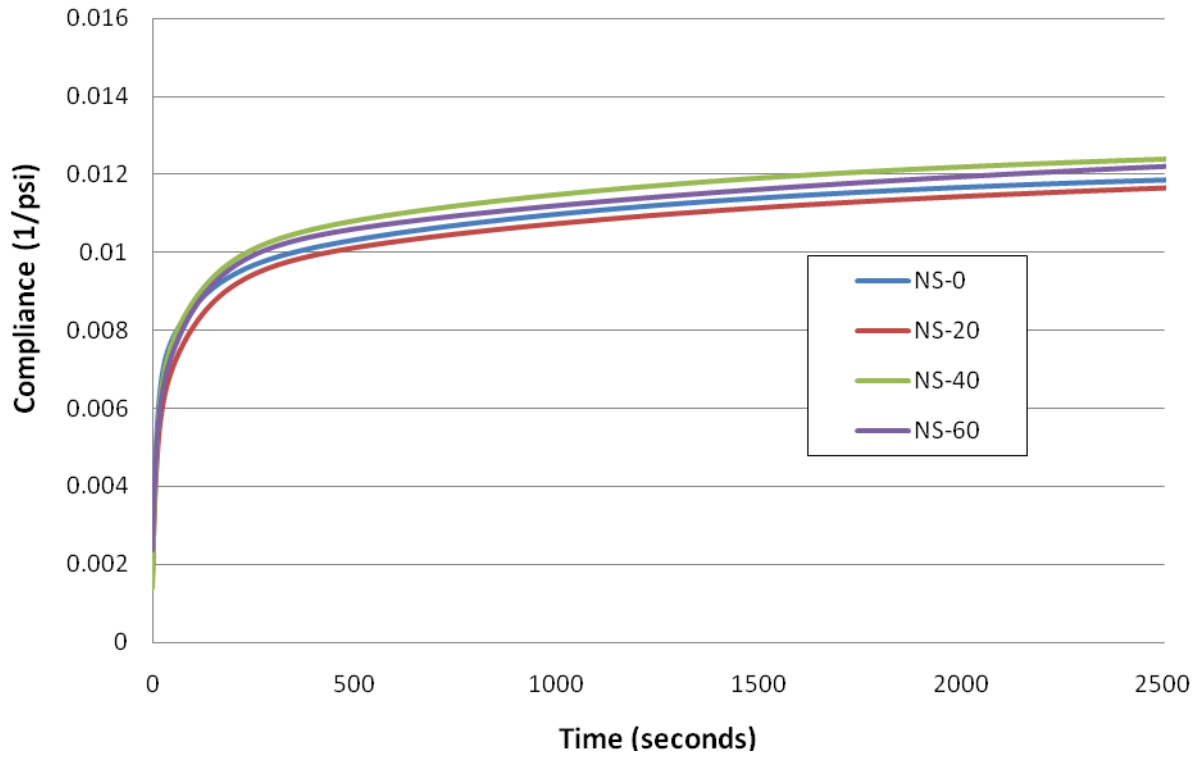

Figure 5-21. Temperature sensitivity results for non-self-leveling sealant

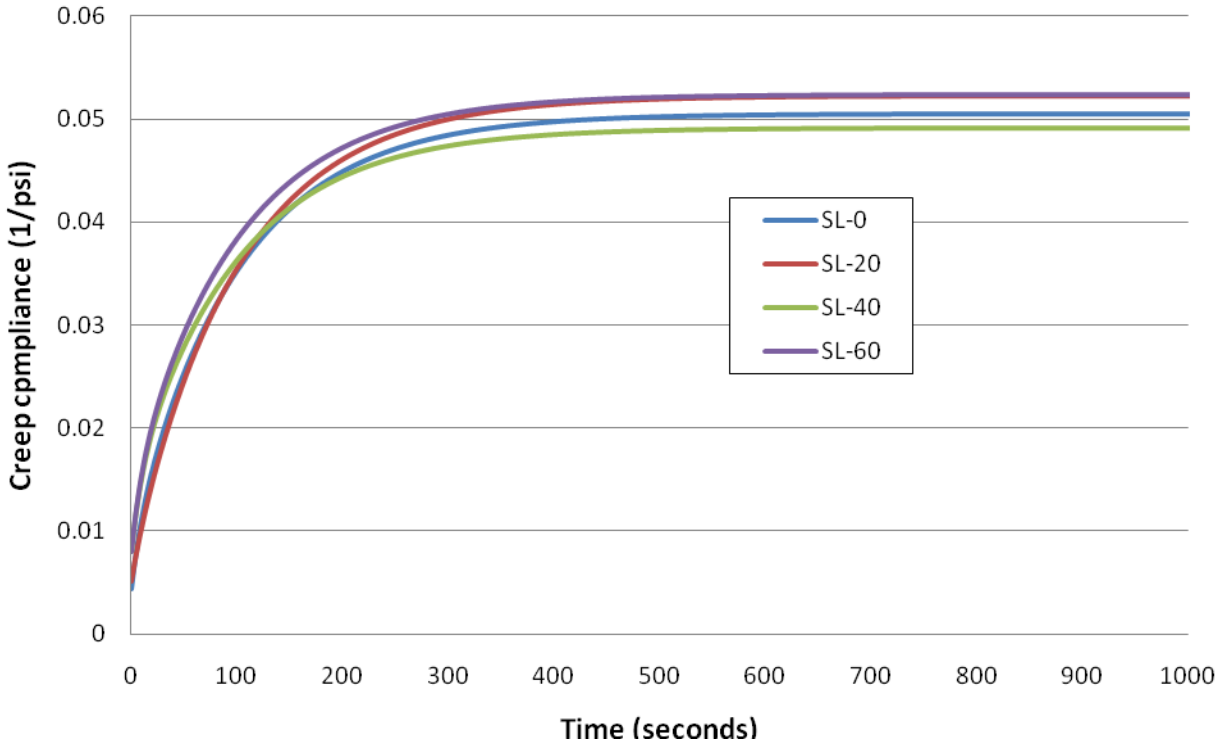

Figure 5-22. Temperature sensitivity results for self-leveling sealant

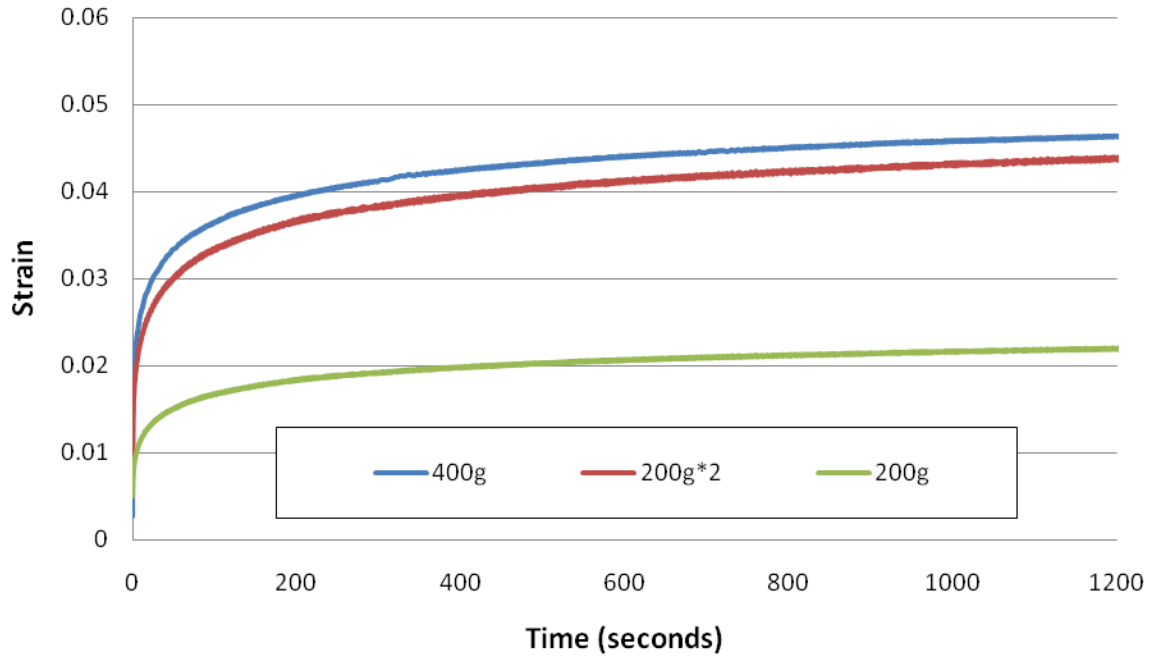

Figure 5-23. Proportionality test results for non-self-leveling sealant

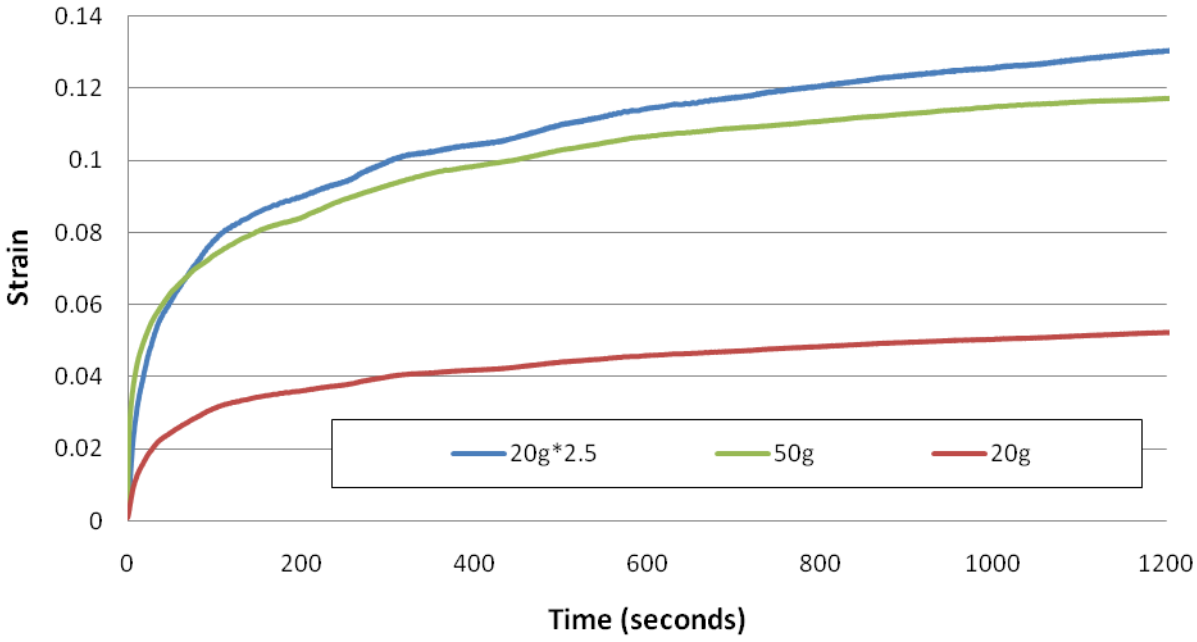

Figure 5-24. Proportionality test results for self-leveling sealant

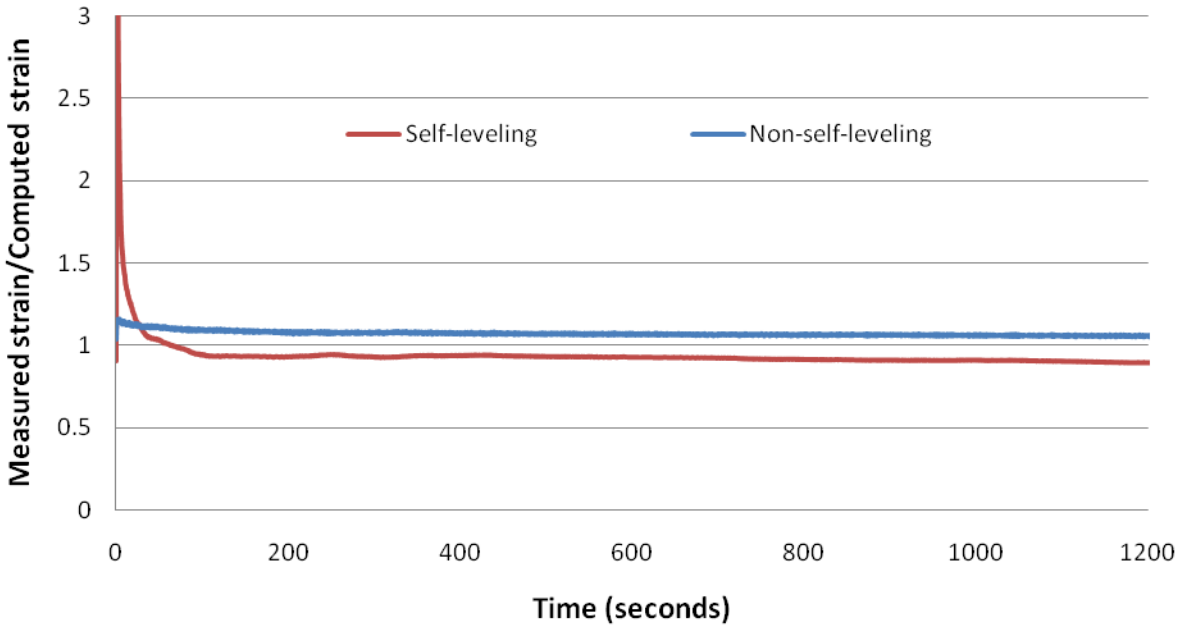

Figure 5-25. Strain ratio of proportionality test

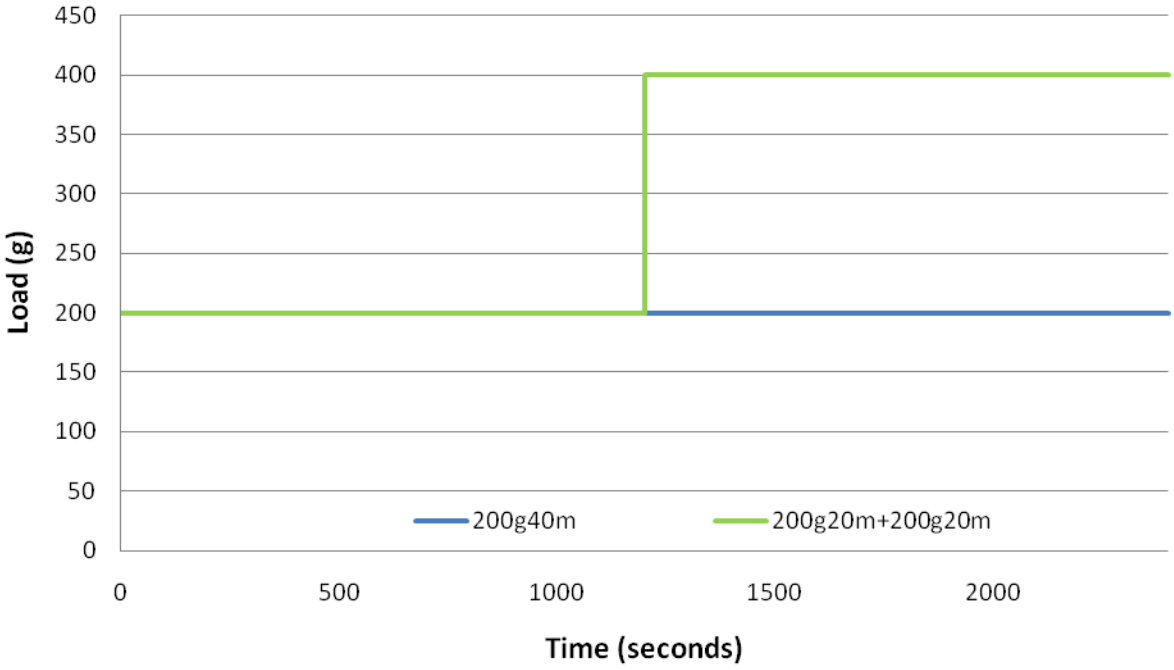

Figure 5-26. Constant load applied to non-self-leveling specimen

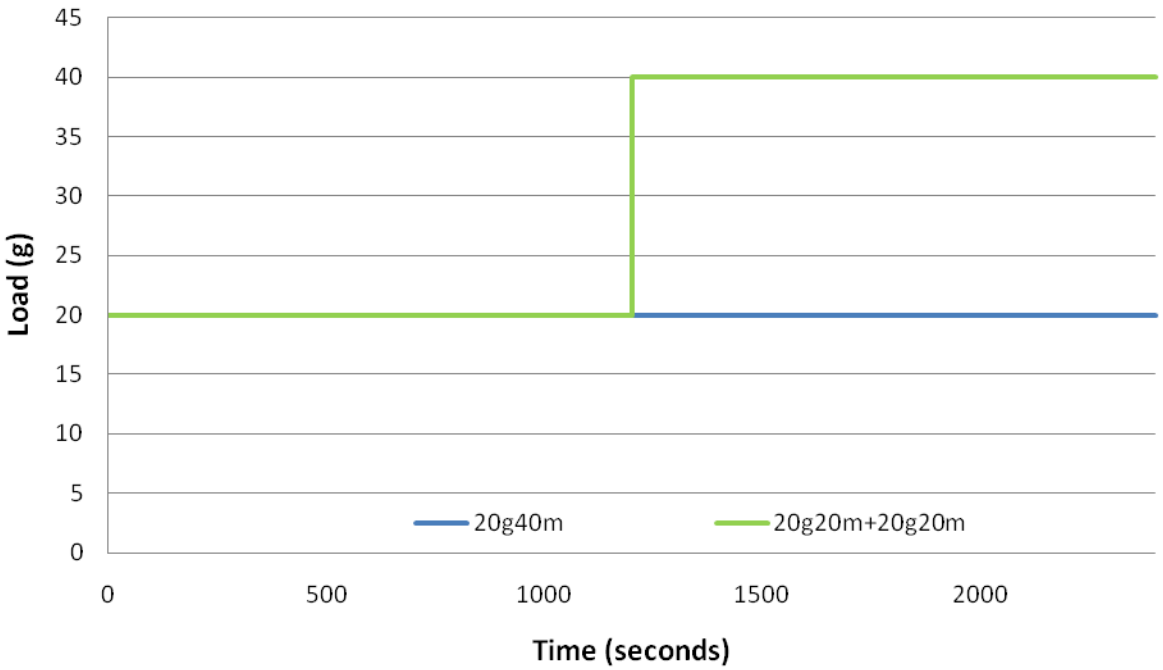

Figure 5-27. Constant load applied to self-leveling specimen

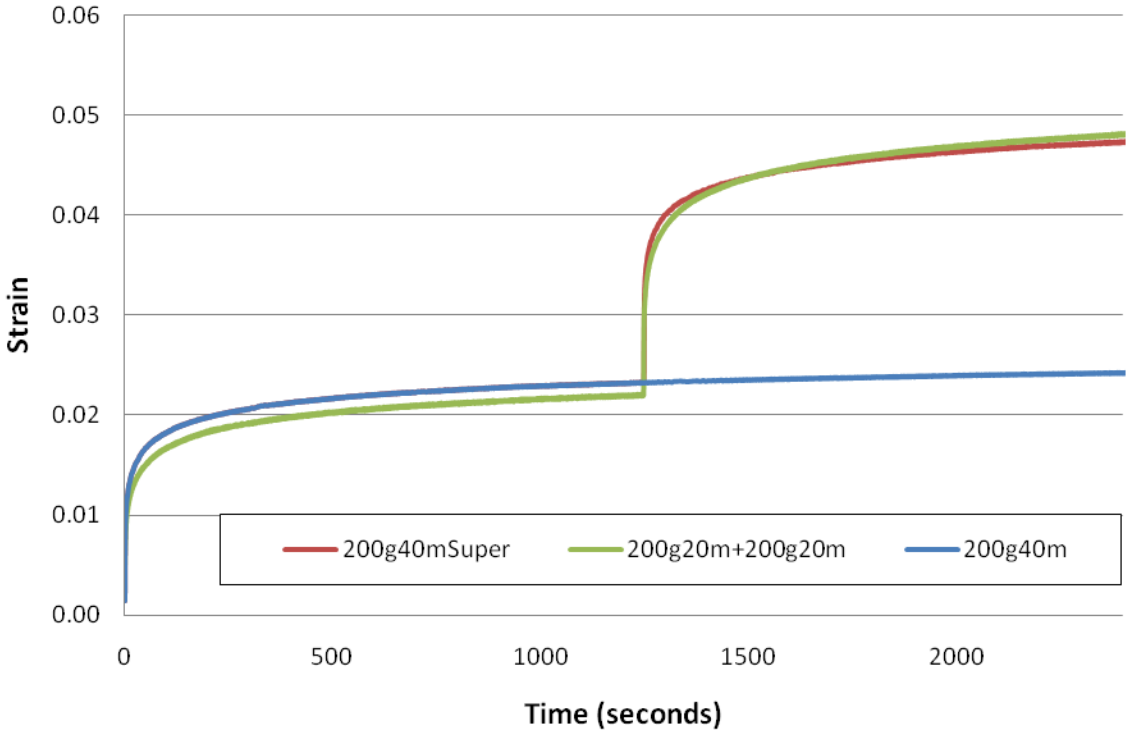

Fiugre 5-28. Superposition test for non-self-leveling sealant.

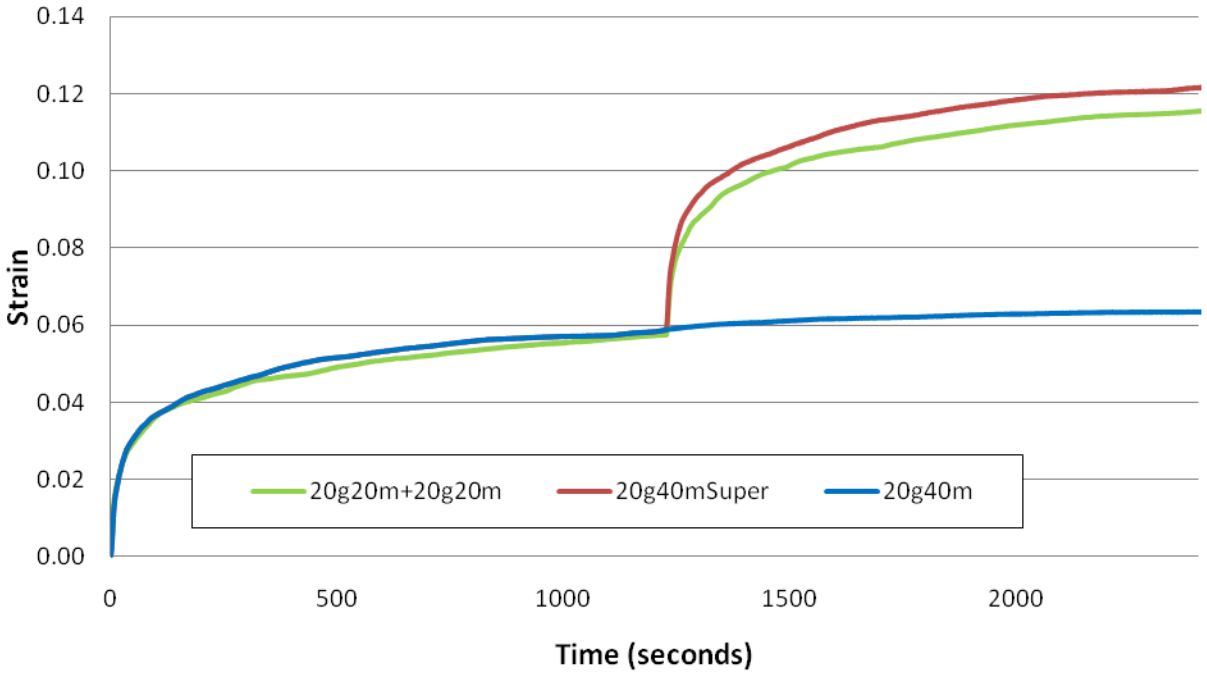

Fiugre 5-29. Superposition test for self-leveling sealant.

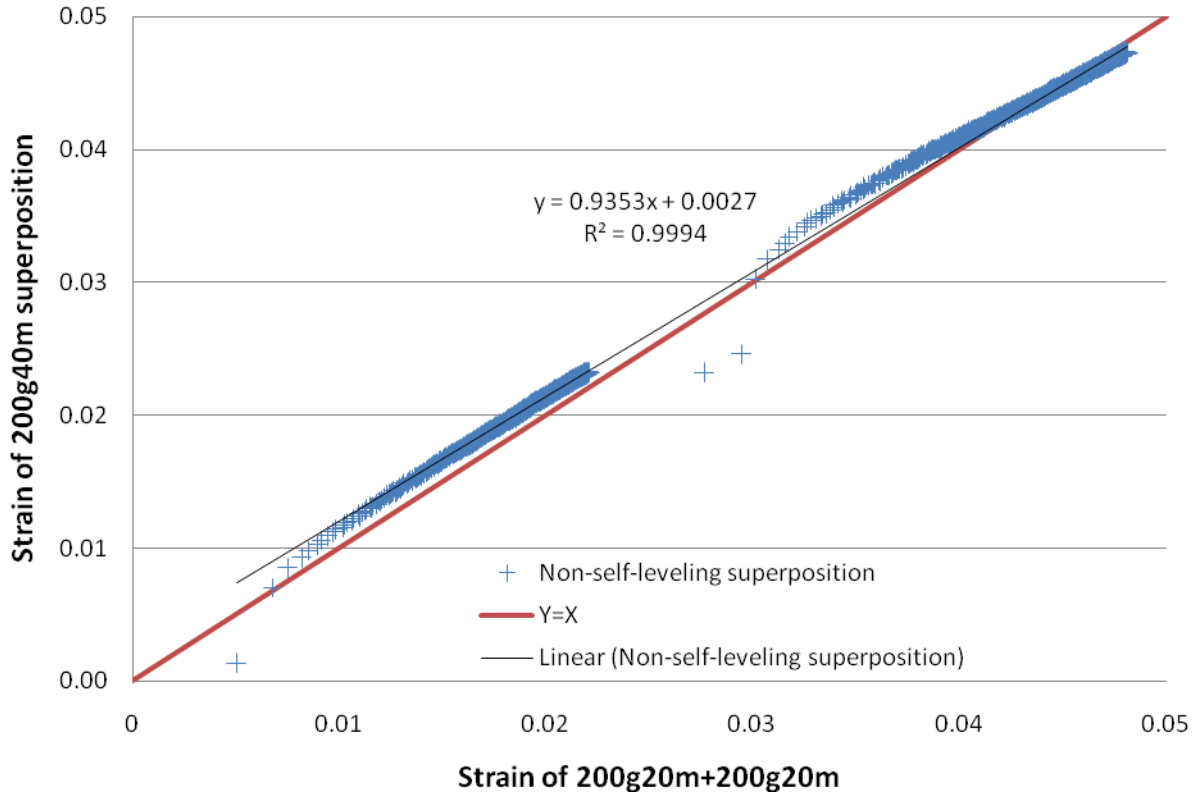

Fiugre 5-30. Superposition test for non-self-leveling sealant.

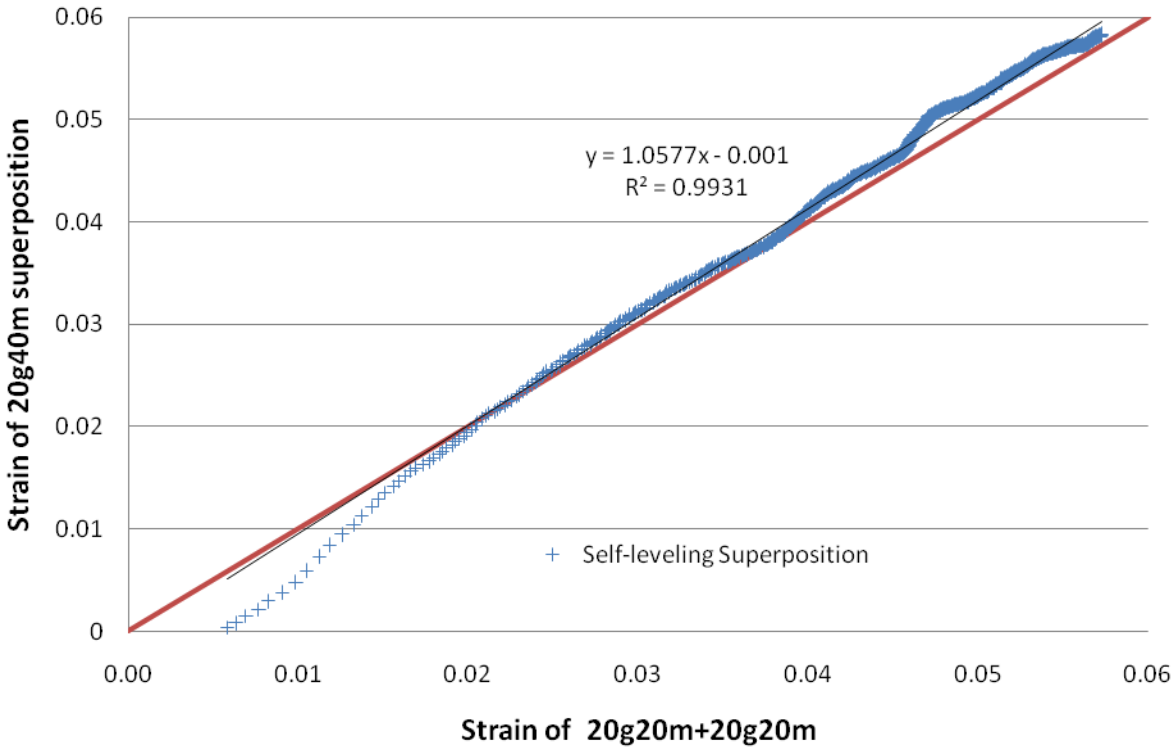

Fiugre 5-31. Superposition test for self-leveling sealant.

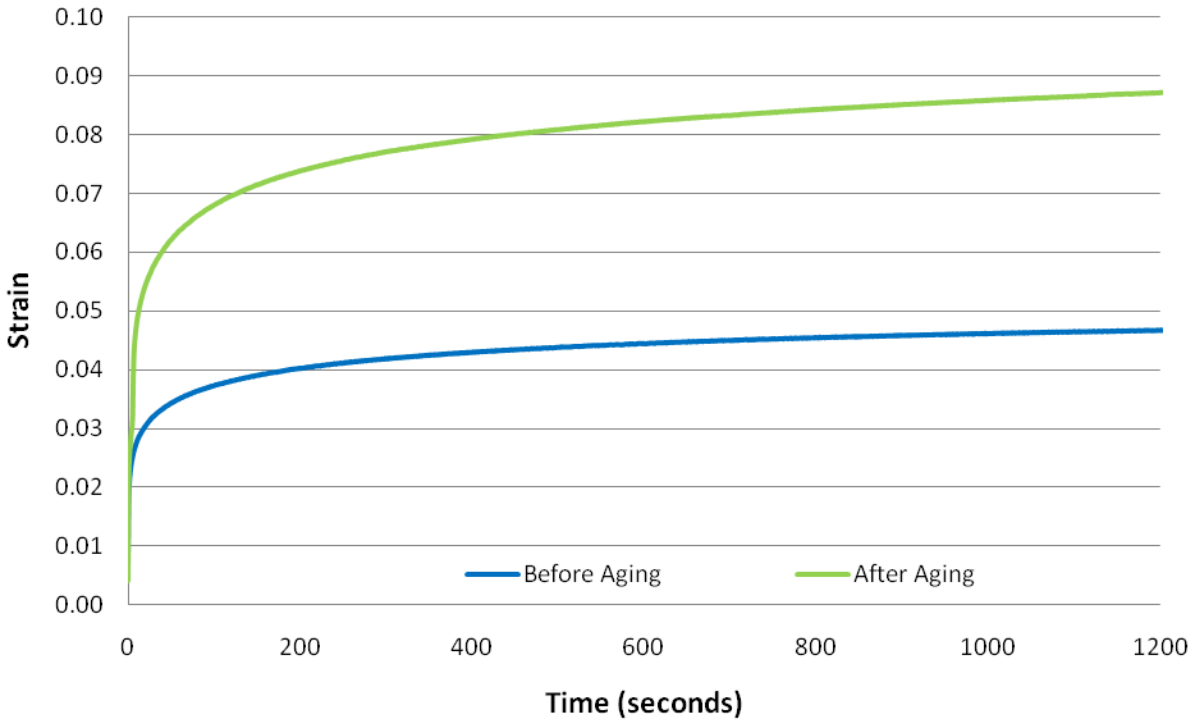

Figure 5-32. Non-self-leveling silicone sealant water aging

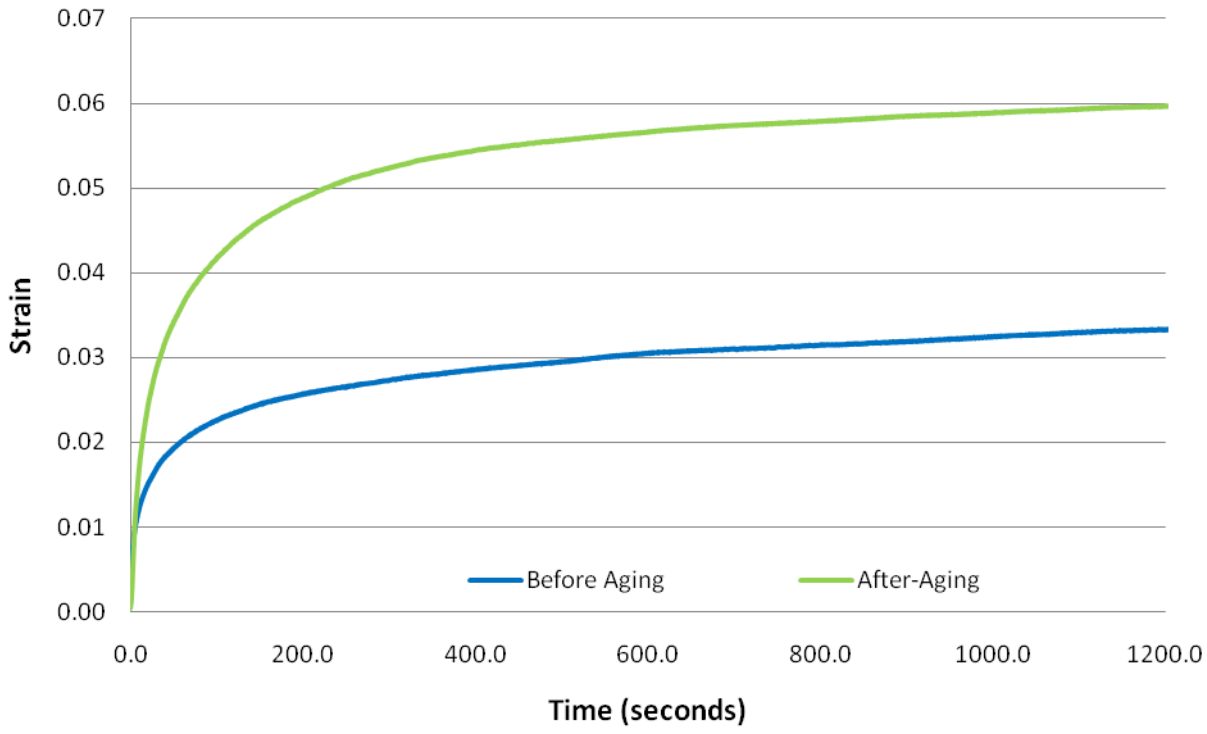

Figure 5-33. Self-leveling silicone sealant water aging

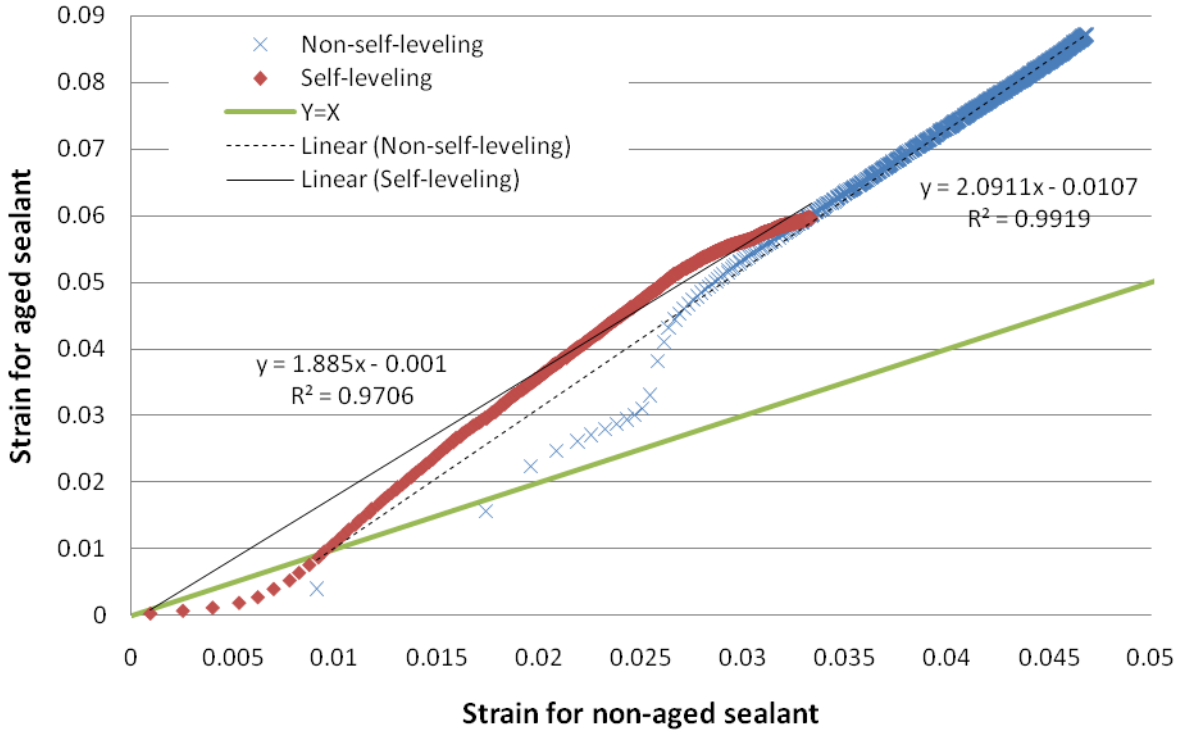

Figure 5-34. Hot water aging non-dimensional results

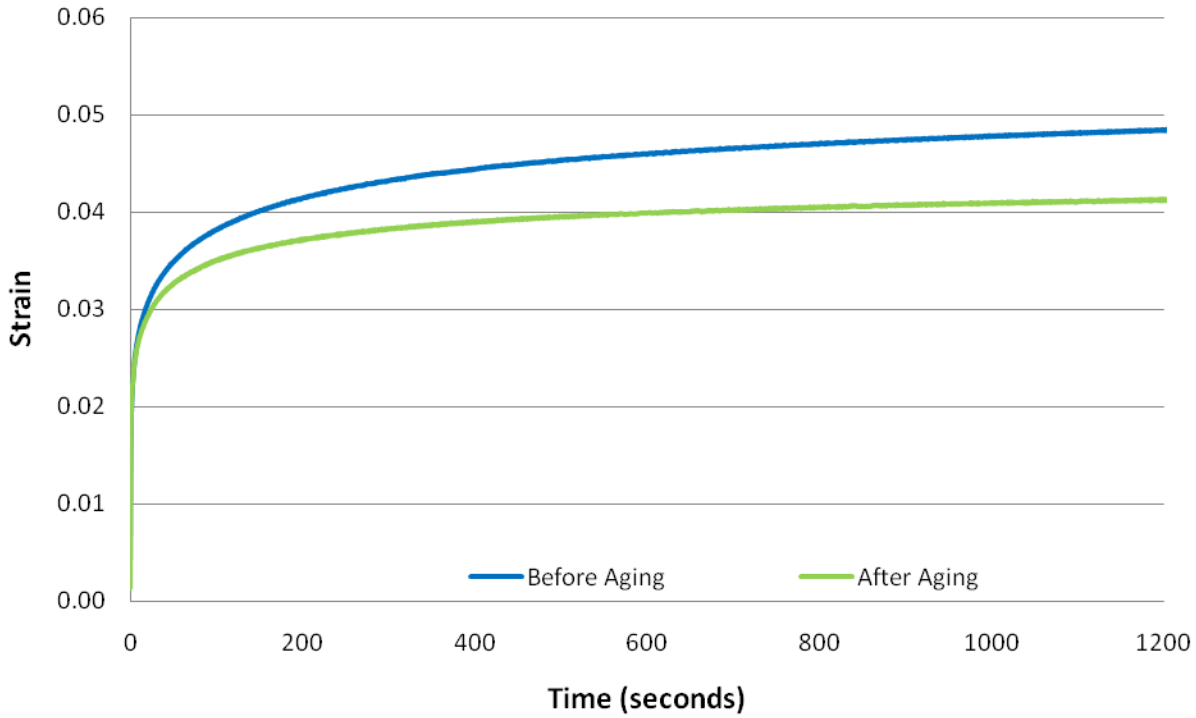

Figure 5-35. Non-self-leveling silicone sealant oven aging

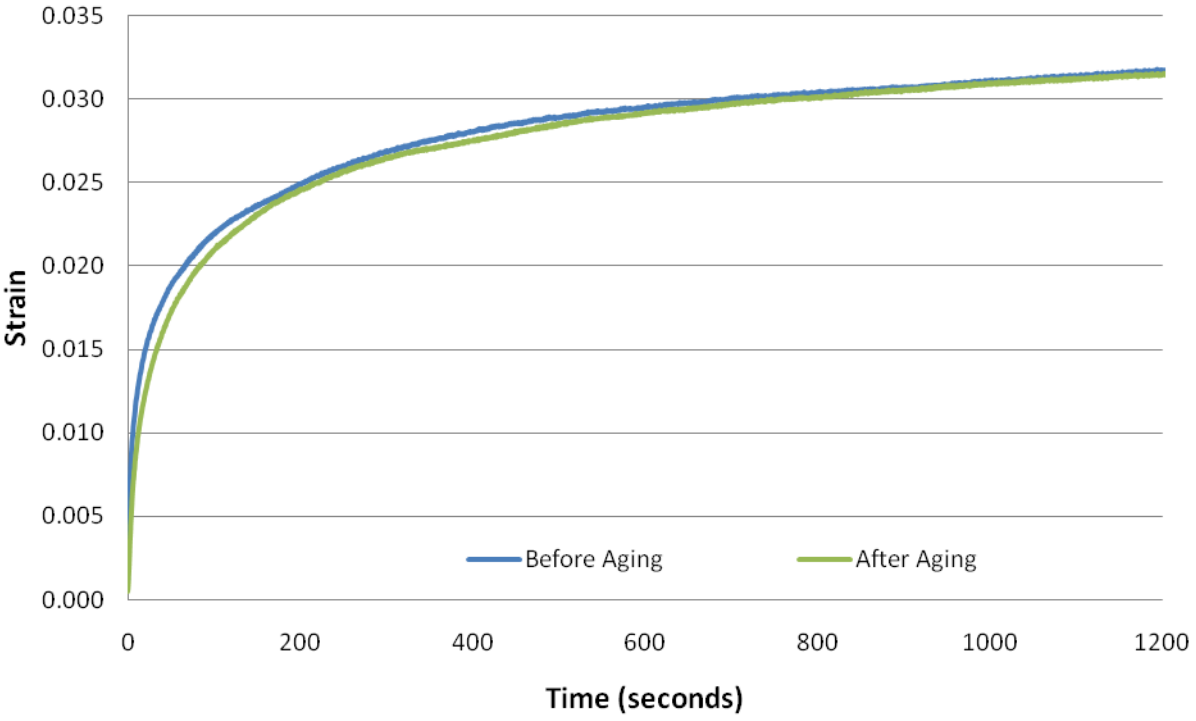

Figure 5-36. Self-leveling silicone sealant oven aging

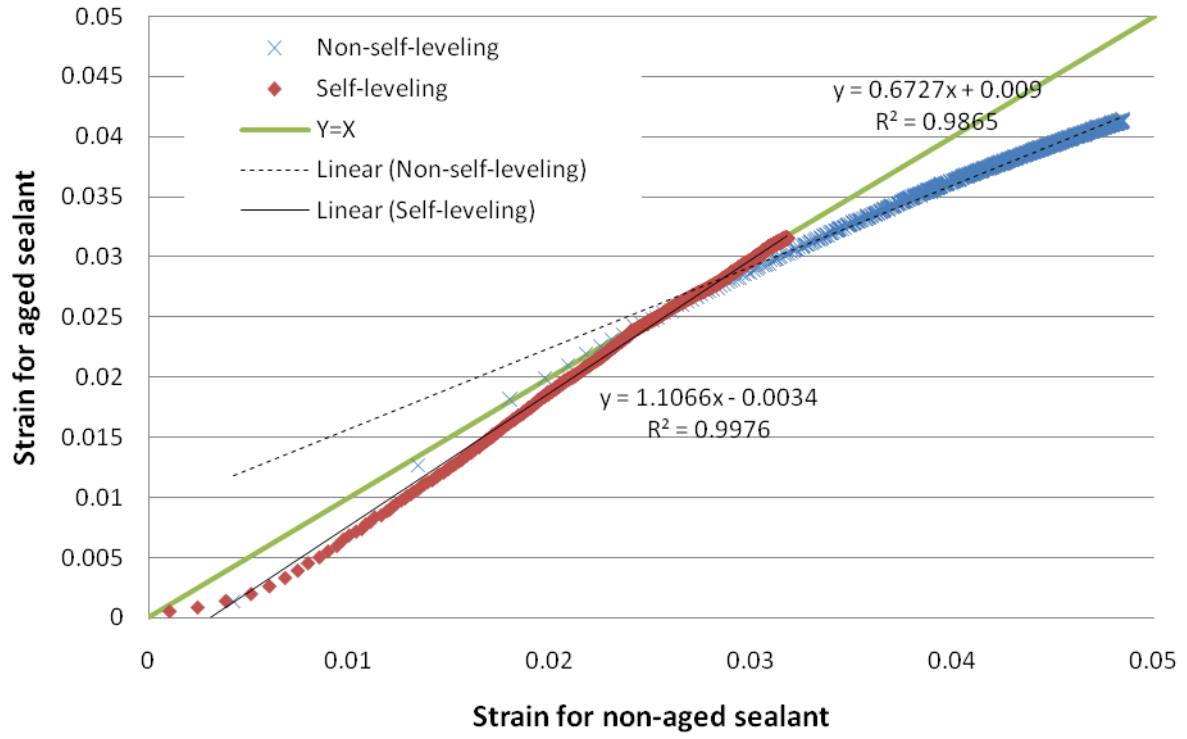

Figure 5-37. Non-dimensional oven-aging data

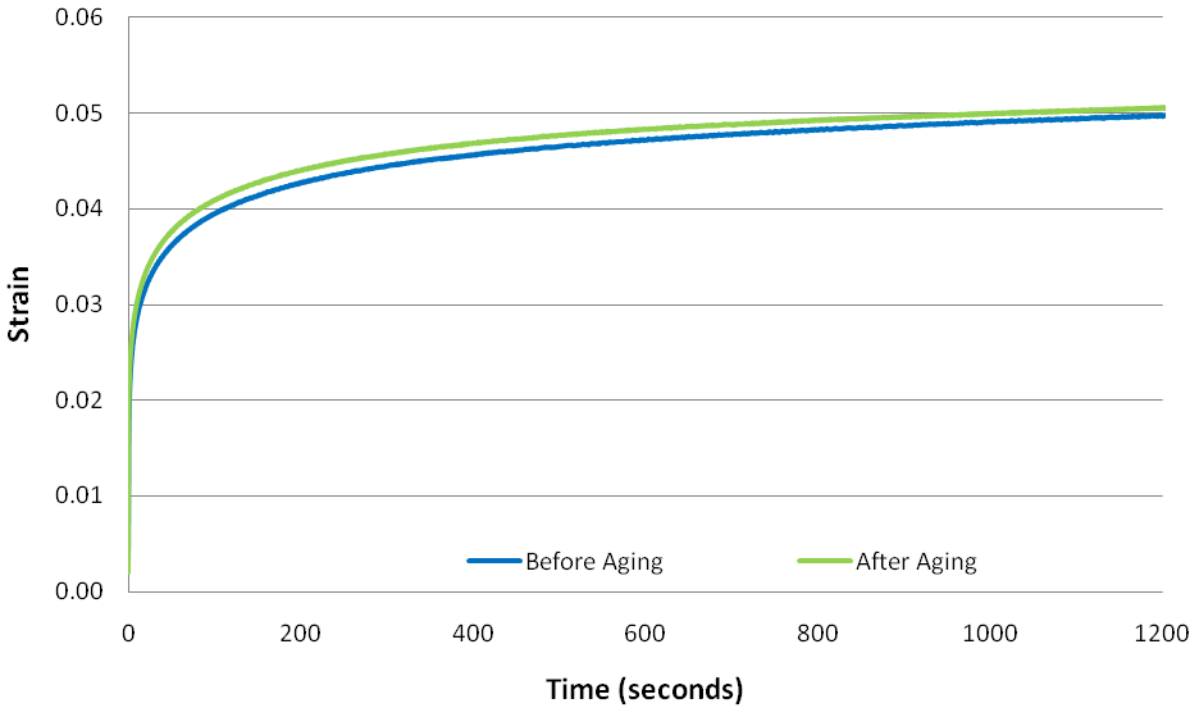

Figure 5-38. Non-self-leveling silicone sealant freeze-thaw results

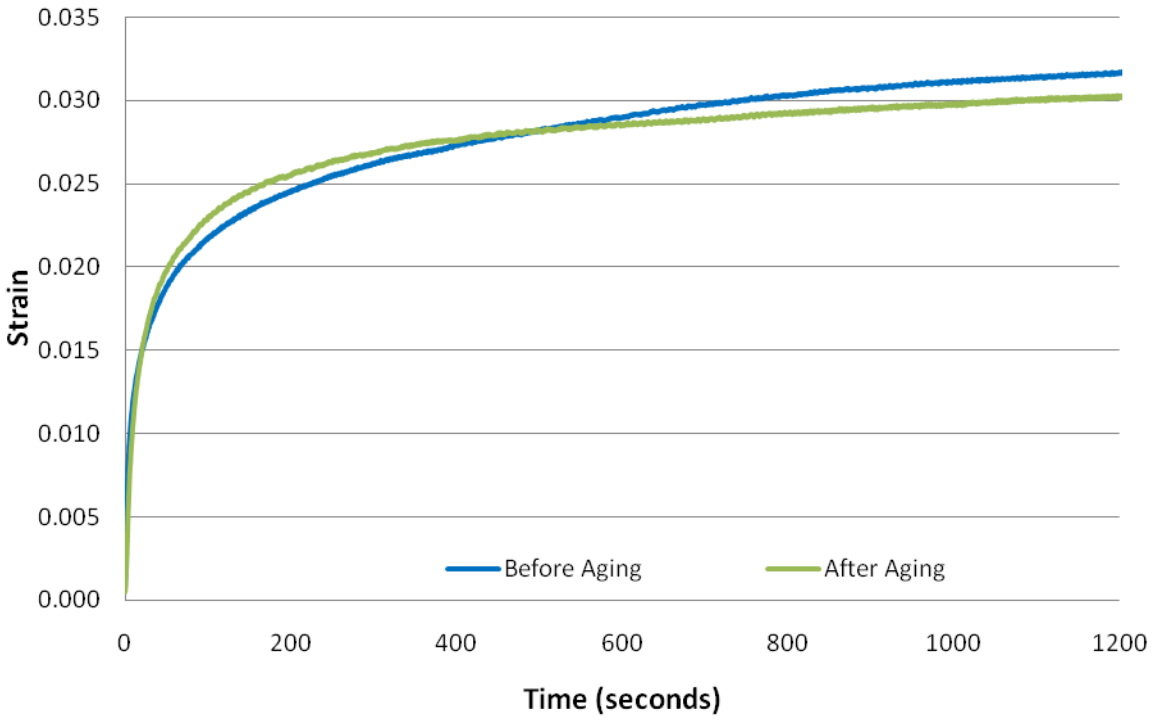

Figure 5-39. Self-leveling silicone sealant freeze-thaw results

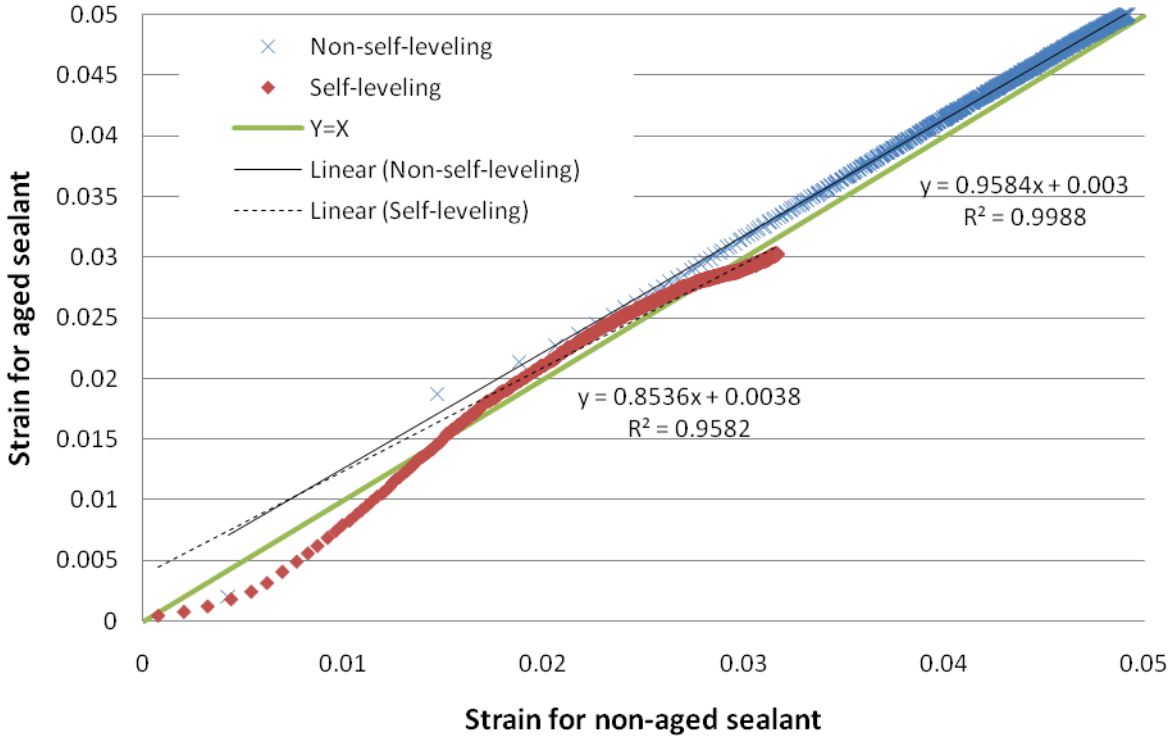

Figure 5-40. Self-leveling silicone sealant freeze-thaw results

CHAPTER 6
ADHESIVE STRENGTH TEST FOR SILICONE SEALANT

As discussed in Chapter 2, adhesive bonding between concrete and sealant is a significant factor that must be taken into account when transverse joints are cut into a concrete roadway. Because reliable tests did not yet exist for evaluating this property, a new laboratory testing method was developed to quantify adhesive strength. As discussed in Chapter 2, surface moisture, roughness, and cleanliness of concrete joint cuts may affect adhesive bonding strength. Therefore, this testing method focused on determining the effects of these variables.

Sample Preparation

Before tests could be initiated, a series of concrete-sealant samples was created. Sample preparation can be divided into four stages:

- Concrete blocks were cut and cast.
- Block surfaces were prepared.
- Teflon film was adhered to the concrete blocks.
- Silicone sealant was poured and allowed to cure.

This section will describe each stage in detail.

Casting and Cutting Concrete Blocks

Concrete was prepared in accordance with Florida Department of Transportation's (FDOT) standard specification for road and bridge construction (FDOT 2007a). Concrete aggregate (6% air entrainment) and Type I Portland Cement were used. The initial water-cement ratio of the concrete slurry was 0.45. Concrete was poured into a 4.0 in. × 4.0 in. × 12.0 in. mold and allowed to cure for 28 days. Once concrete had cured, the 12.0 in. concrete block was cut into 2.0 in. × 1.5 in. × 0.5 in. pieces using a concrete saw. Cutting debris was collected for future use.

Concrete Surface Preparation

Because one of the purposes of this study was to evaluate the effects of surface conditions on adhesive strength, several surface preparation techniques were used. For the “cleanliness test” and the “roughness test,” concrete surfaces were dirtied via particle addition and roughened via sand blasting respectively. For the “moisture test” and the “aging test,” sand blasting was omitted.

Teflon Film

To ensure that only the sealant test-section would adhere to the concrete blocks, thin Teflon film (0.01325 in.) was prepared. First, the film was cut to the block’s dimensions (2.0 in. by 1.5 in.). Then, 1.0 in. holes were drilled through the film’s center. Finally, these film sheets were glued to half of the concrete blocks using 3M Scotch-Weld Super Glues CA5 (Figure 6-1).

Casting Silicone Sealant

Once the Teflon film had been applied, a 1.0 in. diameter sealant section was poured into the hole in the Teflon film. Several sealant thicknesses were used during testing to find a suitable standard, although ultimately a 0.01325 in. standard was employed. A block without attached Teflon was placed on top of the block with attached Teflon and sealant such that the two blocks adhered to one another. The two blocks were clamped together and allowed to cure for 21 days.

Adhesive Strength Testing

Generally, an adhesive strength test involves applying a tensile force to two adhered materials until adhesive failure occurs. In the case of sealant-concrete block interaction, the goal is to pull the concrete blocks away from one another. While both cohesive and adhesive failures are possible with such a test, as discussed in Chapter 2,

adhesive failure was expected to be more common, as was born out by experiment. The following is a description of testing procedures used for the silicone-concrete block samples in this test.

The Adhesive Strength Testing Apparatus (ADHESTA)

To apply tensile forces to the sealant-concrete block samples, a new apparatus was developed – The Adhesive Strength Testing Apparatus, or ADHESTA (Figure 6-2). Loctite E-05CL was used to glue the samples to each half of the ADHESTA "wings." Next, the sample (with attached wings) was placed in a special mold (Figure 6-3) to ensure that the wings' loading holes remained aligned along the same plane (Figure 6-4). Once the Loctite had dried (24 hours per manufacturer specifications), the sample was removed from its mold. Each of the ADHESTA's wings was attached to an MTS Model 810 tensile strength tester (Figure 6-5) and tensile forces were applied to the sample. Force and deformation were recorded as a function of time.

Adhesives Strength Test Data

Typical test results of non-self-leveling and self-leveling sealant adhesive strength are presented in Figure 6-6. As implied in Chapter 5, non-self-leveling sealants are stiffer than self-leveling sealants. Therefore, generally, non-self-leveling sealants tend to fail at relatively lower strains than self-leveling sealants.

While stress and strain are continuously recorded during an adhesive strength test, a few important benchmarks must be highlighted. Maximum load, F_M is used to calculate adhesive strength:

$$AS = \frac{F_M}{A} \tag{6-1}$$

where *AS* is adhesive strength and *A* is the contact area between the sample and concrete (0.785 sq. in.). Adhesive failure energy (AFE), which is defined as the area under a loading curve (Figure 6-6) is a measurement of the amount of energy used to initiate failure.

Adhesive Strength Testing Parameters

Several factors were shown to influence results from adhesive strength tests:

- Sealant thickness
- Tension strain rate
- Curing time

The following is a discussion of these variables, and a rationale for why the standards presented were chosen.

Sealant thickness

Sealant thickness is important because of "necking" during testing. Thicker sealant sections may stretch significantly as they deform. This means that the samples' cross-sectional areas may change –which would lead to incorrectly computed stresses. Thinner samples may not "neck" or stretch significantly, but thinner samples are more difficult to prepare. Therefore, the goal of this series of tests was to find the maximum sealant thickness that provides nearly-constant data for both self-leveling and non-self-leveling samples.

Six sealant thicknesses (0.015in±0.002in, 0.02in±0.002in, 1/32in±0.003in, 1/16in±0.004in, 3/32in±0.005in and 1/8in±0.007in) were tested. All samples were allowed to cure for 21 days prior to testing. All tests were conducted at 20 degrees Celsius. A strain rate of 400 mm/min was used during all tests. Each test was repeated three times, and averages were computed. Figure 6-7 and Figure 6-8 show the reuslts

Figure 6-7 indicates that that 3/32 in. is a “critical thickness” for non- self-leveling sealant. Above this point, adhesive strength appears to rapidly decrease while below this point, results remain nearly constant. Qualitatively, investigators noticed “necking” during the 1/8 in test but not during the 3/32 in test. This would indicate that sealant thicknesses less than 3/32 in. are appropriate for testing non-self-leveling sealant.

Figure 6-8 appears to indicate that 1/32in may be defined as the “critical thickness” for self-leveling sealants. SL sealant thicker than 1/32 in. appears to exhibit increasingly weaker adhesive strength while SL sealant thinner than 1/32 in. exhibits nearly constant adhesive strength. This suggests that sealant thicknesses less than 1/32 in are a suitable standard for self-leveling sealant testing. Because the goal was to find a standardized “upper limit” for both tests, the more stringent limit (1/32 in) was chosen for both self-leveling and non-self-leveling tests.

Strain rate

Because sealant is a viscoelastic material, applied strain rate may significantly influence recorded adhesive strength test results. A series of tension strain-rate tests was conducted to determine sealant’s adhesives strength sensitivity to variable strain rates. Four different strain rates were used during this test series (50 mm/min, 200 mm/min, 400 mm/min, and 800 mm/min). Tests were conducted on both self-leveling and non-self-leveling sealant. Each test was repeated three times, and results were averaged. Results are shown in Figure 6-9 and Figure 6-10.

Figure 6-9 indicates that strain rate has minimal effect on adhesive strength readings for non-self-leveling sealant. Figure 6-10, on the other hand, implies that strain rate may have a significant effect for self-leveling sealant when lower strain rates are applied to the material. For self-leveling sealant, the adhesive strength results for

200 mm/min, 400 mm/min, and 800 mm/min are similar. When strain rate is reduced to 100 mm/min, measured adhesive strength appears to decrease. This decrease in measured adhesive strength may be because self-leveling sealant is much softer than non-self-leveling sealant. As such, stress may be "released" when loaded more slowly.

The goal of this test was to identify a strain-rate standard. This test suggests that strain rates between 200 mm/min and 800 mm/min are appropriate for both tests. Therefore, 400 mm/min was selected as the standard strain rate.

Cure time

All aforementioned sealant samples were cured for 21 days in accordance with ASTM (ASTM 2006b). However, investigators hypothesized that cure time may be dependent on sealant volume. Because a relatively small quantity of sealant was used during these tests, investigators sought to determine whether or not they could reduce the amount of required cure time.

To this end, a series of samples was cured for 1 day, 3 days, 5 days, 7 days, and 21 days. Adhesive strength tests were conducted on both self-leveling and non-self-leveling samples at 20 degrees Celsius. Each test was repeated three times, and results were averaged. The results are shown Figure 6-11 and Figure 6-12.

Figures 6-11 suggests that after one day of curing, the non-self-leveling samples gain nearly 85% of their 21 day adhesive strength. After five days, the sample appears to be fully cured. Figure 6-12 indicates that self-leveling sealant may be fully cured in as little as 7 days. This implies that in the future, the standard for these adhesive strength tests may be modified such that samples will only be required to be cured for 7 days.

Adhesive Strength Testing Results

After determining appropriate standard conditions for testing procedures as described above, a series of tests was administered to investigate the effects of moisture, roughness, and aging on sealant-concrete adhesive strength. Standards developed were used to administer all tests. While previously described results indicate that a 7-day cure time may be acceptable, cure time was held at 21 days to maintain consistency with ASTM.

Moisture Effects on Adhesive Strength

When joints are prepared in the field, the joints must be cleaned using pressurized water prior to sealant installation. If joints are not given sufficient time to dry, retained water may prevent sealant from properly bonding to its concrete joint surface. A series of tests was conducted to quantify the effect of water on adhesive strength. Because one of the goals of this study was to evaluate the effectiveness of a 3/8 in. joint compared to the effectiveness of a 1/8 in. joint, a test was conducted to quantify the evaporation rate within each of these joints. Investigators hypothesized that 1/8 in. joints may dry more slowly than 3/8 in. joints because there is less surface area in a 1/8 in. joint on which water can evaporate. This section discusses these tests in detail.

Wet and dry adhesive strength tests

During these tests, four sample recipes were studied:

- "Dry-dry" samples. Samples were prepared such that both concrete surfaces were dry. Then, the sample was allowed to cure for 21 days in a desiccator.
- "Dry-wet" samples. Samples were prepared such that both concrete surfaces were dry. The samples were allowed to cure for 24 hours and then submerged for 21 days.
- "Wet-dry" samples. Samples were prepared such that concrete was submerged in water for 24 hours. Samples were cleaned with a wet towel such that all debris

was removed from their surfaces. Then, sealant was applied to the wet surface and allowed to cure for 21 days in a desiccator.

- "Wet-wet" samples. Samples were prepared such that concrete was submerged for 24 hours. Samples were cleaned with a wet towel such that all debris was removed from their surfaces. Then, sealant was applied to the wet surface and allowed to cure for 24 hours. After 24 hours, the sample was submerged for 21 days.

Each test was repeated three times, and results were averaged. Data is presented in Figure 6-13 and Figure 6-14. These figures suggest that both self-leveling and non-self-leveling sealant samples are highly dependent on the presence of water. Generally, as water exposure increases, adhesive strength decreases. Results were the most significant during wet-wet tests. Both self-leveling and non-self-leveling sealant under wet-wet conditions was only approximately 25% as strong as similar sealant under dry-dry conditions.

Evaporation rates of 1/8 inch joint vs. 3/8 inch joints

In the previous section, adhesive strength tests were conducted on saturated and dry concrete surfaces. It was found that moisture has a significant effect on sealant adhesive strength. To investigate the moisture effect on adhesive strength, the surface moisture was quantified using a Delmhorst BD-2100 moisture meter (Figure 6-15) and a new series of tests was conducted. This device uses three scales.

- Wood Scale; 6% to 40% moisture range. This scale is used for flooring and building material such as wood studs, floor joists, and subfloors.
- Reference Scale; reads from of 0 to 100 on a relative basis. This scale is used on non-wood materials such as concrete, plaster, and insulation.
- Gypsum Scale; 0.2%-50% moisture range. This scale is used on drywall.

Since the reference scale is suitable for concrete surfaces, it was used for this investigation. The first objective of this test was to calibrate the moisture meter for use

with concrete. Six half-samples (1.5 in by 2.0 in by 0.5 in) were soaked for 24 hours to ensure saturation. Six different relative moisture tests were run at random locations on the six samples' surfaces (Table 6-1) and an average was computed. This number, 73.5, was denoted as the "saturation point." Six other half-samples were placed into an oven for one hour to ensure that they were nearly completely dry. These samples' moisture content was also tested at 6 different locations per sample. Because all samples read 0.00, the "zero-point" was said to be 0.00. Linear interpolation was used to develop Table 6-2 such that readings from the reference scale could be correlated to relative concrete surface moisture.

Once the instrument had been calibrated, the second phase of testing involved comparing evaporation rates for 1/8" vs. 3/8" joints. One joint of each dimension was prepared and cleaned with pressurized water. Six probes were inserted into the joint to measure water content and averages were computed. Temperature during testing was 20 degrees Celsius and the ambient air's relative humidity was 58%. Data was collected for 10 hours. Results were plotted in Figure 6-16.

The results indicate that evaporation is much slower for a 1/8 in. joint. At first, both joints were completely saturated, but 1/8 in. joint evaporation with respect to 3/8 in. joint evaporation became increasingly slower with respect to time. Thus, investigators' hypothesis appears to be correct – a reduction in surface area appears to reduce evaporation rate significantly. As shown, moisture appears to affect silicone's adhesive strength significantly. Therefore, in the field, contractors would be required to wait longer after pressure cleaning to install sealant for a 1/8 in. joint. This longer wait time

implies that there will be more opportunity for debris to enter the joint – which may reduce adhesive strength.

Critical concrete surface moisture

Investigators hypothesized that there may be a "critical surface moisture condition" for sealant-concrete interaction. Below this critical point surface moisture would not significantly affect adhesive strength. Above this critical point, adhesive strength would be reduced significantly. To test this hypothesis, a series of tests was conducted. Based on the calibration curve developed in Table 6-2, four water contents were selected (20%, 60%, 80%, and 100%). Samples were submerged for 24 hours to ensure saturation, and then dried to the appropriate surface moisture levels. Once moisture level reached the specified value, silicone was applied to the concrete, and the sample was allowed to cure for 21 days. During curing, ambient air conditions were fixed at 58% relative humidity and 20 degrees Celsius. Once cured, adhesive strength was tested for each sample. Both self-leveling and non-self-leveling samples were prepared and tested using this technique. Each test was repeated three times. Results were plotted (Figure 6-17 and Figure 6-18).

Results suggest that adhesive strength reduces significantly for moisture levels above 80% saturation. From 0% to 60% saturation, adhesive strength appears to be minimally affected. Accordingly, 80% surface moisture appears to be the critical value for concrete-sealant interaction. This result is interesting when compared with Figure 6-19. According to Figure 6-16b, 1/8 in. concrete joints should reach 80% moisture after four hours. Conversely, 3/8 in. joints appear to reach 80% moisture after only 30 minutes. Two scenarios are possible if a 1/8 inch joint is used. First, sealant may be prematurely installed. As discussed, this would likely reduce adhesive strength and

lead to frequent adhesive failures. Secondly, contractors could wait four hours before installing sealant, but this wait-time defeats the purpose of installing the smaller joint to begin with. From a sealant-concrete adhesion perspective then (with respect to moisture), there does not appear to be an advantage to using a narrower joint.

Roughness and Cleanliness Effects on Adhesive Strength

A series of tests was conducted to quantify roughness and cleanliness effects on concrete-sealant adhesion.

Sample preparation

A series of samples was prepared using sandblasting to roughen their surfaces. Three different "roughness degrees" were used in this study: low (R0), medium (R1), and high (R2). Low-roughness samples are defined as samples whose saw-cut surfaces were not sandblasted. Medium-roughness samples are defined as samples whose surfaces were sand-blasted at 14.5 psi (100 kPa) and with a volumetric flow rate of 20 cf/min (0.57 m^3/min). High-roughness samples are defined as samples whose surfaces were sand-blasted at 14.5 psi using and with a volumetric flow rate of 100 cf/min (2.83 m^3/min).

During initial sample cutting, debris was collected and dried in an oven at 150 degrees Celsius. This debris was used to create three "cleanliness degrees" for testing: low (D0), medium (D1), and high (D2). Low-debris samples are defined as samples where no debris was added. Medium-debris samples are defined as samples where 0.15g of debris was added to samples' surfaces. High-debris samples are defined as samples where 0.45g was added to the samples' surfaces.

Roughness measurements using the Aggregate Image Measurement System (AIMS)

The University of Florida's Aggregate Image Measurement System (AIMS) was used to quantify surface roughness for each rough and unclean sample. The AIMS (Figure 6-19) is a new tool that provides information about surface geometry of aggregate samples. This surface geometry may be characterized by the properties of the particles comprising the aggregate. In general, the AIMS device specifies three independent particle geometry parameters: form, angularity, and surface texture (Figure 6-20). Form, a first order property, reflects variations in the proportions of a particle. Angularity, a second order property, reflects variations at the corners; that is, variations superimposed on shape. Surface texture is used to describe the surface irregularity at a scale that is too small to affect the overall shape (Eyad A. Masad 2004).

In this study, surface texture was used as the indicator of surface roughness since investigators hypothesized that surface variations would probably be relatively small. The AIMS functions by using high-resolution digital photography to take a photograph of a material's surface. Analysis software, which uses pixelated color differences, is then used to calculate texture index corresponding to the intuitive notion of roughness.

Fifty-six concrete blocks were prepared for AIMS surface roughness testing. Additionally, three grades of sandpaper, P180 (180 μm grit size), P220 (220 μm grit size), and P320 (320 μm grit size) were prepared for AIMS testing to form a basis for roughness comparison. Concrete blocks and sandpaper samples were tested using the AIMS, and a roughness distribution was plotted (Figure 6-21). Results appear to indicate that sample roughnesses reside between P320 and P220 sandpaper. AIMS

testing confirmed that sand blasting effectively roughened the samples' surfaces as designed.

Results and discussion

The three roughness scenarios were combined with the three cleanliness scenarios to yield nine total testing conditions. Each testing condition was conducted for self-leveling and non-self-leveling sealant yielding a total of 18 different tests conditions (Figure 6-22). Each test was conducted three times for a total of 54 tests. Results were plotted (Figure 6-23 and Figure 6-24) such that adhesive strength and adhesive failure energy were compared for each testing condition.

Results appear to indicate that generally, for a given surface condition, non-self-leveling sealant exhibits a greater adhesive strength. As discussed in Chapter 2, two types of joint movement are common with concrete pavement – shear joint movement and horizontal joint movement. Recall that horizontal joint movement is associated with large movement magnitudes. Sealant with greater adhesive strength may resist this movement. Therefore, these test results imply that non-self-leveling sealant may be more resistant to horizontal joint movement than the self-leveling sealant.

To resist relatively high-frequency shear movements, sealants must exhibit high adhesive strength and high levels of adhesive failure energy. This is because repetition of relatively smaller magnitude shear stresses during shear movement can lead to a stress-build-up condition in the sealant. While self-leveling sealant typically exhibits lower adhesive strength for a given roughness when compared to non-self-leveling sealant, adhesive failure energy behaves oppositely. For a given roughness, self-leveling sealant typically implies higher adhesive failure energy when compared with the non-self-leveling sealant variety.

Results show an interesting phenomenon: a rougher surface does not necessarily imply a greater adhesive strength. There are two explanations for this. First, high-level sandblasting damages the concrete's surface and may create localized cracks or failure planes along the surface. Secondly, the rougher surface may be "too rough" for sealant to penetrate completely into the surface's cracks or pits. Air pockets may become trapped between the sealant and concrete surface. The combination of these effects appears to produce stress concentrations during loading. Ultimately, adhesive strength is reduced. This implies that there may be an optimal roughness condition for sealant application. Further research should be conducted to quantify this optimization point.

For self-leveling and non-self-leveling sealant, debris-induction generally reduces adhesive strength. Results also indicate that the debris effect increases as surface roughness increases. This is probably caused by the fact that rougher surfaces will tend to entrain debris more effectively than smoother surfaces. Because of the increase in the number of pits in rougher surfaces, debris has more surface area on which to rest. The sealant is unable to take advantage of the increase in surface area along the sealant-concrete interface, and instead sticks to more-and-more debris. The debris-induction issue seems to be even more significant for self-leveling sealant. This may be due to the fact that self-leveling sealant is less viscous than non-self-leveling sealant when it is poured. The reduction in viscosity implies that self-leveling sealant is capable of "absorbing" more debris into its matrix. The result appears to be a significant adhesive strength reduction.

Aging Effect on Adhesive Strength

As discussed in Chapter 5, aging appears to affect viscoelasticity of silicone sealant during creep. Investigators hypothesized that similar reductions in adhesive

strength and adhesive failure energy may occur for aged sealant. Similarly to Chapter 5, a series of tests was conducted to quantify the effect of hot water aging, oven aging, and freeze-thaw aging.

Sample preparation was similar to methods used in Chapter 5. Samples were prepared in accordance with the specifications discussed in this chapter. Oven-aged samples were placed into an oven at 150 degrees Celsius for seven days. Water-aged samples were submerged in 90 degree Celsius water for seven days after curing. Freeze-thaw samples were subjected to five freeze-thaw cycles in which samples were moved back-and-forth between a freezer at -5 degrees Celsius and a room at 20 degrees Celsius for 24 hours. Once samples were prepared, a series of adhesive strength tests was conducted. Each test was repeated three times for a total of nine tests. Results were recorded and plotted (Figure 6-25 and Figure 6-26).

Results were similar to those of the creep test. For non-self-leveling sealant, oven aging appeared to be insignificant. For self-leveling sealant, however, oven aging reduced adhesive strength. Hot-water aging and freeze-thaw aging both appeared to reduce adhesive strength by a similar ratio for both non-self-leveling and self-leveling samples. The reason for strength-reduction during adhesive tests is similar to that for strength-reduction during creep tests, and thus, this discussion will not be repeated here.

Summary and Conclusions

The following is a summary of adhesive strength testing including important conclusions:

A new device, the Adhesive Strength Testing Apparatus (ADHESTA) was designed and constructed. A series of standardization tests was run so that investigators could develop testing procedures for the new instrument.

A series of tests was conducted with the ADHESTA to determine the adhesive strength of concrete-silicone sealant samples under baseline conditions. Results indicate that non-self-leveling sealant is stronger and more brittle than self-leveling sealant.

A series of tests was conducted with the ADHESTA to determine the adhesive strength of concrete-silicone sealant samples under several initial surface-moisture conditions. Results appear to indicate that a “critical initial moisture level” may be present, such that below this critical value, surface moisture does not significantly affect adhesive strength.

Tests were conducted on 1/8 in. and 3/8 in. joints to determine evaporation rates. Results show that the 1/8 in. joint reaches its critical moisture level eight times more slowly than 3/8 in. joints. This implies that any advantage gained by using the 1/8” in. joint may be negated by the need to wait for the joint’s surface to dry prior to sealant installation.

A series of tests was conducted to study roughness and debris-induction. Results appear to indicate that a “critical roughness level” may exist for concrete-silicone samples such that above a certain roughness, adhesive strength ceases to improve.

A series of tests was conducted to study aging. Results were similar to creep-test results. Oven-aging significantly reduced adhesive strength for self-leveling samples. Non-self-leveling samples, on the other hand, appeared to be largely unaffected by

oven-aging. Hot-water aging and freeze-thaw aging reduced adhesive strengths for both sealant recipes studied in a similar manner.

Table 6-1. Reference scales for saturated concrete surface

Specimens	Reference Scale					
1	74.6	77.5	73.6	74.2	73.2	67.5
2	73.7	72.6	73.2	75.1	72.6	75.1
3	77.0	70.5	74.6	71.6	77.0	76.0
4	72.8	71.0	69.0	75.6	70.0	70.2
5	76.0	77.5	73.2	74.6	72.6	77.0
6	72.3	72.1	73.1	73.2	71.8	75.6

Table 6-2. Reference scales with corresponding concrete surface moisture

Concrete surface moisture	Reference scale
100%	73.5
80%	58.8
60%	44.1
20%	14.7

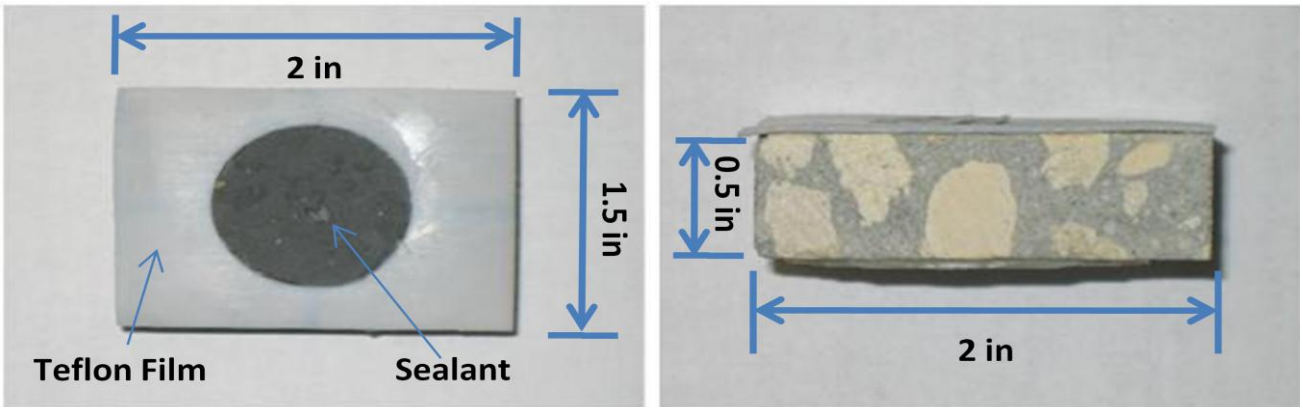

Figure 6-1. Test sample details (Photo courtesy of Qiang Li)

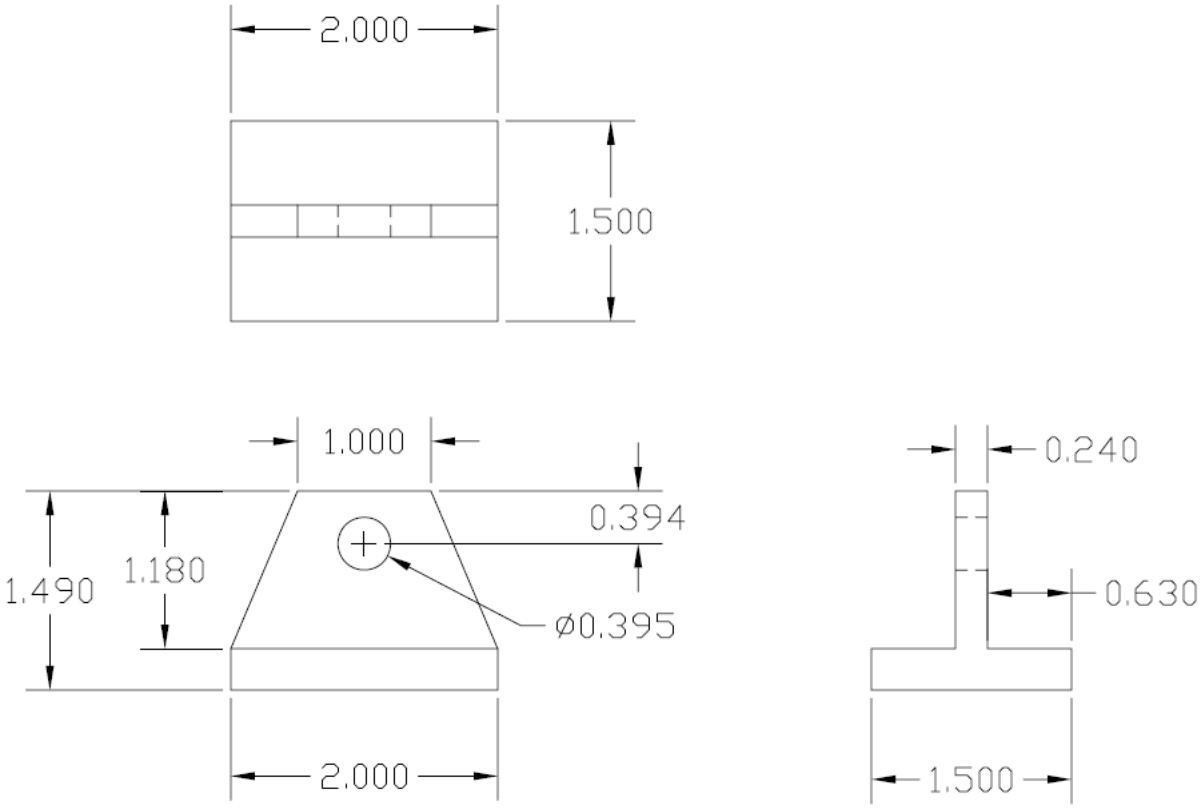

Figure 6-2. Adhesive Strength Testing Apparatus (ADHESTA) schematic (inches)

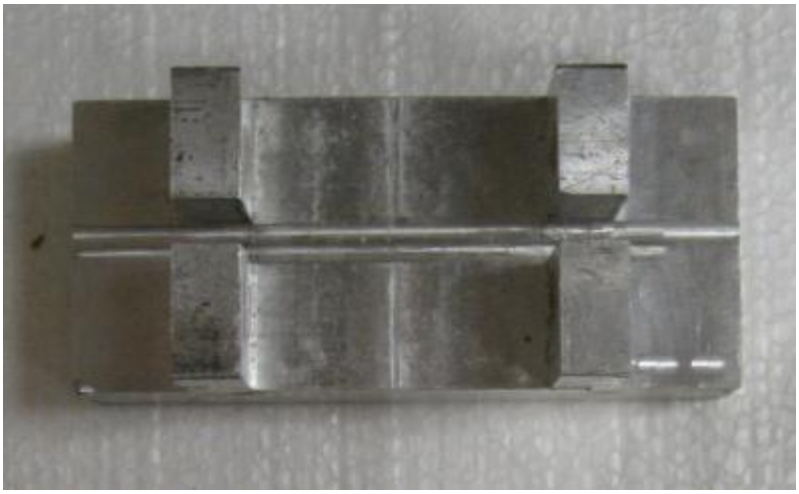

Figure 6-3. ADHESTA mold (Photo courtesy of Qiang Li)

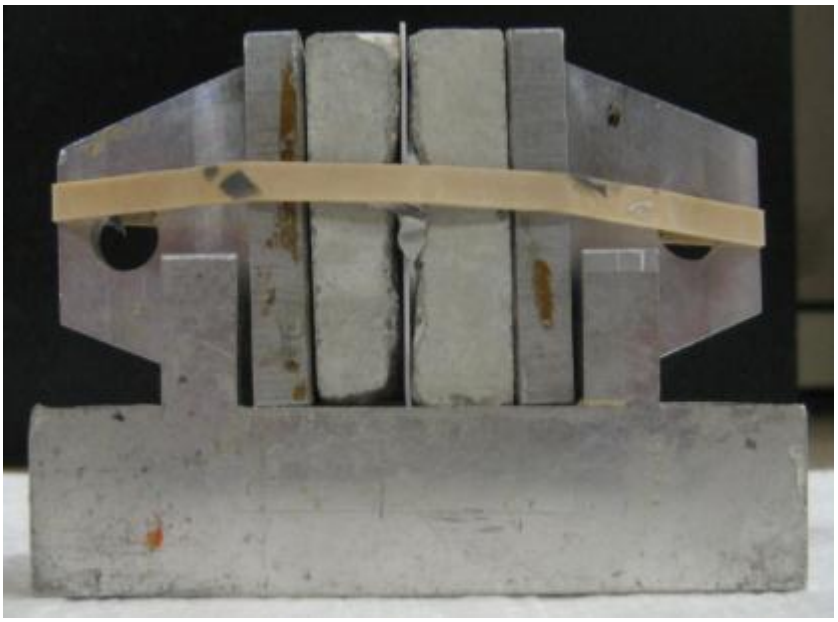

Figure 6-4. ADHESTA with sample (Photo courtesy of Qiang Li)

Figure 6-5. Adhesive strength test setup (Photo courtesy of Qiang Li)

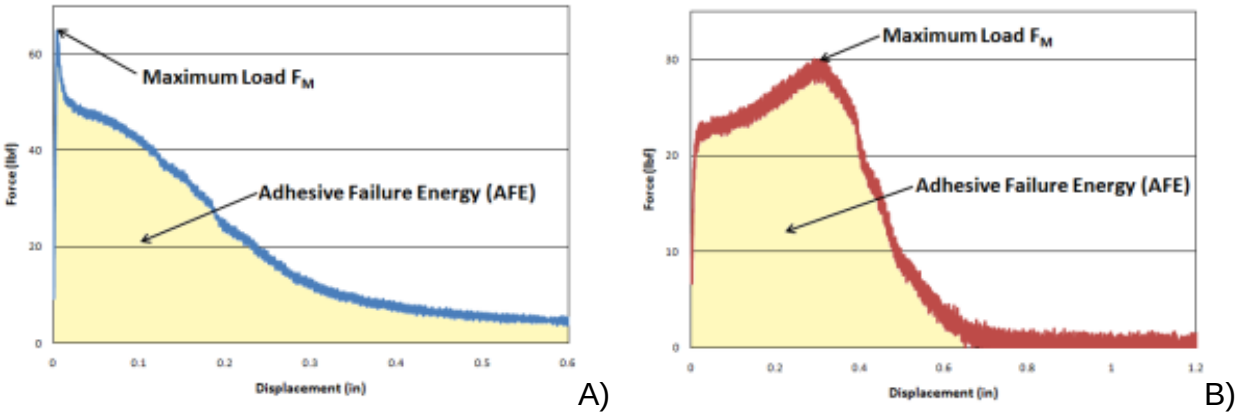

Figure 6-6. Typical adhesive strength test results, (A) non-self-leveling, (B) self-leveling.

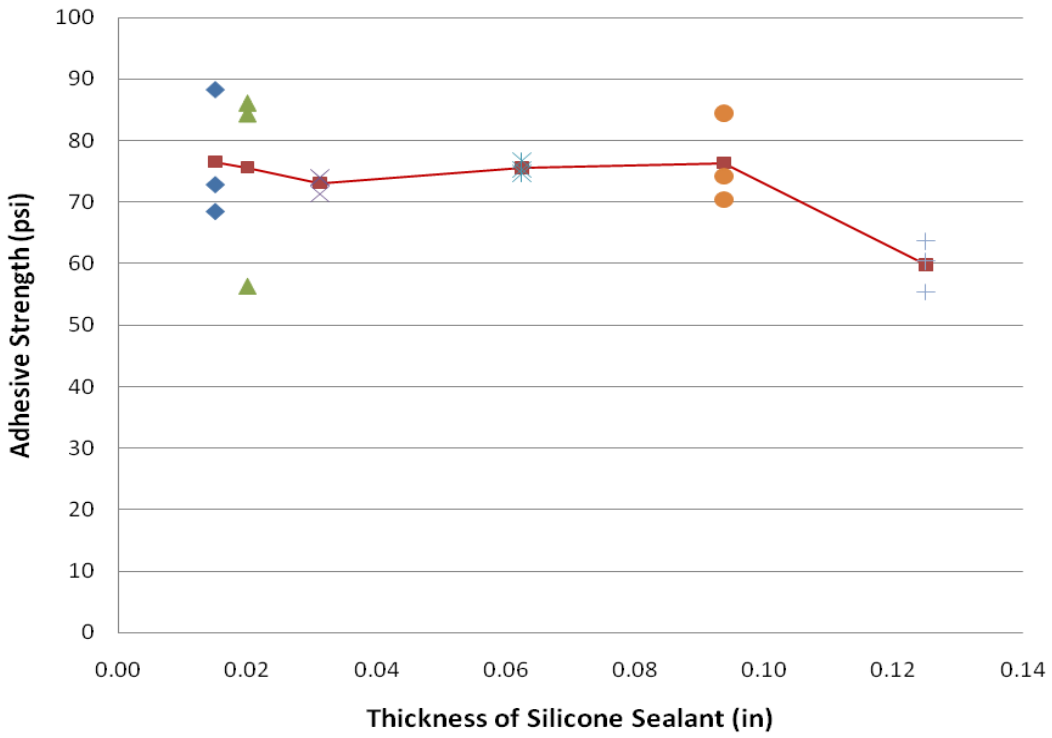

Figure 6-7. Effect of sealant thickness on AS for non-self-leveling sealant

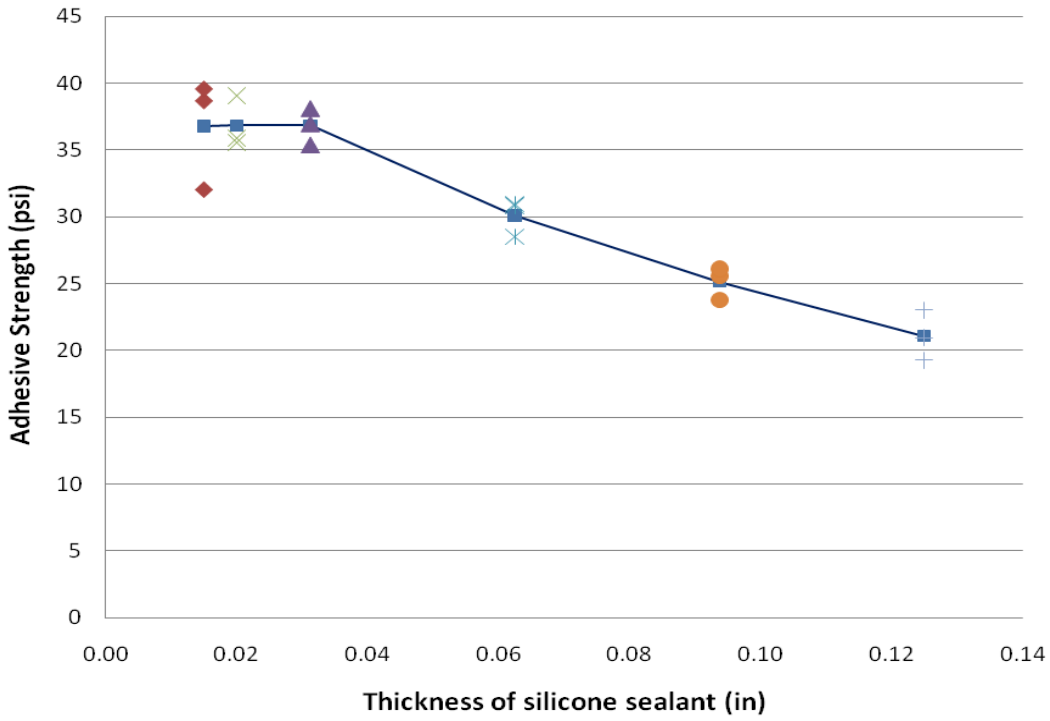

Figure 6-8. Effect of sealant thickness on AS for self-leveling sealant

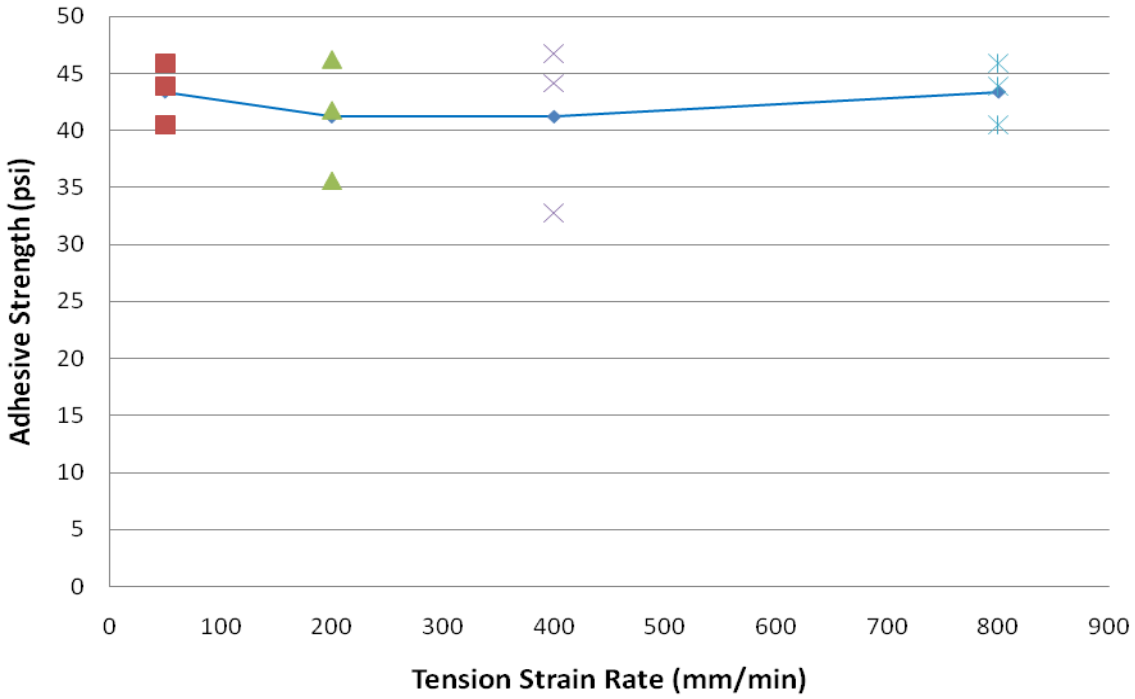

Figure 6-9. Effect of strain rate on adhesive strength for non-self-leveling sealant

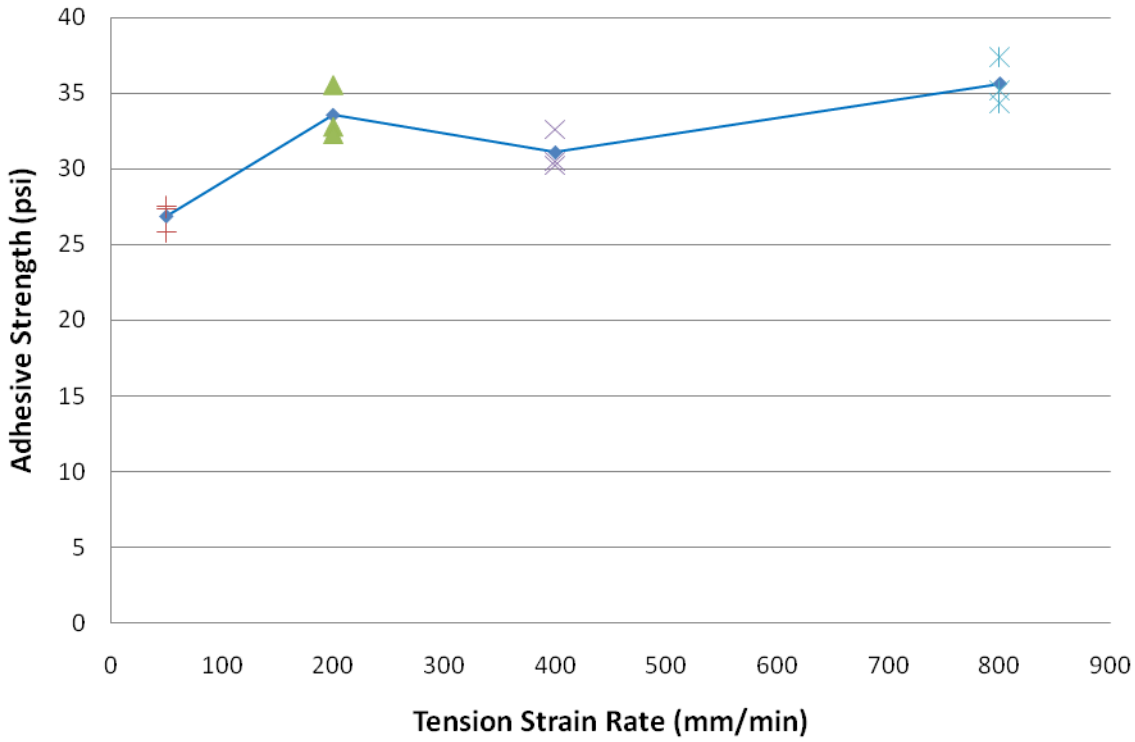

Figure 6-10. Effect of strain rate on adhesive strength for self-leveling sealant

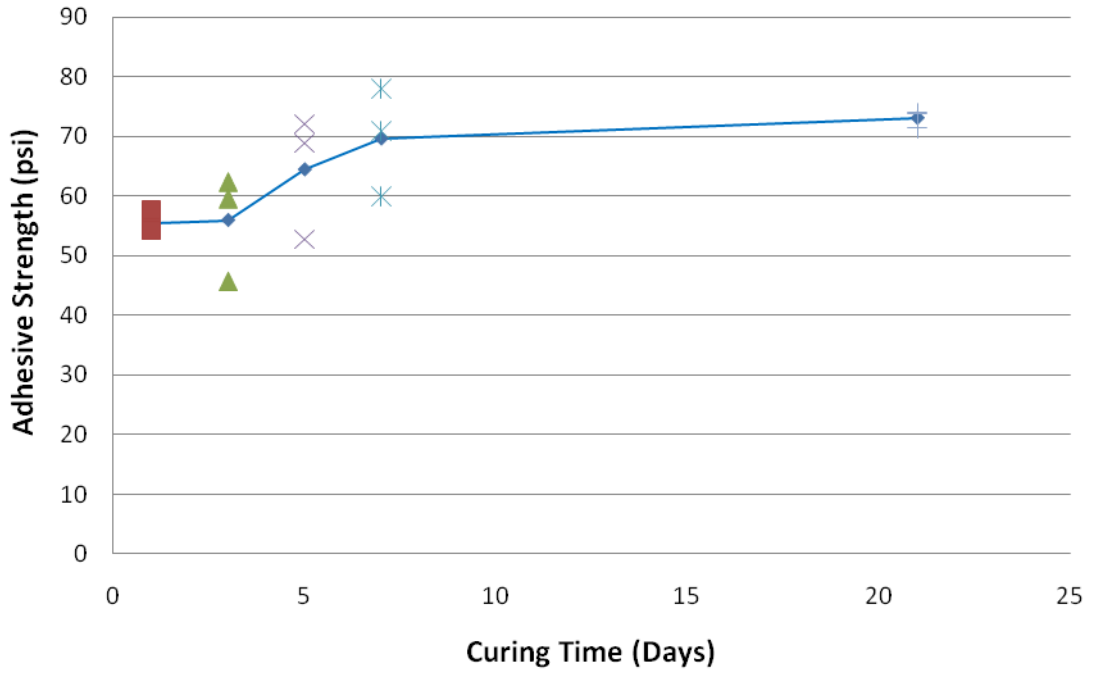

Figure 6-11. Effect of curing time on adhesive strength for non-self-leveling sealant

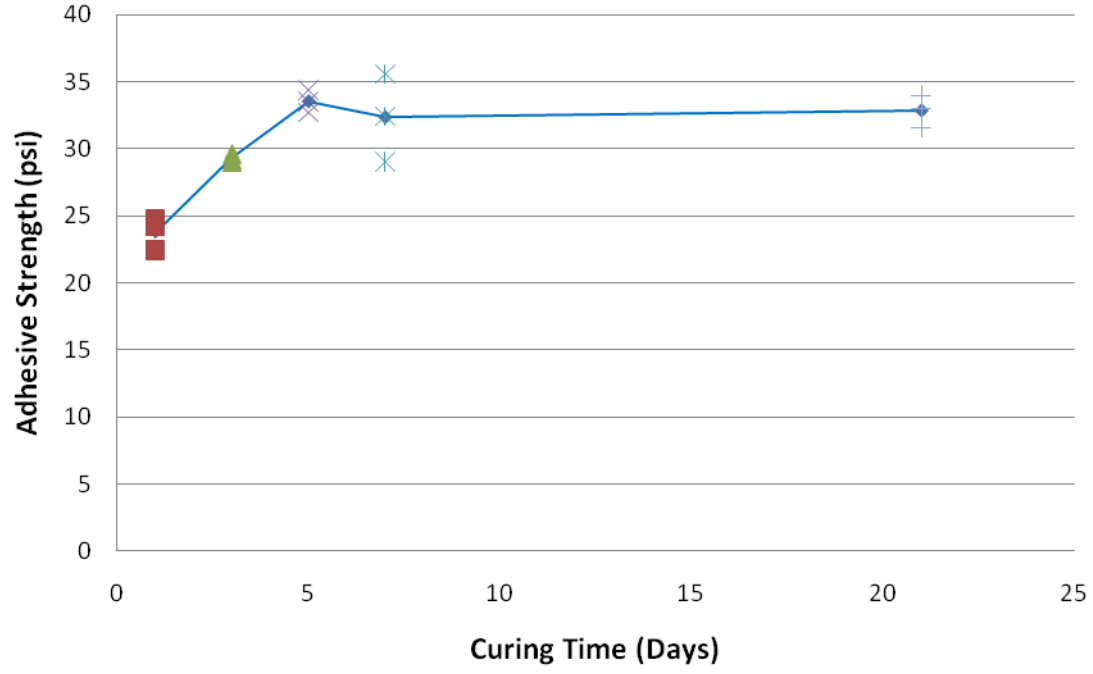

Figure 6-12. Effect of curing time on adhesive strength for self-leveling sealant

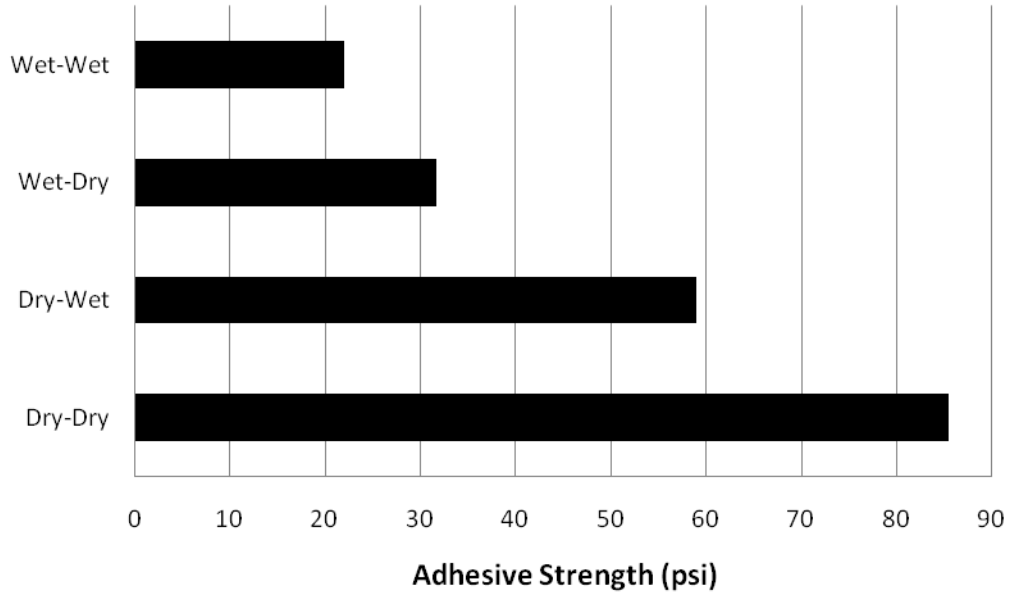

Figure 6-13. Non-self-leveling silicone sealant wet and dry adhesive strength test results

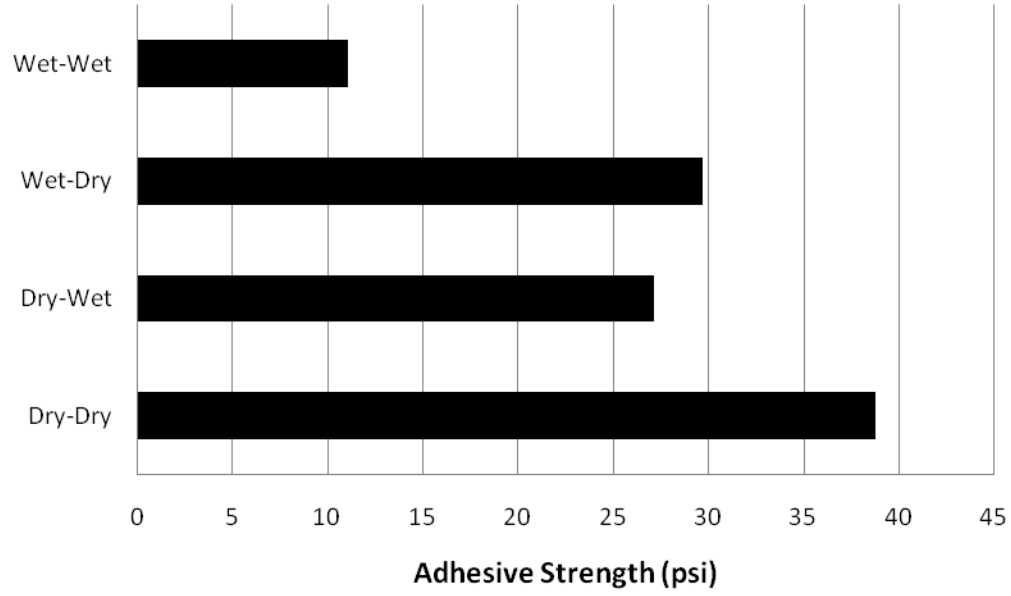

Figure 6-14. Self-leveling silicone sealant wet and dry adhesive strength test results.

Figure 6-15. Delmhorst BD-2100 Moisture Meter (Photo courtesy of Qiang Li)

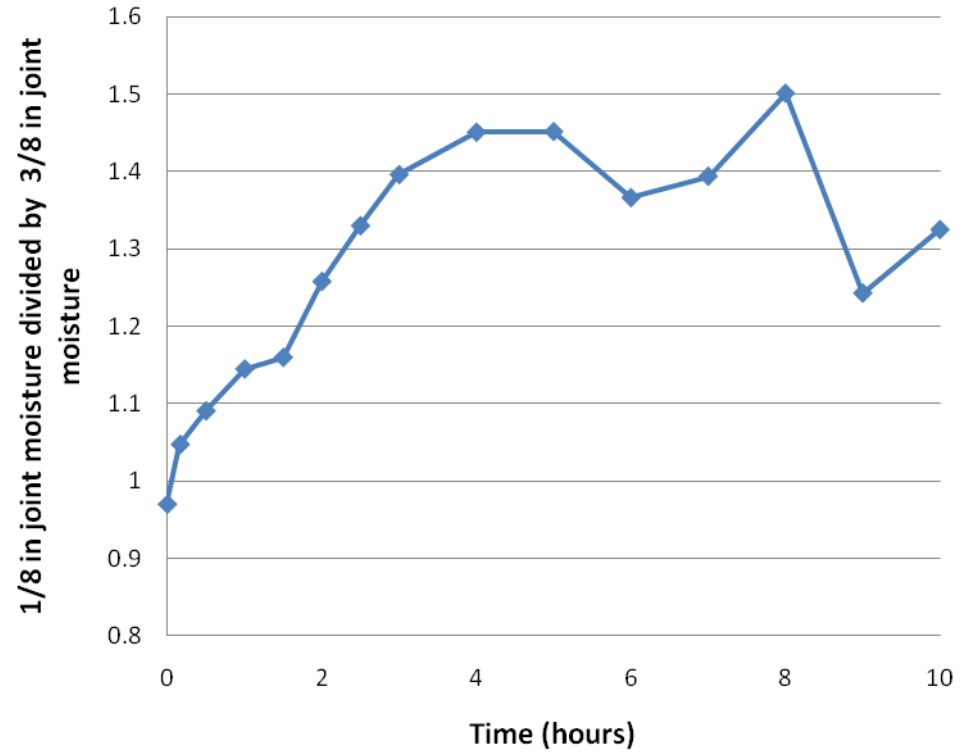

A)

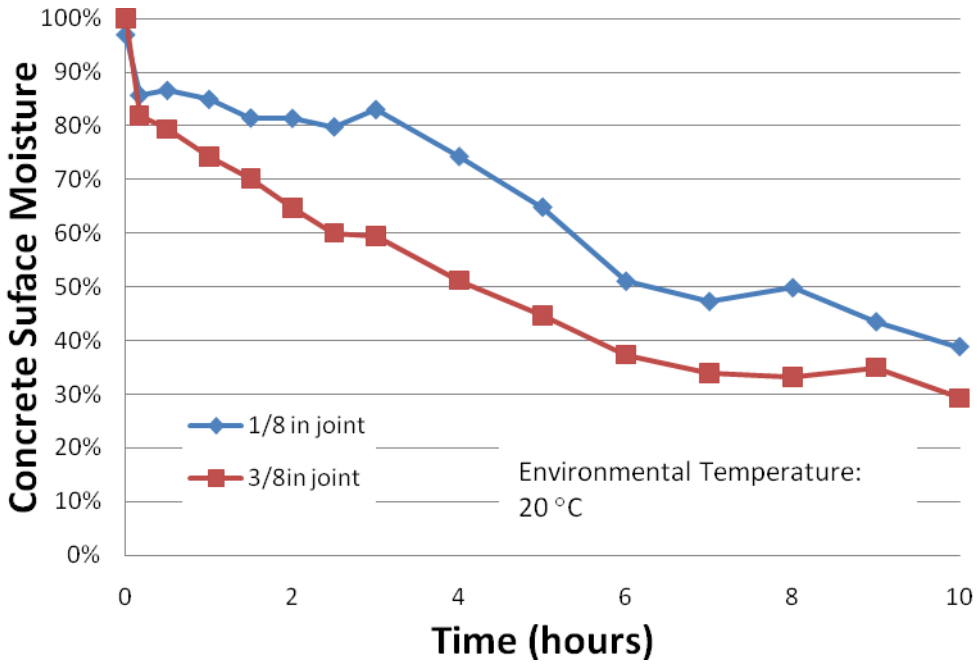

B)

Figure 6-16. Dry-time raw data for 1/8 in. and 3/8 in. joints; A) is non-dimensionalized data and B) is raw data.

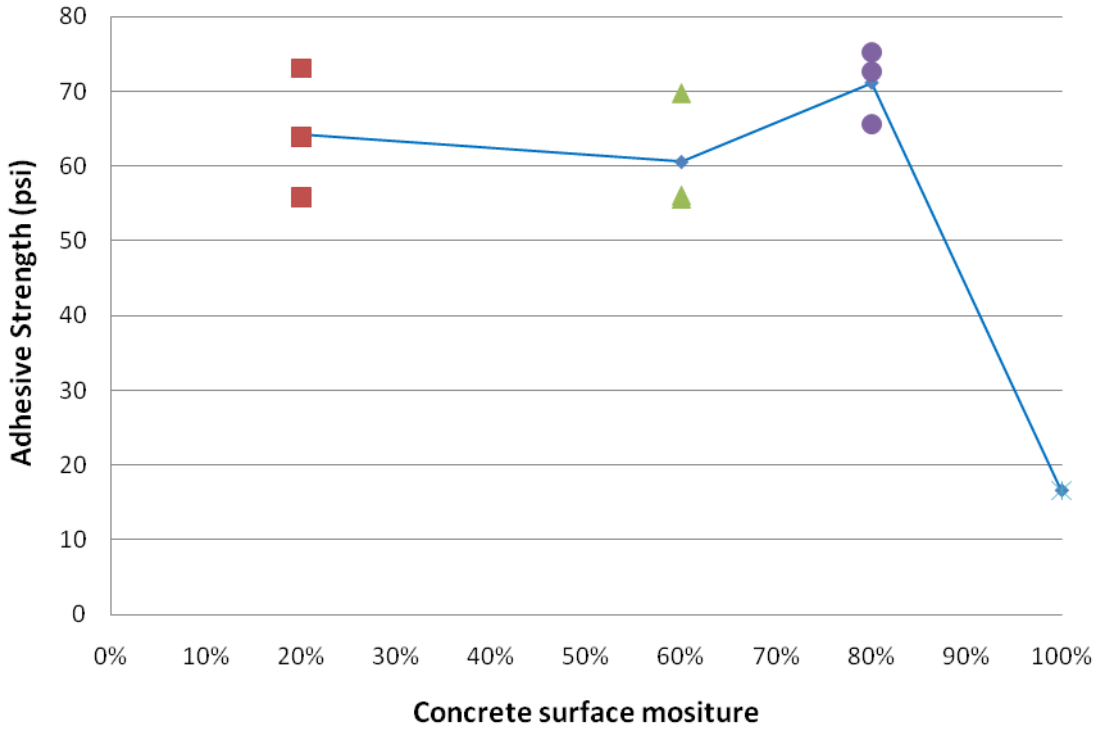

Figure 6-17. Effect of moisture on adhesive strength for non-self-leveling

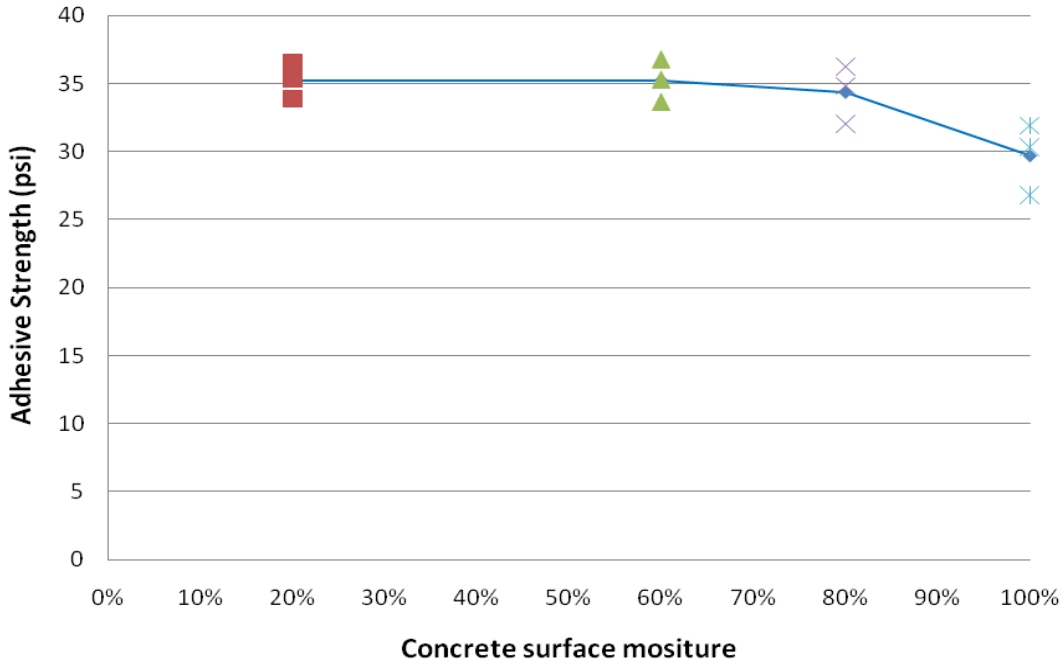

Figure 6-18. Effect of moisture on adhesive strength for self-leveling

Figure 6-19. Aggregate Image Measurement System (AIMS) (Photo courtesy of Masad)

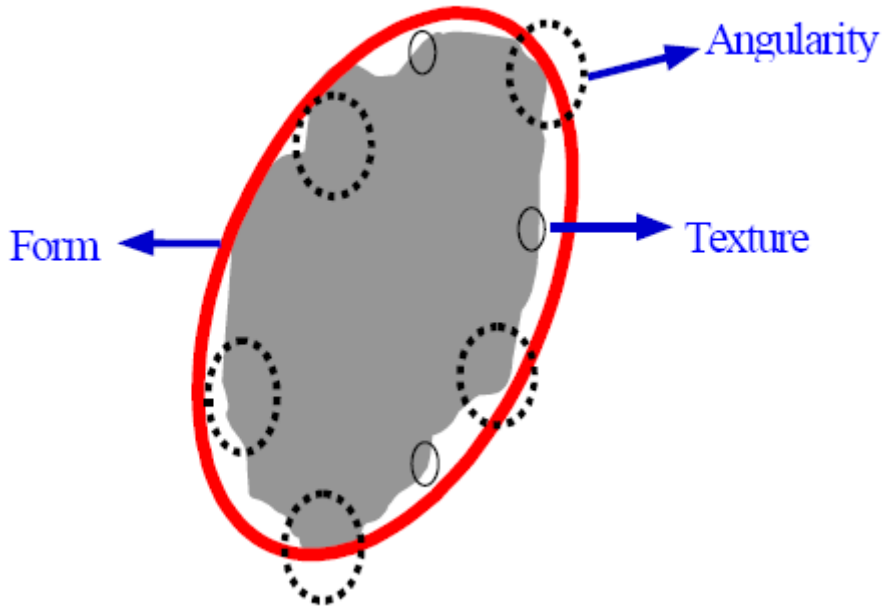

Figure 6-20. Aggregate shape properties schematic (Masad 2004)

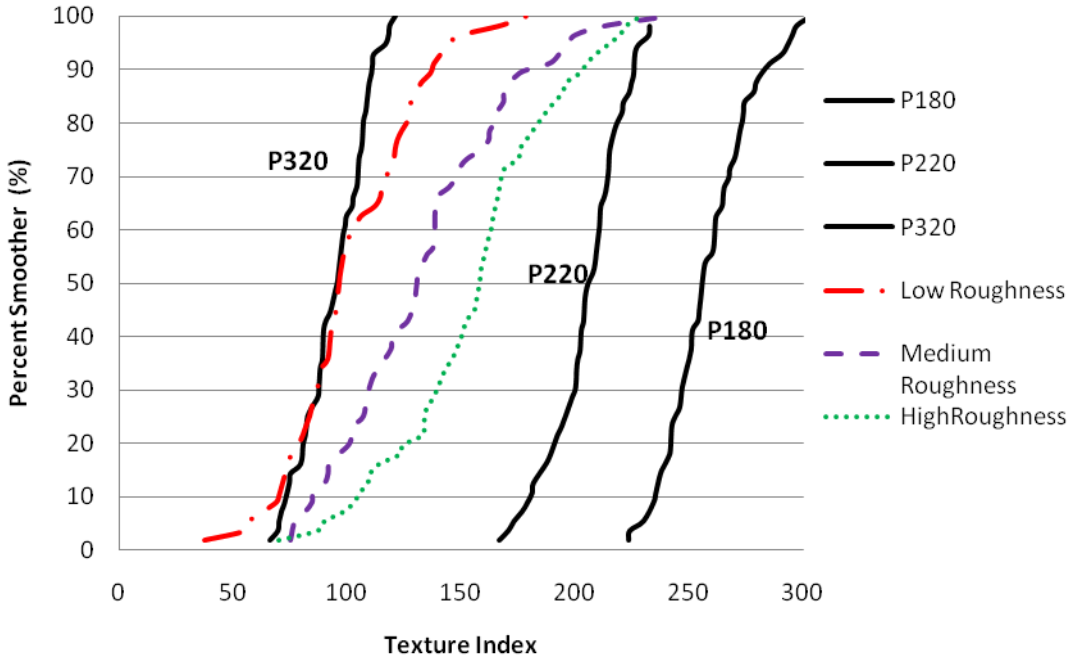

Figure 6-21. Texture indices of concrete surface and sandpaper

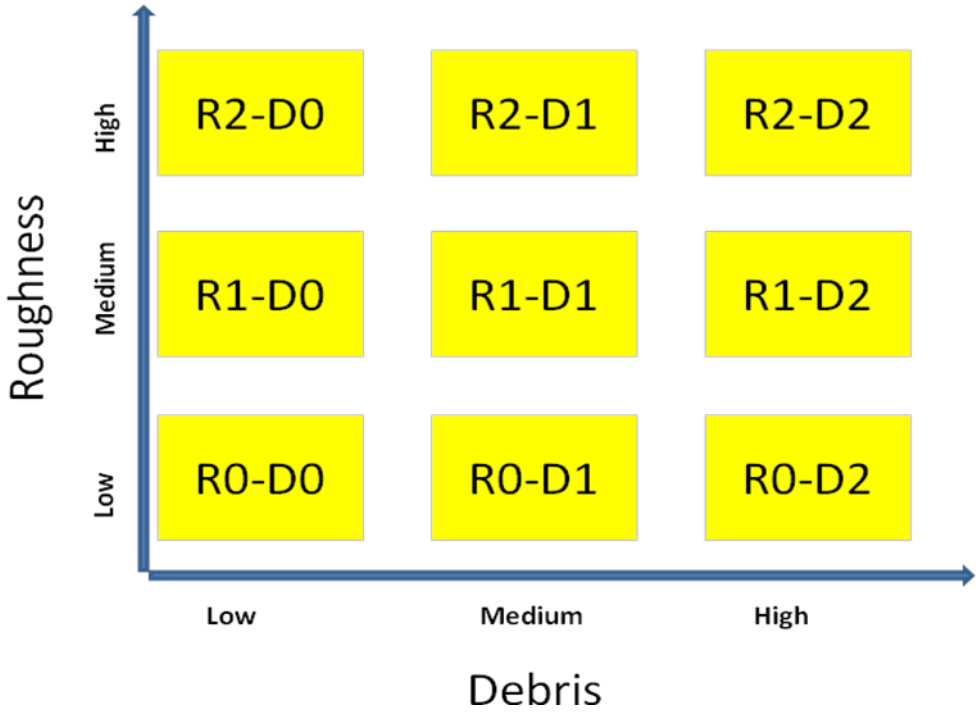

Figure 6-22. Adhesive strength test design matrix for roughened and debris-induced samples.

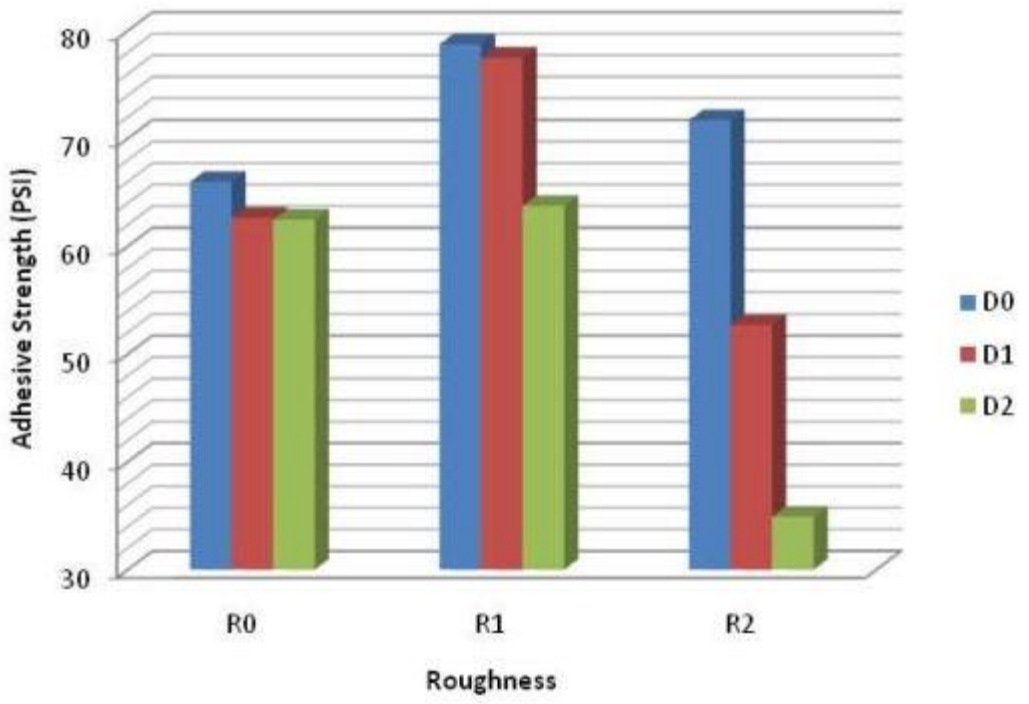

A)

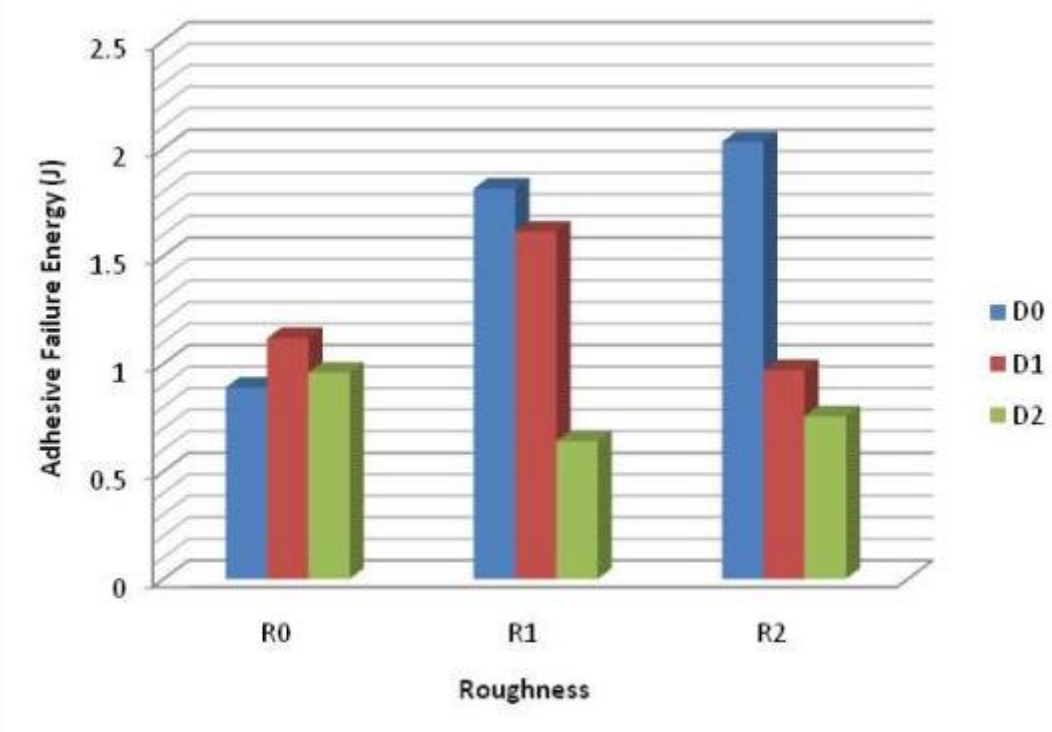

B)

Figure 6-23. Non-self-leveling sealant adhesive strength test results showing (A), Adhesive Strength (AS); and (B) Adhesive Failure Energy (AFE)

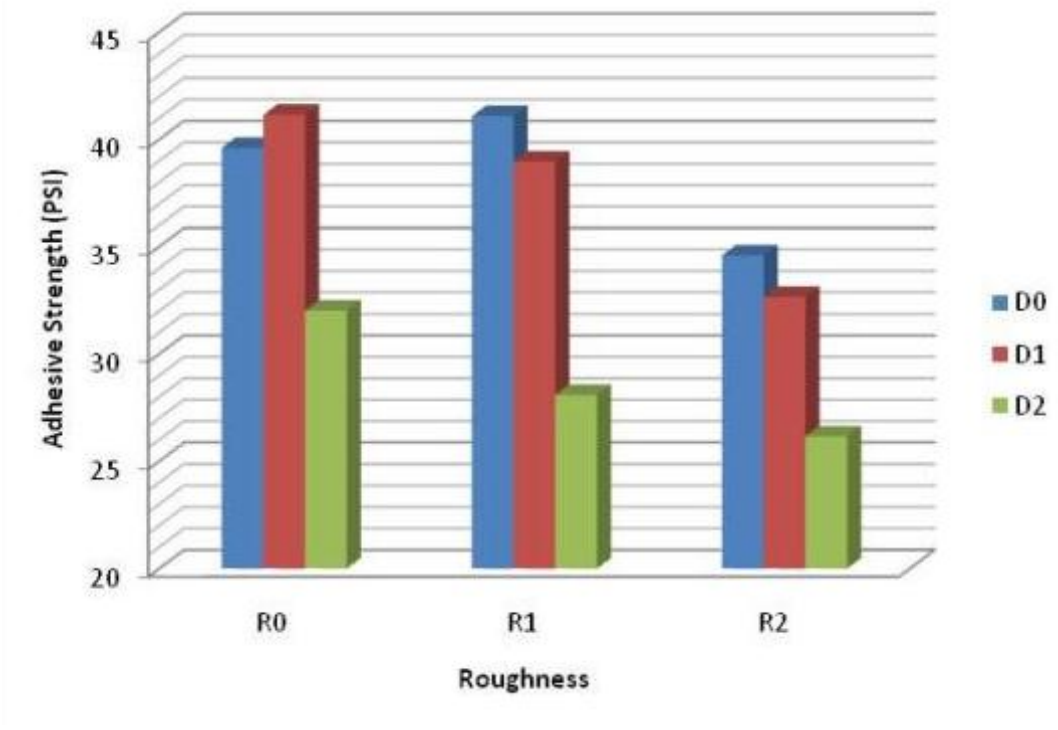

A)

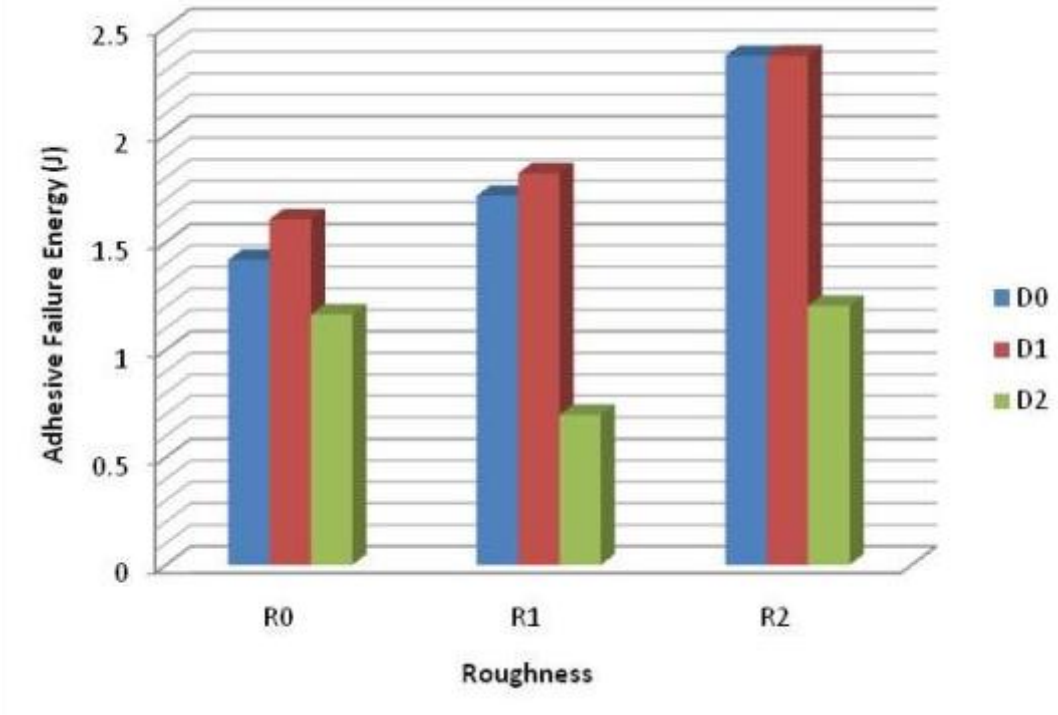

B)

Figure 6-24. Self-leveling sealant adhesive strength test results showing (A) Adhesive Strength (AS); and (B) Adhesive Failure Energy (AFE)

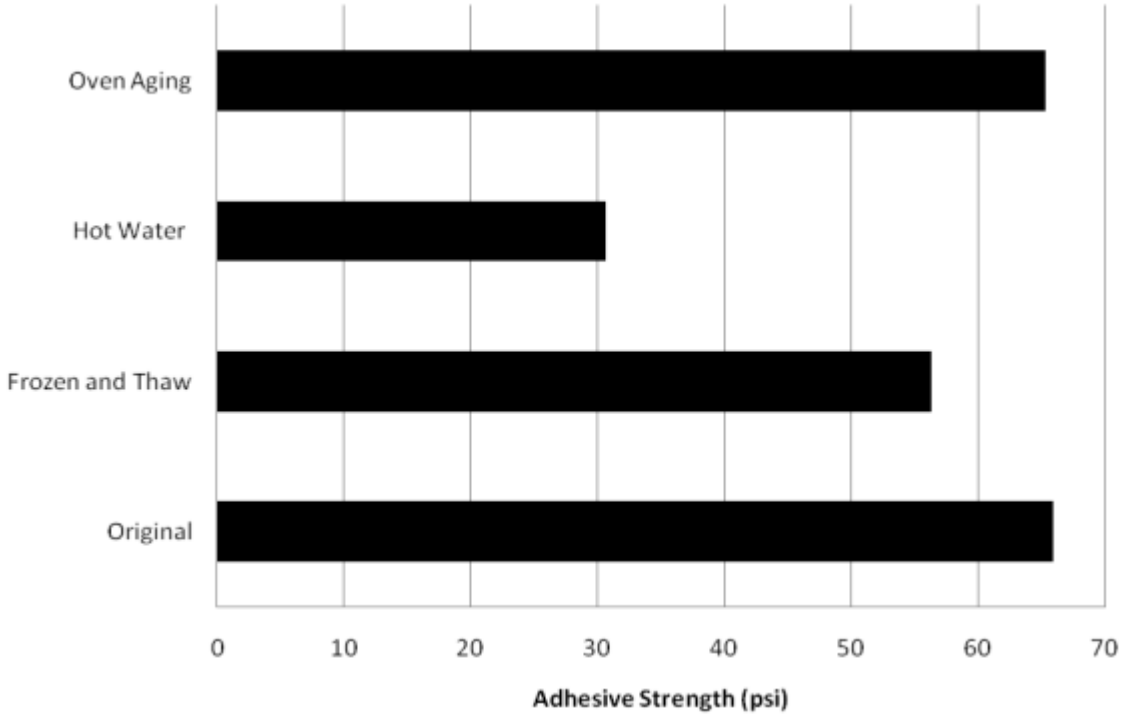

Figure 6-25. The effect of aging on the adheisve strength for non-self leveling sealant

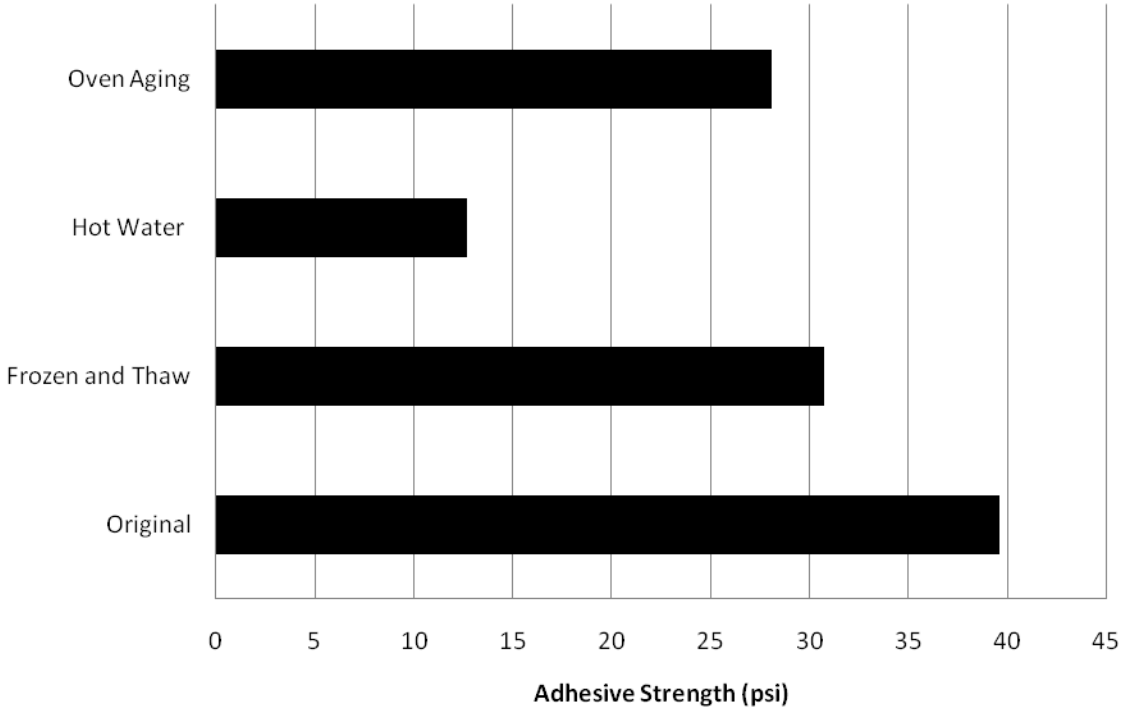

Figure 6-26. The effect of aging on the adhesive strength for self leveling selant

CHAPTER 7
DEVELOPMENT OF JOINT PREPARATION QUALITY CONTROL DEVICE

The preparation of a transverse contraction joint has a direct effect on sealant adhesive strength. Previous results have indicated that the roughness and cleanliness of the concrete surface were two significant variables that determine adhesive strength. The joint preparation quality control device was developed to test joint preparation in the field before sealing.

Design of Joint Preparation Quality Control Device

The objective of this portion of the project was to design a joint preparation quality control device and to use this device to investigate the effect of debris and moisture on adhesive strength. The Joint Preparation Quality Control Device (JPQCD) was designed to meet the following specifications:

- The device must be applicable to 3/8” and 1/8” concrete joints.
- The device must evaluate variables affecting adhesive strength.
- The device must be portable (reasonable size and no AC power requirement), convenient to use, and reliable.
- The device must be appropriate for evaluation of the adhesive area.
- The device must be reusable and consistent between tests.
- The device must function in a timely manner.
- The testing procedure must not affect surface prior to test.
- Device design (materials and manufacturing) should minimize cost.

Based upon these criteria, a portable device was designed for a quantitative and qualitative inspection of the prepared joint surface. The JPQCD consists of a disk-shaped aluminum insert which is fitted with two pins that support the insert at the joint surface (Figure 7-1 and Figure 7-4A). The device is slid into the joint and the square

shaped hollow in the device serves as a form which is filled with Medium Body ReproRubber. This two-part rubber fills the mold between the concrete joint surfaces. When the rubber is cured, the device and rubber are pulled out by a “Force Multiplier” device (lever/fulcrum, Figure 7-2). The elastic rubber retains its shape after being pulled out of this joint. A DC powered load cell and digital meter are used to record the load during removal (Figure 7-3).

Testing Procedure

The testing procedure was conducted as per the following:

- The insert is first placed in the joint as indicated in Figure 7-4A.
- “ReproRubber” is injected into the insert and allowed to cure for a minimum of 10 minutes (Figure 7-4B).
- Once the “ReproRubber” has cured, the force multiplier is placed directly above the JPQCD, and it is connected using the hook hanging from the load cell.
- The digital meter is powered on and set to record and configured to take a reading.
- The extension handle is used to apply a force to the JPQCD such that the device is lifted out of the joint.
- Data from the test is stored and eventually uploaded to a PC using a USB cable.

Test Preparation

Several combinations of joints surfaces were prepared for testing. Pairs of clean and debris-covered surfaces were used to test the effect of debris on adhesive strength, while dry and moistened joint-pairs were prepared to investigate the effect of moisture on adhesive strength. The following is a description of preparation and testing procedures associated with these tests.

Preparation of Testing Apparatus

The testing apparatus consisted of a 1.50 in. x 0.75 in. steel tube-section bracket. The bracket's steel tube halves were attached to two 2x4's with 1 in. x 1 in. x 9/16 in. concrete blocks with variable surface conditions attached (Figure 7-5). The 2x4's were adjusted such that the desired separation was achieved. Once separation was correct, the brackets were clamped to prevent movement of the testing apparatus during testing. Once clamped, tests were conducted in accordance with the testing procedure.

Preparation of Clean Joint Surfaces

Clean joint surfaces were prepared such that concrete was sawed to the appropriate size and pressure-washed. Once washed, the concrete was dried in a climate-controlled environment for a minimum of three days. Tests were conducted on one joint pairs for and 3/8 in. joint; tests were repeated 14 times.

Preparation of Debris Joint Surfaces

Similar to clean joint-surface blocks, "debris blocks" were cut to the appropriate size, pressure-washed, and dried in a climate-controlled environment. Then, approximately 0.03 grams of debris were applied evenly to the concrete blocks' testing surfaces with a Teflon applicator such that a debris-density of 0.03 g/in^2 was achieved. Tests were conducted on one joint pairs for and 3/8 in. joint; tests were repeated 14 times.

Preparation of Dry and Moistened Joint Surfaces

"Moisture-test blocks" were cut, sawed, and dried in the same manner as debris blocks and clean blocks. Then, using a dropper, 20 drops of water were applied to the moisture-block testing surface in a prescribed pattern. Two series of tests were conducted: samples were either tested immediately or allowed to dry for 15 minutes.

Tests were conducted on one joint pairs for and 3/8 in. joint. When “immediate” testing was conducted, tests were administered 21 times; when 15-minute drying time was used, tests were conducted 7 times.

Results and Discussion

During testing, investigators simply left the JPQCP “on” and allowed it to collect a continuous time-series of data. In other words, a test was conducted where the device was removed from the artificial joint; the joint was reinserted; allowed to cure; pulled out again; etc. Raw data of clean test (Figure 7-8) appears to be a dormant signal interspersed with load peaks which is displayed using red dot. The peak loads were summarized and shown in Table 7-1 and Table 7-2.

Debris Test Results

The average peak load for a clean 3/8 in. joint was 65.7 lbs. The average peak load for a 3/8 in. joint with debris was 55.5 lbs. Figure 7-6 shows the a comparison between debris and clean tests for the 3/8 in. joint. The red dot in this figure represents the average of 14 peak loads and the blue line represents the associated 95% confidence interval from these tests. A T-test was conducted on two set of samples to determine whether the clean joints achieved a greater peak load than the debris-joints. Results from the T-test returned a value of 12%. In other words, statistically one can say with 88% confidence that clean joints achieve a higher peak load than debris joints.

Moisture Test Results

Results from moisture tests indicate that under dry conditions a 3/8 in. joint required a peak pullout load of 70.20 lbs. Under immediate wet conditions, peak load was reduced to 54.10 lbs. Under 15-minute drying conditions, the average peak load was 63.10 lbs. Figure 7-7 presents the test results for the effect of moisture. The red

dot represents the average of 7 peak loads and the blue line denotes the 95% confidence interval. A T-test was conducted on dry and immediate wet conditions. Results from the T-test returned a value of 8%. This means that one can say with 92% confidence that on average, dry conditions produce a higher peak load when compared with “immediate” wet conditions. The corresponding T-test for comparing dry and the 15-minute drying condition was 49% while the T-test comparing immediate-wet versus 15-minute wet conditions was 37%.

Summary and Conclusions

The following is a summary of work discussed in this section including all relevant conclusions:

A new testing device, the Joint Preparation Quality Control Device (JPQCD) was designed and built. A new testing procedure was built using the new device to evaluate concrete joint adhesive strength.

The JPQCD was used to test 3/8 in under clean conditions and debris-induced conditions. Results appear to indicate that debris may reduce peak load.

The 3/8 in. joint was tested under two dry-time conditions. When a test was run immediately after moisture-induction, adhesive strength appeared to be reduced significantly.

Because the JPQCD functioned as designed, it should be used in the future to compare 1/8 in. versus 3/8 in. joints both under field conditions and in a highly controlled laboratory environment.

Table 7-1. Peak load (lbf) for 3/8 in. concrete joints for clean vs. debris conditions.

Run Number	Clean Test	Debris Test
1	53.33	23.00
2	53.33	64.00
3	70.00	57.67
4	74.67	99.33
5	74.00	23.33
6	90.33	73.67
7	53.33	62.00
8	61.67	46.33
9	90.67	47.67
10	70.00	42.67
11	71.00	55.33
12	56.67	57.33
13	50.33	54.00
14	51.00	71.33

Table 7-2. Peak load (lbf) for 3/8 in. concrete joints for dry vs. immediate and 15 min dry time.

Run Number	Dry	Wet immediate	Wet w/ 15 min. dry time
1	86.33	54.00	35.67
2	68.00	49.00	77.00
3	97.33	67.33	96.00
4	60.67	54.33	67.67
5	48.67	56.67	63.00
6	61.67	25.33	40.67
7	69.00	72.33	62.00

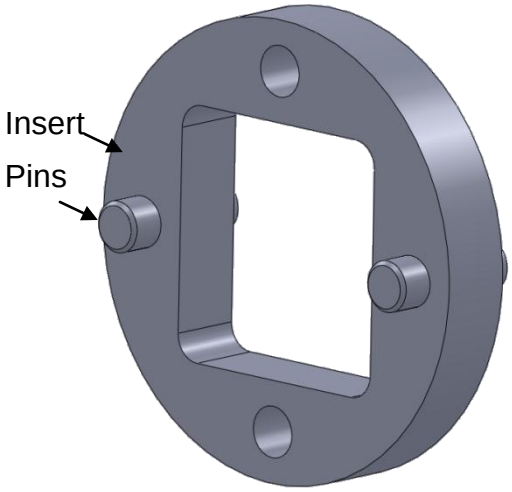

Figure 7-1. Aluminum insert and two pins for JPQCD

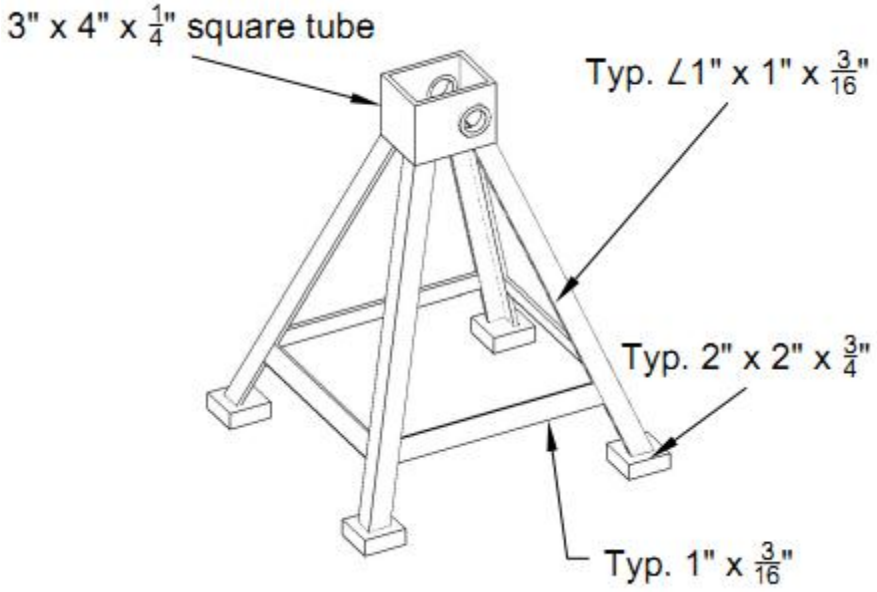

Figure 7-2. "Force Multiplier" (lever/fulcrum) device for JPQCD

Figure 7-3. Digital meter used to record load during JPQCD removal (Photo courtesy of Robert Ferguson)

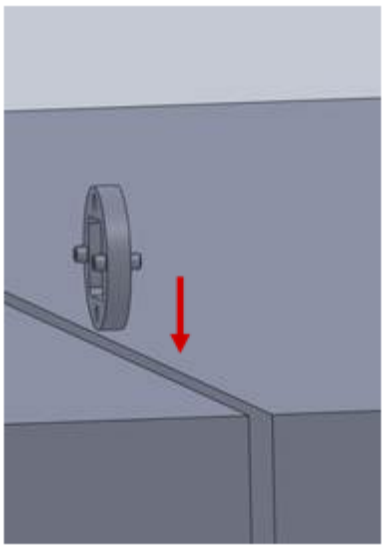
A)
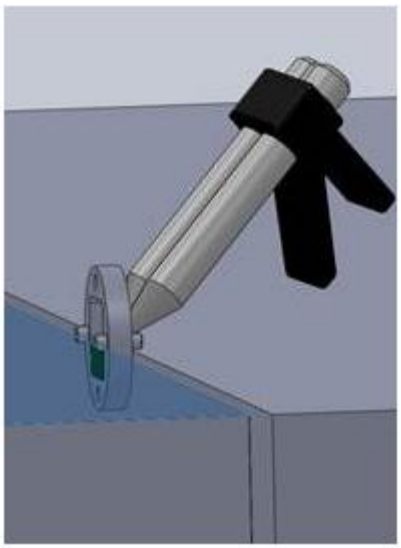
B)

Figure 7-4. JPQCD testing procedure: (A) Step 1; (B) Step 2

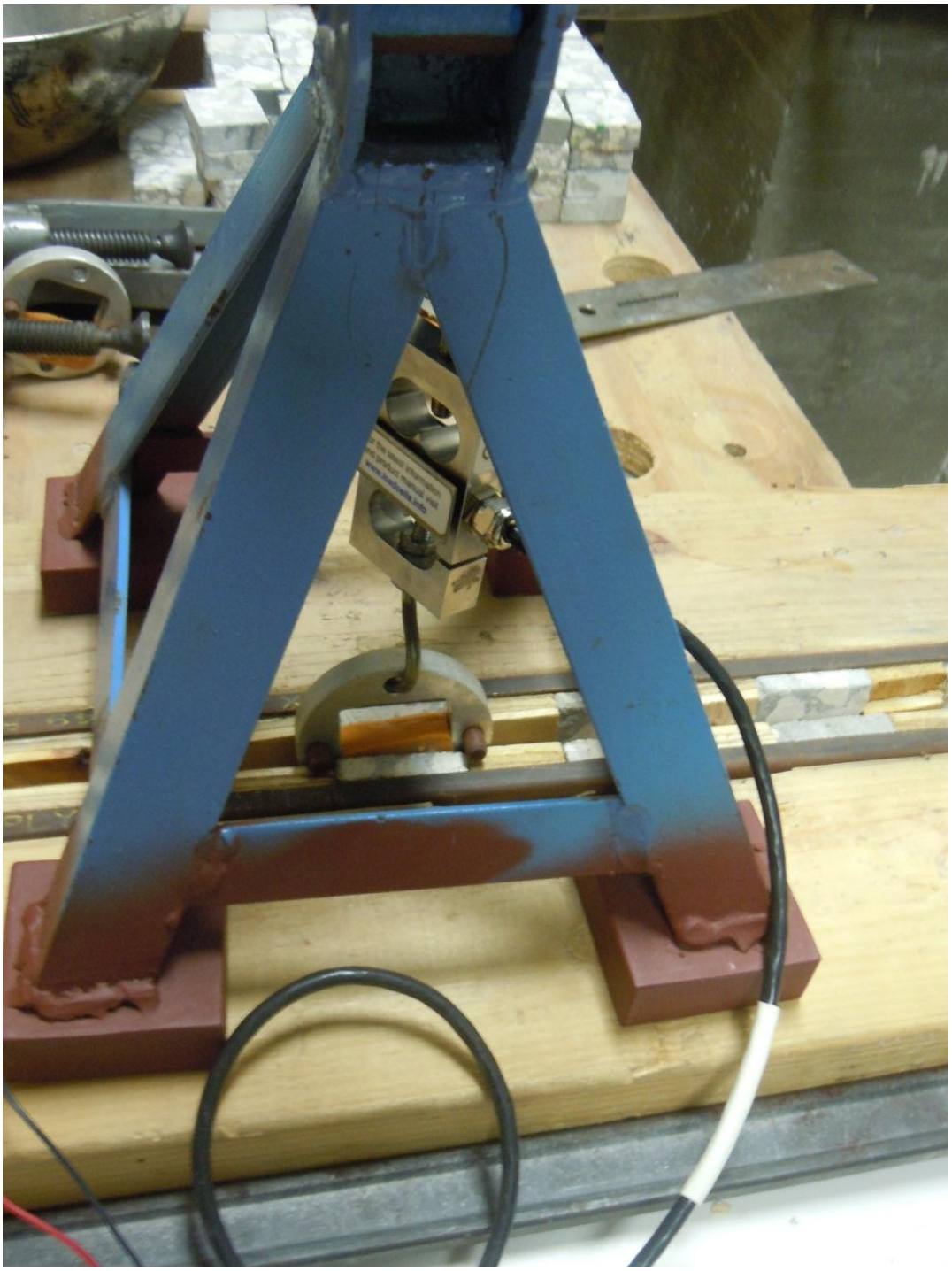

Figure 7-5. Photograph of joint testing setup (Photo courtesy of Raphael Crowley)

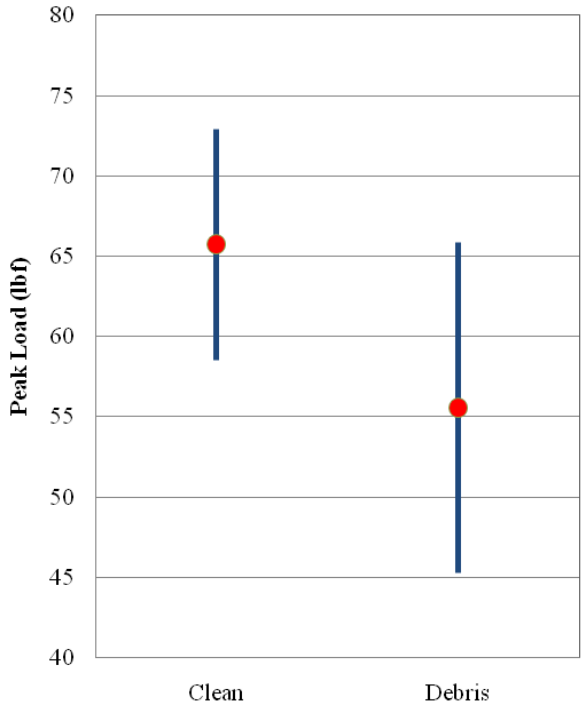

Figure 7-6. Debris test results

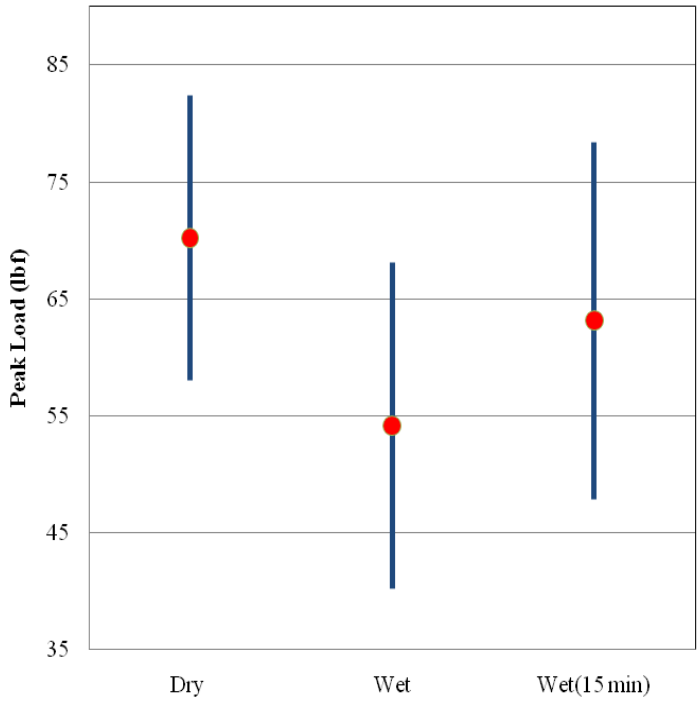

Figure 7-7. Moisture effect test results

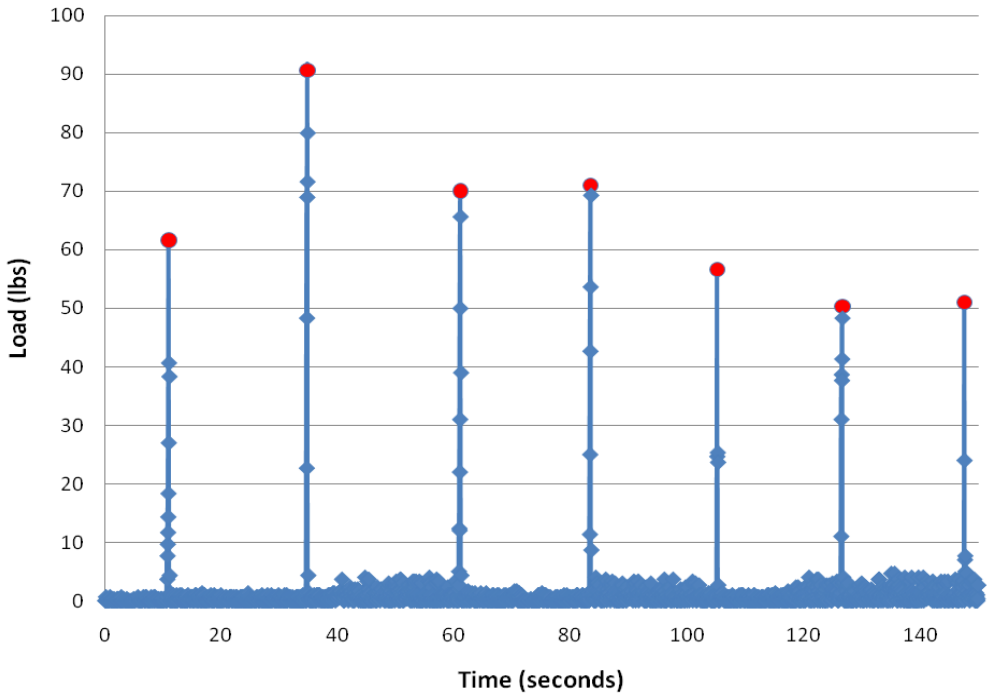

Figure 7-8. Raw data for half of clean test (7 peak loads)

CHAPTER 8
EVALUATION OF NARROW AND STANDARD JOINT USING JOINT PERFORMANCE EVALUATION MODEL

The objective of this chapter is to develop a Joint Performance Evaluation Model (JOPEM) based on discussion from Chapter 4 through Chapter 7, and to use this model to compare the standard 3/8 in. joint with the proposed 1/8 in. joint.

Horizontal joint movement, which was quantified in Chapter 4, was used as strain load input in the JOPEM. Creep test results, developed in Chapter 5, were used to model sealant's viscoelastic properties. As discussed several times in this paper, adhesive failure is the most common failure mode for silicone sealant. Therefore, adhesive strength as discussed in Chapter 6 was used as the failure criterion.

Shear Movement of Concrete Pavement

A FEACONS-ADINA finite element model was developed to determine the shear movement of a concrete joint. The Finite Element Analysis of Concrete Slabs (FEACONS) model (Figure 8-1 and Figure 8-2) was used to determine shear movement magnitude. The Automatic Dynamic Incremental Nonlinear Analysis (ADINA) model (Figure 8-3) was used to determine sealant stresses resulting from this movement. A 12.0 ft. by 15.0 ft. slab was used in the FEACONS model; such dimensions are typical for roadways. As shown, dual tire loads were applied to the slab and represented as 6.0 in. by 8.0 in. rectangles. These tire loads were placed at the slab's corner such that maximum shear movement was achieved. According to the model, maximum deflection was computed to be 0.24 mm.

The ADINA model consisted of a two-dimensional solid, plain-strain element with nine nodes. Maximum deflection was applied to the right side of the joint, and the principle tensile stress along the left side of the joint was computed. According to

ADINA, the maximum principle stress' locus was at the model's upper-left (P1). This maximum was compared with adhesive strength, which as discussed was used as the model's failure criterion. Since the maximum principle tensile strength is greater than the tensile strength in the horizontal direction, this method is inherently conservative. This is important because it implies that all results presented in this section are conservative – which may indicate that further research may be required to design a more precise model. This model was run with the two different joint widths discussed in this study (1/8 in. vs. 3/8 in.) and two types of silicone sealant (self-leveling vs. non-self-leveling).

Silicone Sealant Modulus of Elasticity

Since field poured silicone sealant is a viscoelastic material, its modulus of elasticity is not constant. Rather, its modulus is highly dependent upon the rate at which loading is applied to it. Sealant is very stiff when deformation is applied at a high rate. Conversely, if a low deformation rate is used, silicone sealant releases significant amounts of stress.

From the perspective of concrete joint sealant, horizontal joint movement is a relatively slow strain rate. Thus, under horizontal joint movement conditions, the sealant has sufficient time to release stress. Creep test results indicate that strain increases slowly after 1000s. Therefore, creep testing results at 1000s were used to quantify sealant's modulus of elasticity under this condition. The elastic modulus of sealant is equal to the reciprocal of creep compliance at 1000s.

In contrast with horizontal joint movement, traffic shear movement occurs at a relatively high rate. Under traffic-load conditions then, sealant becomes stiff in response. Therefore, creep testing results at 1s were used to quantify sealant's

modulus of elasticity under this condition. The elastic modulus of sealant is equal to the reciprocal of creep compliance at 1s. Input moduli are presented in Table 8-1.

In the field, oxidation, water, UV light, and other factors cause sealant to age. As sealant ages, its modulus of elasticity increases (i.e. the sealant becomes more stiff and more brittle). While creep testing was conducted on laboratory-aged sealant as discussed in Chapter 4, it is unlikely that techniques used during these tests accurately simulated "true" field-aging. Oldfield and Symes (1996) studied long-term in-situ aging of silicone sealant in which sealant samples were aged in natural environments for 20 years. Their results indicate that sealant's modulus increases by approximately 60% over 20 years. Oldfield and Symes provided a series of aging parameters to quantify a sealant's modulus as a function of time (Figure 8-3). These aging parameters were multiplied by the original sealant moduli such that modulus used for this model was defined as a function of time.

Adhesive Strength of the Silicone Sealant

The adhesive strength of original field-poured silicone sealant used in the JOPEM is presented in Table 8-2. Aging tests in Chapter 6 indicate that adhesive strength decreases with aging. While this trend was apparent, a similar argument to the modulus discussion can be used to describe adhesive strength: Chapter 6 results may not accurately mimic field data. Because of the lack of reliable field data, investigators assumed that adhesive strength decreased by 60% over twenty years, or put another way, adhesive strength was inversely proportional to modulus of elasticity. An adhesive strength aging parameter was developed based on Oldfield and Symes' modulus aging parameter. These reduction factors were multiplied by original adhesive strengths such that adhesive strength was quantified over the duration of the model.

Predicting Sealant Performance for Narrow and Standard Joints

Adequate performance for a sealant means that joint closure is maintained without adhesive failure. The purpose of this model then, is to predict when adhesive failure will occur. As implied, since both horizontal and shear movement may affect sealant performance, both of these movement types were considered in this model.

Horizontal Joint Movement Model

Horizontal joint movement (Figure 4-7) was applied to silicone sealant; stress was plotted as a function of time; and compared with nominal adhesive strength (Figure 8-5 and Figure 8-6). Results indicate that adhesive failure occurs after approximately one year of service life for non-self-leveling joints if 1/8 in. joints are used. Conversely, over a 20 year service life, 3/8 in., non-self-leveling joints should not experience adhesive failure. Under self-leveling conditions, results indicate that adhesive failure will not occur in either the 1/8 in. or 3/8 in. joint condition.

Shear Joint Movement Model

Shear joint movement was applied to silicone sealant; stress was plotted as a function of time; and compared with nominal adhesive strength (Figure 8-7, Figure 8-8, Figure 8-9, and Figure 8-10). Results presented here represent average principal interface stress at the top of the sealant which is the portion that will experience the most stress.

Results indicate that non-self-leveling sealant applied to a 1/8 in. joint will fail from shear joint movement in approximately 16.2 years (Figure 8-8). Conversely, 3/8 in. non-self-leveling joints will not fail from shear movement in 20 years (Figure 8-7). Similarly, self-leveling joints will also fail from shear movement in approximately 16.7 years when

1/8 in. joints are used. Conversely, a 3/8 in. self-leveling joint should be able to withstand shear movement for more than 20 years.

When results are compared against one another (Figure 8-11 and Figure 8-12), they indicate that the 1/8 in. joint experiences approximately 3 more stress than the standard 3/8 in. joint.

Summary and Conclusions

The following is a summary of work completed in this Chapter including all relevant conclusions:

An ADINA finite-element model was developed with results from Chapter 4 – Chapter 7 and existing literature to evaluate horizontal and shear concrete joint movement over a twenty year test cycle. Both 1/8 in. and 3/8 in. concrete joints were evaluated for self-leveling and non-self-leveling sealant.

Results indicate that under horizontal movement, 1/8 in. and 3/8 in. joints perform similarly when self-leveling sealant is used. When non-self-leveling sealant is used, 3/8 in. joints should not fail over a twenty year design-life. However, 1/8 in. joints will fail in approximately one year.

Results suggest that under shear joint movement, 1/8 in. joints perform significantly worse than 3/8 in. joints. When both self-leveling and non-self-leveling sealant are used, 1/8 in. joints fail in about 16 years. Conversely, 3/8 in. joints did not fail in 20 years.

Generally, this model suggests that 1/8 in. joints may not be adequate. The current 3/8 in. design standard appears to be more appropriate because roadways generally have at least twenty year lifespan.

Table 8-1. The original modulus of silicone sealant

Sealant	Modulus 1000 seconds (psi)	Modulus 1 second (psi)
Non-self-leveling	98.67	293.10
Self-leveling	6.98	131.00

Table 8-2. The original adhesive strength of silicone sealant

Sealant	Adhesive Strength (psi)
Non-self-leveling	101.86
Self-leveling	46.41

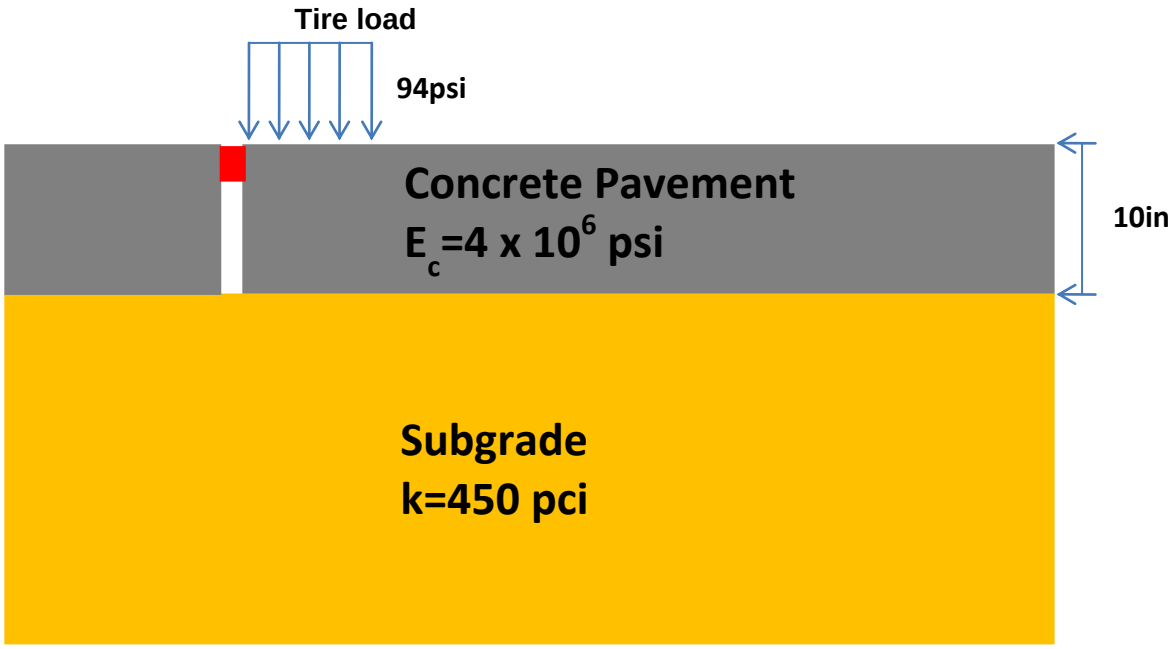

Figure 8-1. Schematic of finite-element model used to compute shear movement

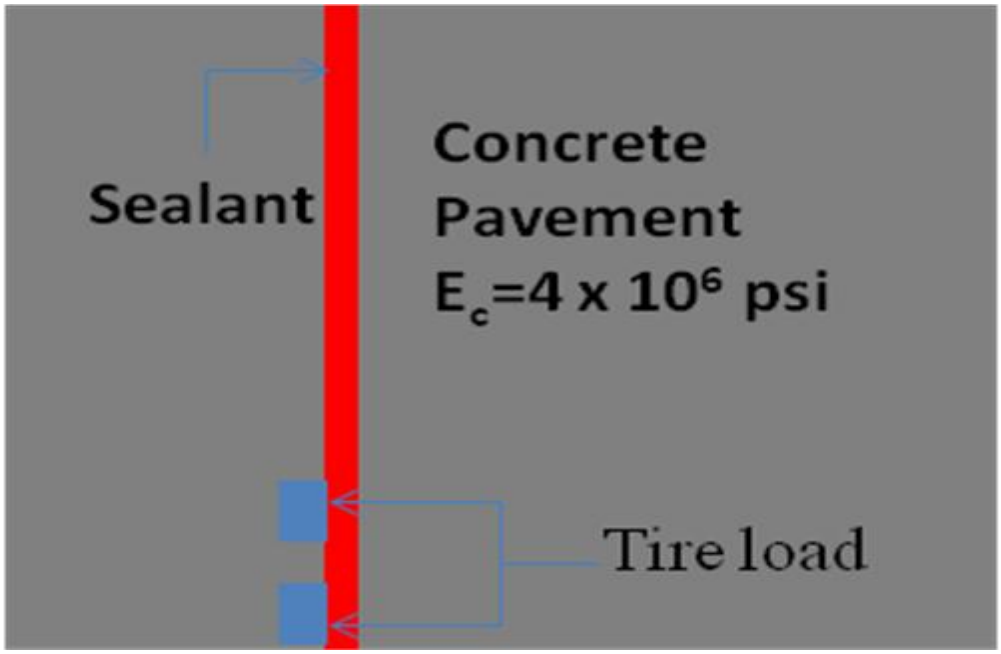

Figure 8-2. Schematic of position of the uniform tire load used in finite-element model

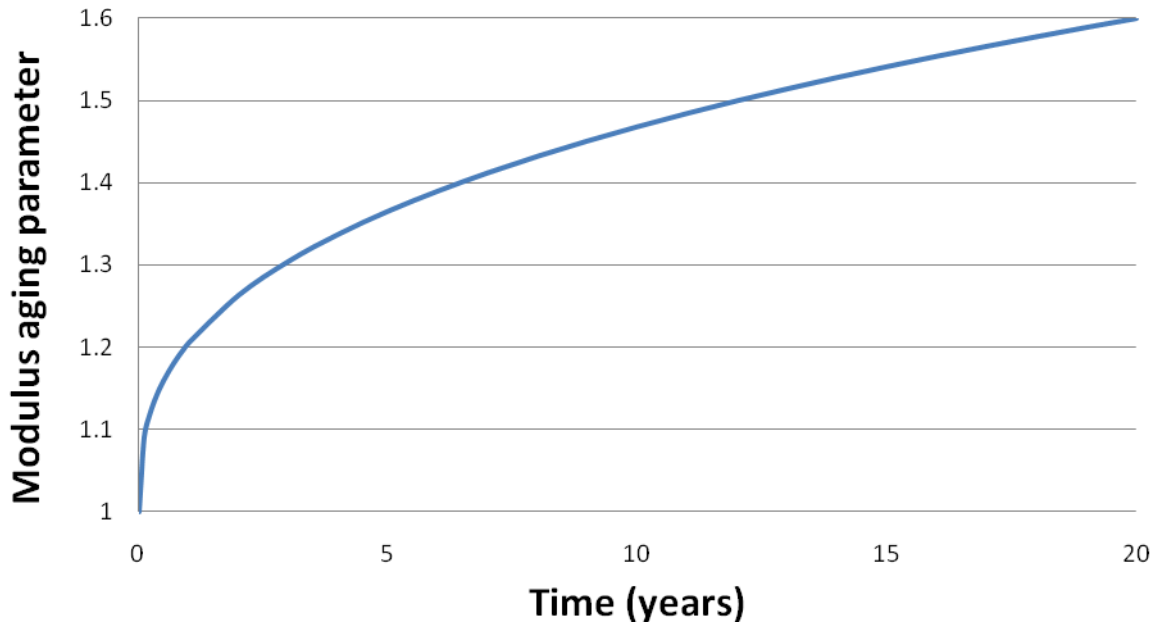

Figure 8-3. Modulus aging parameters (Oldfield and Symes 1996)

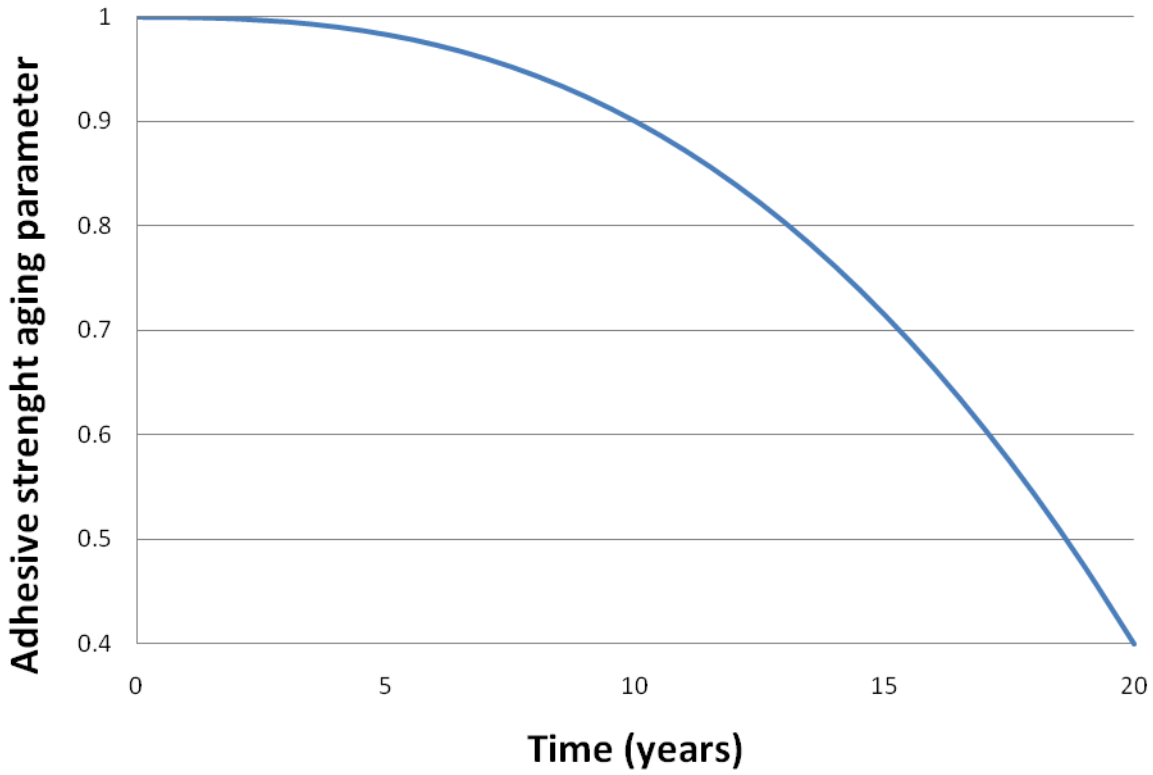

Figure 8-4. Adhesive strength aging parameters

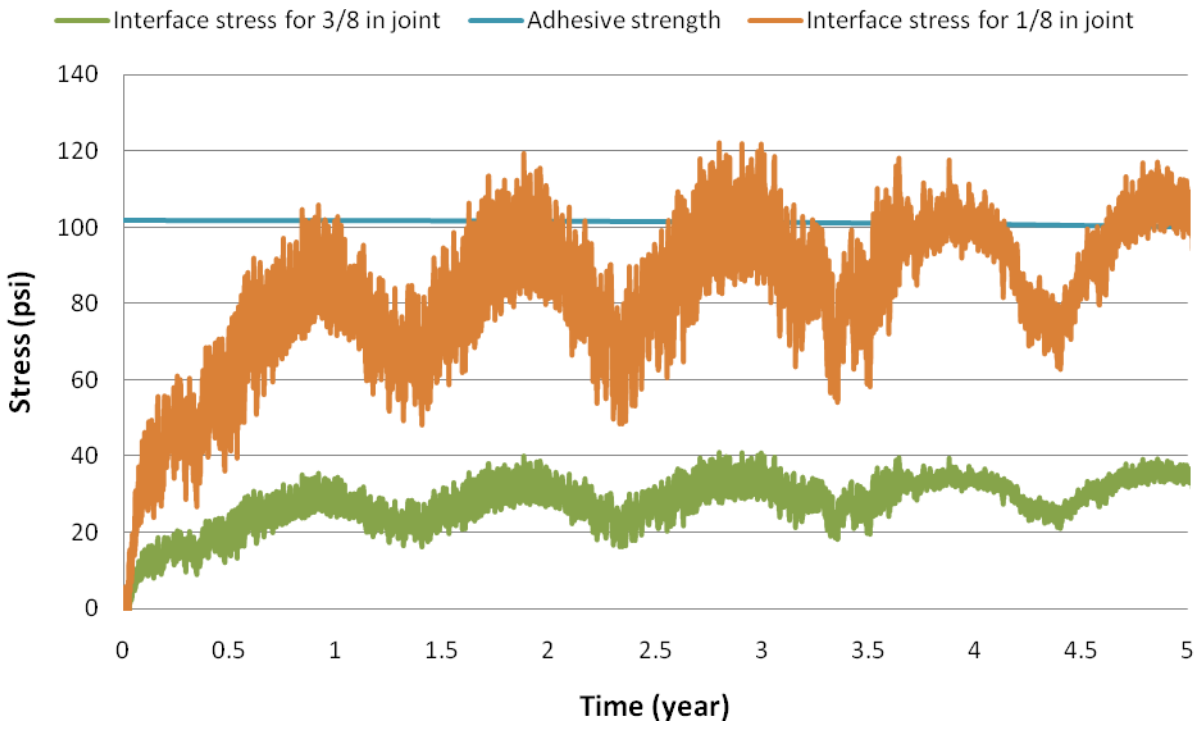

Figure 8-5. Non-self-leveling sealant performance under horizontal joint movement

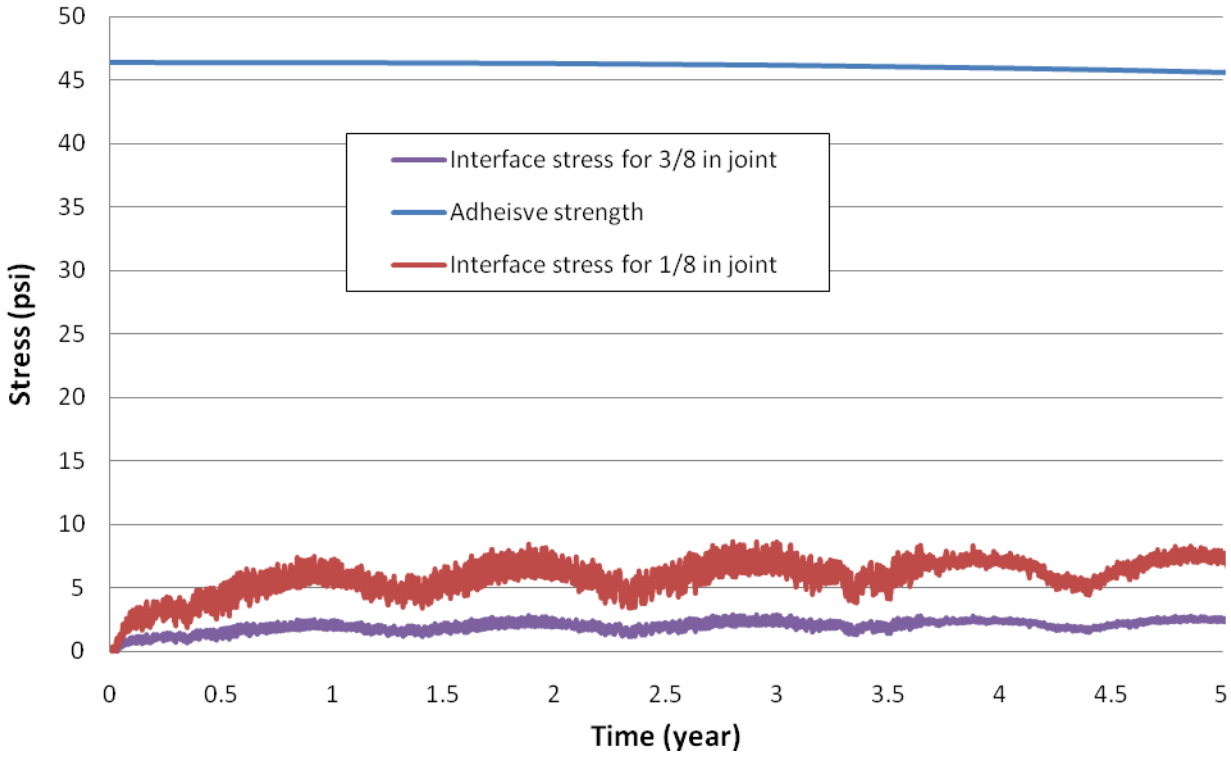

Figure 8-6. Self-leveling sealant performance under horizontal joint movement

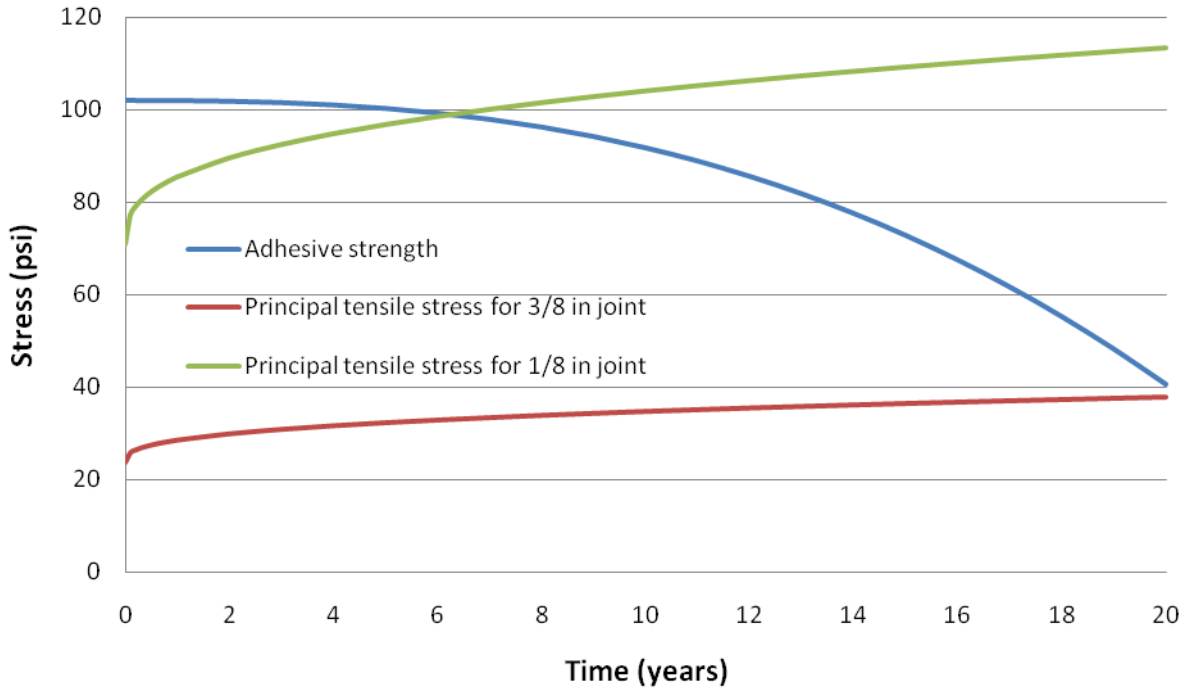

Figure 8-7. Non-self-leveling sealant performance during shear movement

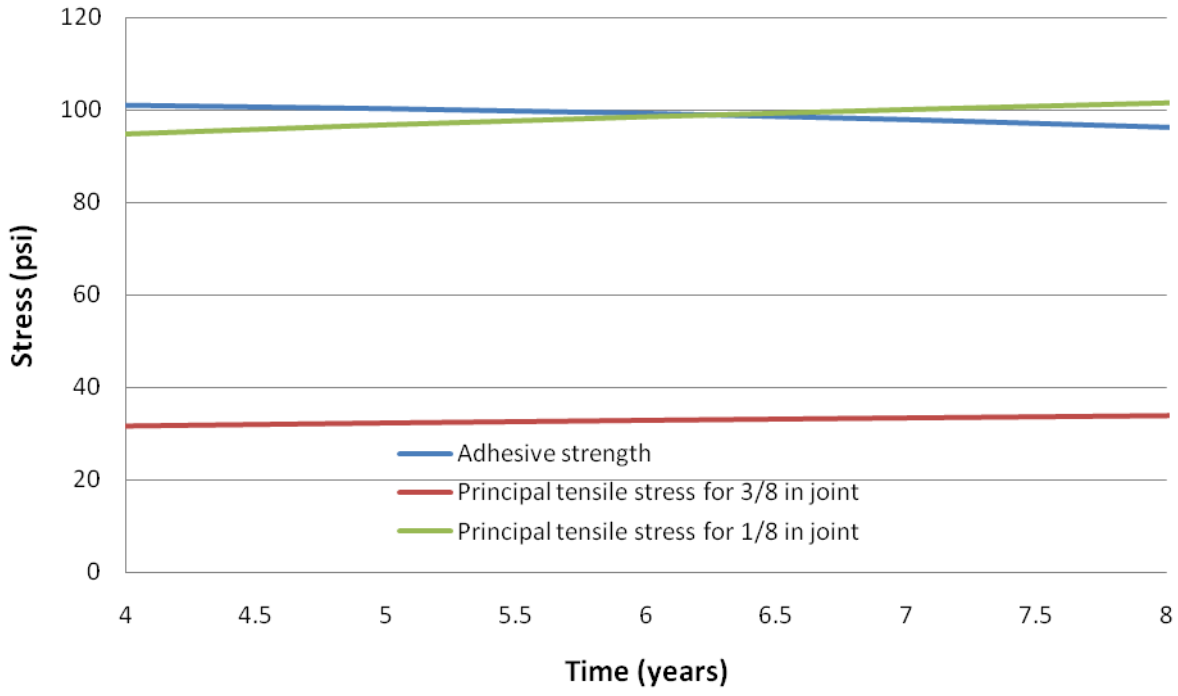

Figure 8-8. Zoom-in of non-self-leveling sealant performance during shear movement

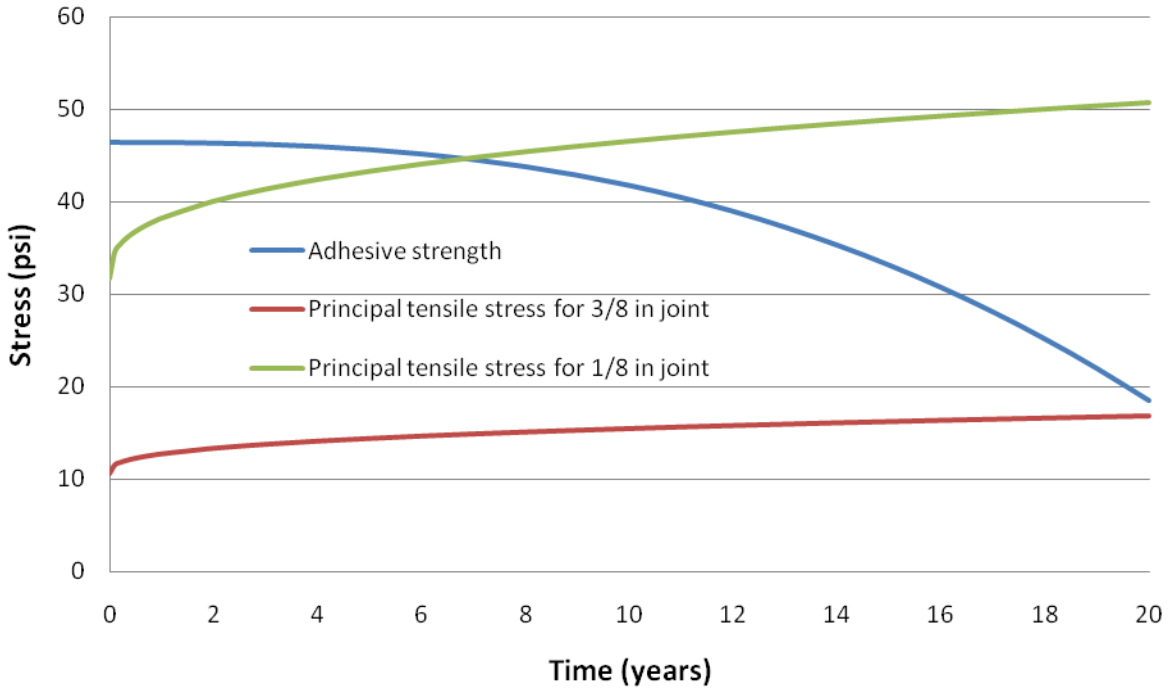

Figure 8-9. Self-leveling sealant performance during shear movement

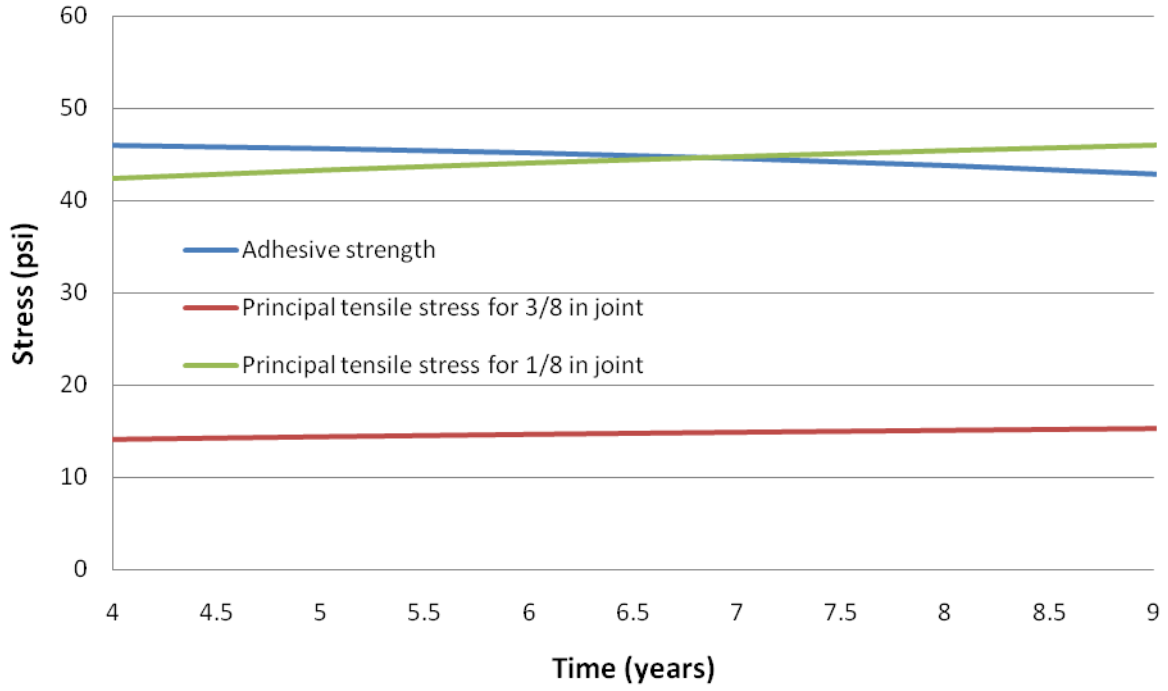

Figure 8-10. Zoom-in of self-leveling sealant performance during shear movement

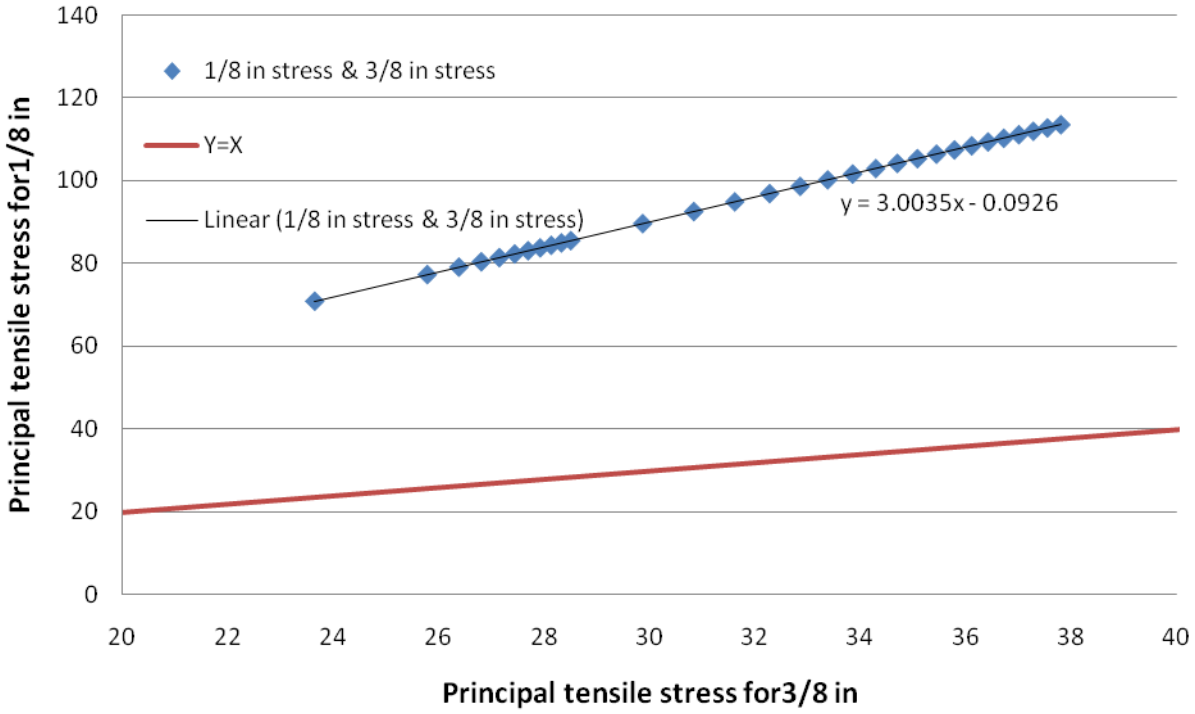

Figure 8-11. Non-self-leveling sealant performance under shear joint movement

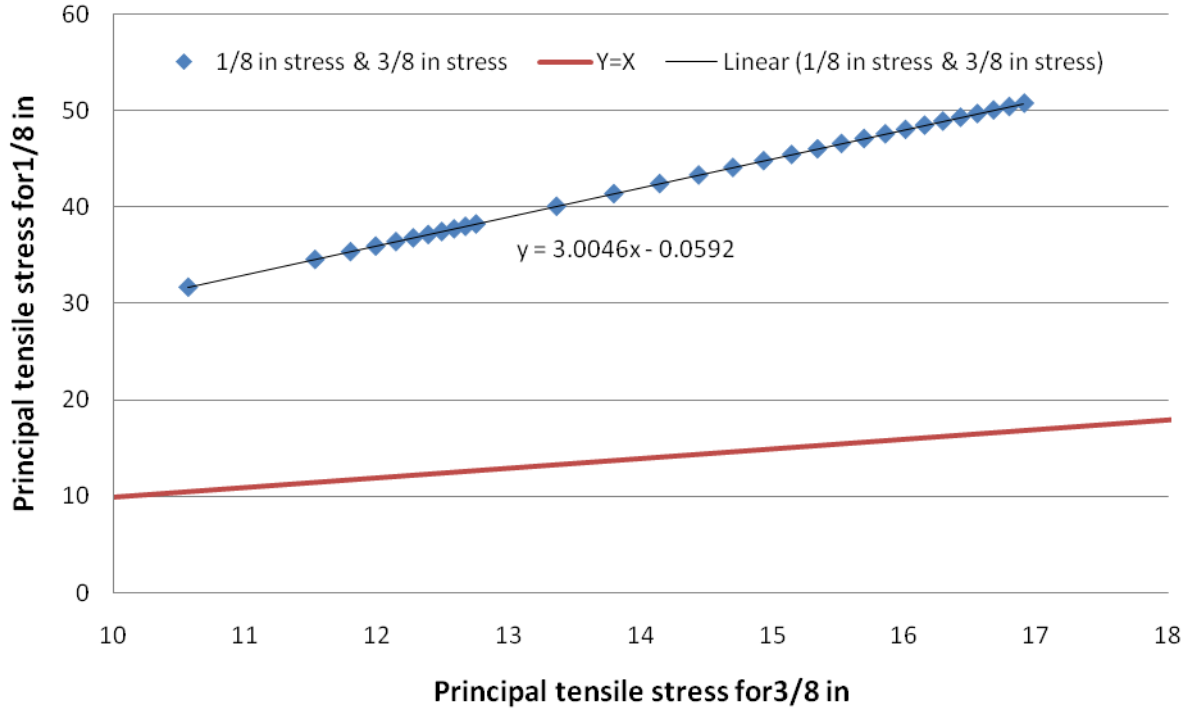

Figure 8-12. Self-leveling sealant performance under shear joint movement

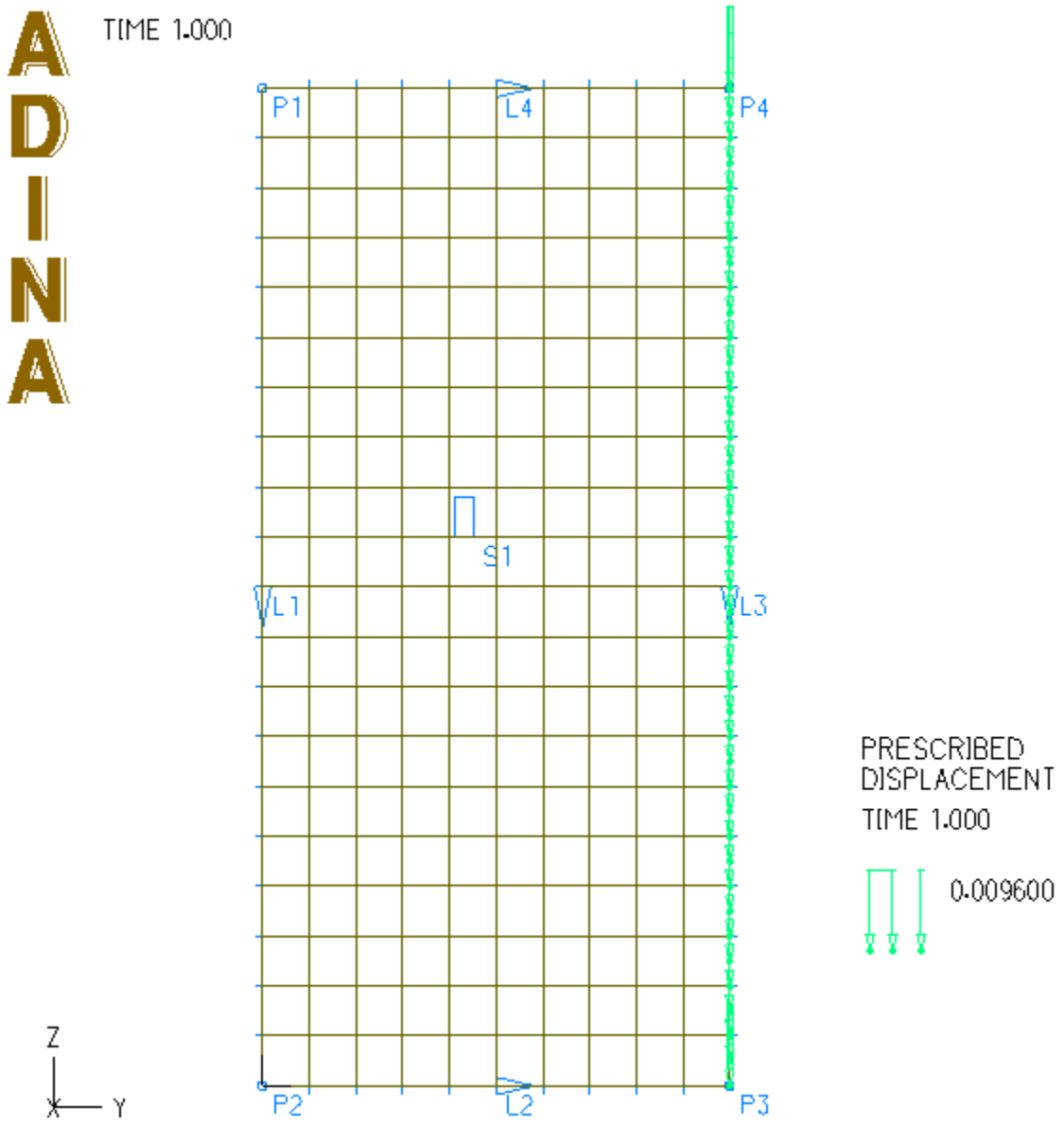

Figure 8-13. Finite element model of silicone sealant

CHAPTER 9
SUMMARY AND FUTURE WORK

Summary

Review of the Goals for This Study

The purpose of this study was to develop a testing system to analyze transverse joints in concrete pavement. Ultimately, the goal was to evaluate joint field performance for 1/8 in. versus standard 3/8 in. joints. The specific goals met in this project were as follows:

- Develop a laboratory testing method which accurately measures the adhesive strength between concrete surfaces and sealant.
- Develop a laboratory creep test to investigate the viscoelastic properties of sealant materials.
- Develop a laboratory method to quantify the roughness of concrete joint surfaces after sandblasting or wire brushing and to evaluate the effect of roughness on adhesive strength.
- Design a laboratory approach to identify the quantity of debris on the concrete joint surfaces after cleaning and to evaluate the effect of cleanliness on adhesive strength.
- Build a relationship between field results and laboratory results by comparing data from Objective (1) through Objective (4) with field data.
- Identify the effect of aging on sealant adhesive strength.
- Develop an approach to predict temperature-induced movement of concrete slabs.
- Develop a finite element model to evaluate the long-term field performance of sealants at different joint widths.
- Develop equipment suited for narrow joint surface preparation.
- Develop a joint preparation quality control device to evaluate surface preparation in the field.
- Determine if narrower joint width allows for adequate slab movement.
- Using results from (1) through (11), determine the overall effects of narrow joints on constructability and service life.

Summary of Work

To achieve those goals, the following was accomplished in this study:

- A sealant adhesive strength test was developed. This test can accurately quantify the adhesive strength between concrete surfaces and sealant. A series of adhesive strength tests was conducted to evaluate the effect of roughness, debris, moisture and aging on the adhesive strength of field-poured silicone sealant.

- A new sealant creep testing apparatus and method were developed. A series of creep tests was conducted to investigate linear viscoelastic properties, temperature sensitivity, and aging effects in field-poured silicone sealant

- The texture index, measured by the Aggregate Image Measurement System (AIMS), was used to quantify roughness of concrete joint surfaces after sandblasting or wire brushing.

- An analytical approach was developed to predict the horizontal movement of a concrete slab due to concrete shrinkage with drying and temperature variations. Additionally, a finite element model was developed to quantify the shear movement due to traffic.

- A joint preparation quality control device was developed to evaluate the effect of debris and moisture on adhesive strength.

- A joint performance evaluation model was developed to evaluate the performance of narrow and standard joints.

Conclusions

The following is a list of conclusions obtained in this study:

- The analytical approach for concrete pavement joint openings is an effective method to calculate dynamic features of the joint opening. In this approach three factors that impact joint openings are considered: thermal strain of the concrete slab, drying shrinkage through the slab thickness, and temperature curling effect. It was found that curling does not have significant effect on the joint opening.

- The sealant creep test is an effective method to measure viscoelastic properties of sealant materials.

- Field poured silicone sealant is a linearly viscoelastic material.

- The viscoelastic properties of field poured silicone sealant do not appear to be sensitive to temperature changes in the range from 0 to 60 degrees Celsius.

- Hot water aging tends to soften field poured silicone sealant while oven aging tends to harden it. Freeze-thaw cycles do not appear to have a significant effect on the viscoelasticity of field poured silicone sealant.

- The adhesive strength test is an effective method to quantify the adhesive strength between concrete and sealant.

- 80% concrete surface moisture (relative to full saturation) is a critical value for field poured silicone sealant. Data suggests that if sealant is applied to a concrete surface with moisture higher than 80%, adhesive strength will be reduced significantly. When the concrete surface moisture is less than 80%, moisture appears to have an insignificant effect. Under identical ambient conditions, 1/8 in. joints dry more slowly than 3/8 in. joints.

- Data suggests that there is a threshold roughness for non-self-leveling silicone sealant. Before reaching this threshold, increasing roughness yields higher adhesive strength. Beyond this threshold, adhesive strength decreases. In addition, adhesive strength decreases with an increase in the amount of debris. This effect becomes more significant at higher levels of roughness.

- Similar to non-self-leveling sealant, self-leveling sealant, also exhibits a critical roughness threshold. However, unlike NS sealant, SL sealant appears to have the ability to absorb a certain amount of debris until it reaches its absorption capacity. Once above this absorption capacity, additional debris reduces adhesive strength and required adhesive failure energy.

- Self-leveling sealant is less sensitive to roughness and debris changes than non-self-leveling sealant. Achieving the proper degree of roughness and reducing debris can improve the performance of silicone sealant. Too much debris can significantly reduce adhesive strength and adhesive failure energy.

- Field poured silicone sealant is very sensitive to water aging, which can lead to a significant decrease in adhesive strength. Freeze-thaw aging also reduces adhesive strength, however, the effect is smaller than hot water aging. Oven aging reduces the adhesive strength of self-leveling sealant but does not appear to have a significant effect on non-self-leveling sealant.

- The joint preparation quality control device can effectively test joint preparation in the field before sealing.

- Concrete slab shear movement due to traffic can produce higher principal tensile stresses in sealant than horizontal movement.

- A 1/8 in. joint will experience much higher interface stress than a 3/8 in. joint. Furthermore, based upon our model, adhesive failure will occur at an early age for the 1/8 in. joint. Thus the 1/8 in. joint cannot perform as well as 3/8 in joint.

- Overall, based on these tests, if a field poured silicone sealant sealed joint was used in concrete pavement, a 1/8 in. joint is not recommended.

Future Work

Field Aging of the Sealant

As discussed, creep and adhesive strength aging tests were conducted on artificially-aged sealant samples, and it is unlikely that these artificial aging techniques accurately match field-aging conditions. Thus, to make predictions about long-term performance, it may be more appropriate to conduct creep and adhesive strength tests on field-aged samples. In the future, researchers should conduct a series of field-aged tests and compare results with laboratory-aged data obtained in this study.

Finite Element Model

As discussed, a two-dimensional finite element model was built to simulate sealant behavior under shear slab movement, while analytical computations were used to solve for horizontal movement. In the future, it may be beneficial to combine these methods and develop a three-dimensional finite element model. It may be possible to improve this model further by using field aging data. Such a model would allow engineers to determine how these movement modes interact and would give more accurate service-life data for sealant in concrete joints.

Slab Movement

Both the finite-element model and the analytical horizontal slab computation used in this study were theoretical in nature. In the future, results from these computations should be verified with field data. If field data proves that these models do not accurately capture slab movement, it may be more appropriate to use field results to quantify long-term field-aged sealant behavior.

APPENDIX A
MATHCAD PROGRAMMING FOR SLAB MOVEMENT

Parameters of the concrete slab

$Tref := 40°C$ Concrete setting temperature

$\alpha := 10.3510^{-6} \cdot \frac{1}{K}$ Coefficent of thermal expansion of concrete

$E28 := 25900MPa$ 28 day Elastic modulus of concrete

$\gamma := 0.2$ Poisson's ratio

$\varepsilon u := 7.810^{-4}$ Ultimate drying shrinkage strain

$L := 4570mm$ Length of concrete slab

$Data :=$

$n := rows(Data) = 2.206 \times 10^{5}$

$i := 0..32000$

$t_i := Data_{i,2}$ Curing time of conrete after casting

$\Delta T_i := \left[\left(Data_{i,1}\right) \cdot \frac{5}{9}\right] \cdot \Delta°C$ Temperature difference between top and bottom

$T_i := \left[\left(Data_{i,0} - 32\right) \cdot \frac{5}{9}\right] °C$ Temperature of concrete slab

$h := 254 \cdot mm$ Thichness of concrete slab

$k := 450 \cdot pci$ Composite modulus of sub-grade reaction

Thermal strain

$$\varepsilon t_i := \alpha \cdot \left(T_i - Tref\right)$$

Drying shrinkage

$$\varepsilon dry_i := \frac{\frac{t_i}{24}}{35 + \frac{t_i}{24}} \cdot \varepsilon u$$

Joint opening without curling

$$JO_i := 0.8L \cdot \left(\varepsilon t_i + \varepsilon dry_i\right)$$

Curling issue

$$l := \sqrt[4]{\frac{E28 h^3}{12\left(1-\gamma^2\right)\cdot k}} = 0.741m \qquad \lambda := \frac{L}{l\cdot\sqrt{8}} = 2.18 \qquad \Delta TT(z) := \Delta T_z$$

$$z0(z) := \frac{(1+\gamma)\cdot l^2 \cdot \alpha \cdot \Delta TT(z)}{h}$$

$$F(x,z) := -z0(z)\cdot\frac{2\cdot\cos(\lambda)\cdot\cosh(\lambda)}{\sin(2\cdot\lambda)+\sinh(2\cdot\lambda)}\left[\begin{array}{l}(-\tan(\lambda)+\tanh(\lambda))\cdot\left(\cos\left(\frac{x}{l\cdot\sqrt{2}}\right)\cdot\cosh\left(\frac{x}{l\cdot\sqrt{2}}\right)\right)\ \ldots \\ +(\tan(\lambda)+\tanh(\lambda))\cdot\left(\sin\left(\frac{x}{l\cdot\sqrt{2}}\right)\cdot\sinh\left(\frac{x}{l\cdot\sqrt{2}}\right)\right)\end{array}\right]$$

$$dF(x,z) := \frac{d}{dx}F(x,z)$$

$$Curl(z) := \begin{cases} -h\cdot\left|dF\left(\frac{L}{2},z\right)\right| & \text{if } \Delta TT(z) \le 0 \\ h\cdot\left|dF\left(\frac{L}{2},z\right)\right| & \text{otherwise} \end{cases}$$

Joint opening with curling

$z := 0..3200$

$JOWC(t) := JO_t + Curl(t)$

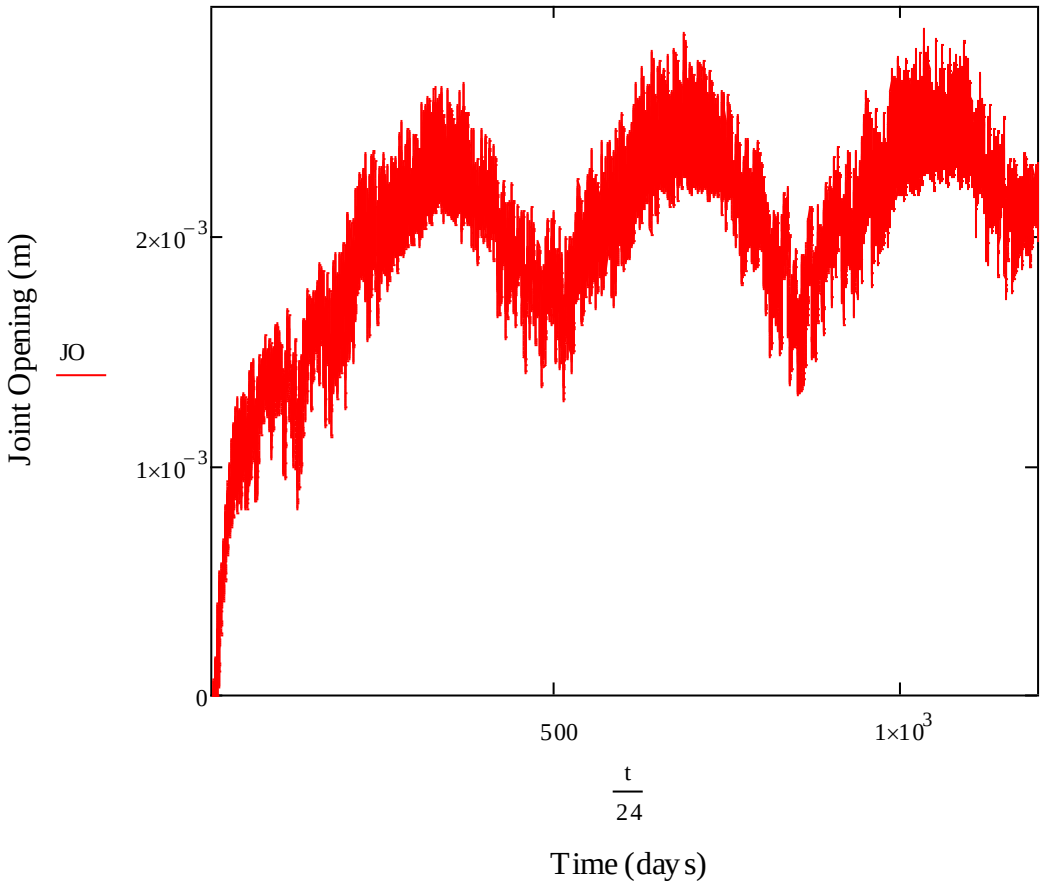

Figure A-1. Joint opening considering curling effect.

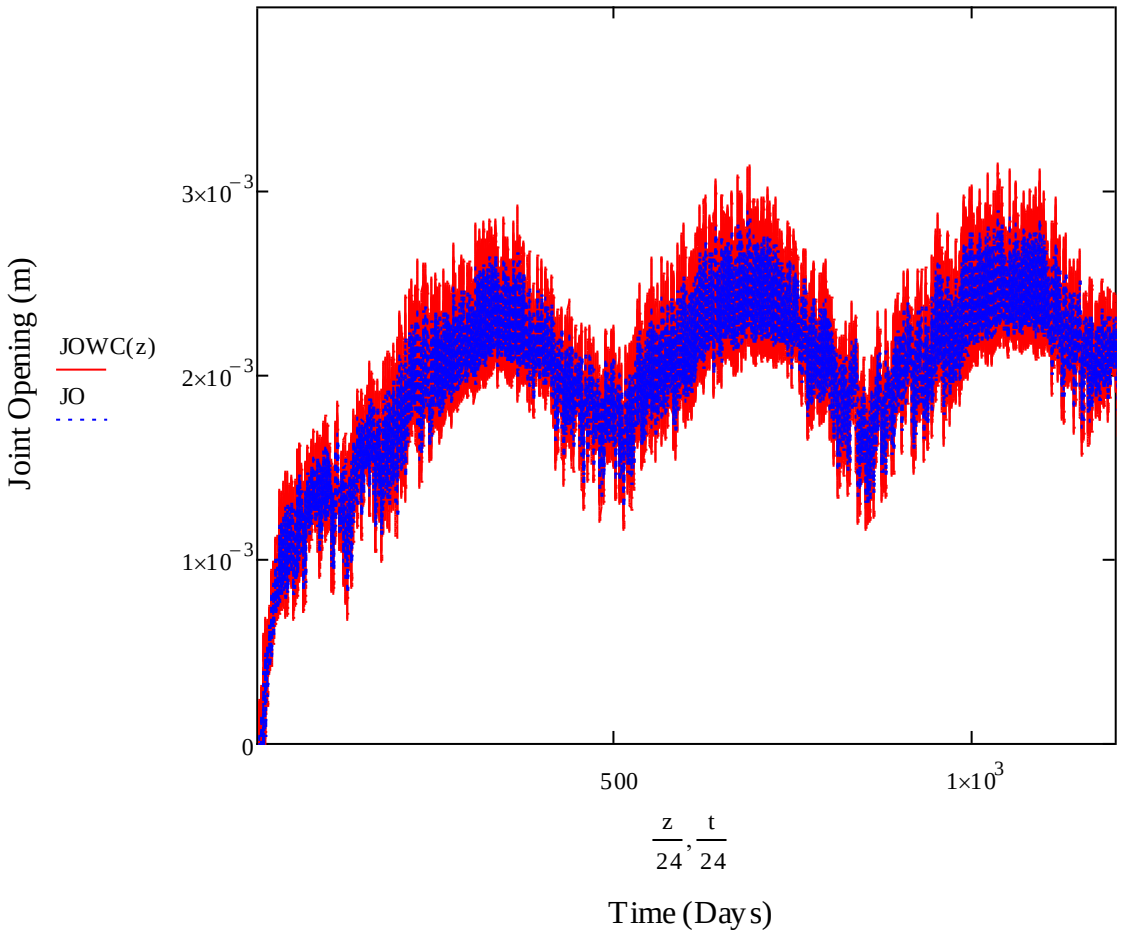

Figure A-2. Joint opening without considering the curling effect

LIST OF REFERENCES

American Association of State Highway and Transportation Officials (2009). *Standard Method of Test for Ductility of Asphalt Materials*. *T 51.*

American Society for Testing and Materials. (2009a). "Standard Test Method for Tack-Free Time of Elastomeric Sealants." C679.

American Society for Testing and Materials. (2009b). "Standard Test Methods for Sealants and Fillers, Hot-Applied, for Joints and Cracks in Asphaltic and Portland Cement Concrete Pavements." D5329.

American Society for Testing and Materials. (2007). "Standard Test Method for Rheological (Flow) Properties of Elastomeric Sealants." C639.

American Society for Testing and Materials. (2006a). " Standard Test Method for Slump of Sealant." D2202.

American Society for Testing and Materials. (2006b). "Standard Specification for Cold Applied, Single Component, Chemically Curing Silicone Joint Sealant for Portland Cement Concrete Pavements." D5893-04.

American Society for Testing and Materials. (2006c). "Standard Test Methods for Vulcanized Rubber and Thermoplastic Elastomers—Tension." D412.

American Society for Testing and Materials. (2005a). "Standard Test Method for Adhesion and Cohesion of Elastomeric Joint Sealants Under Cyclic Movement (Hockman Cycle)." C719.

American Society for Testing and Materials. (2005b). "Standard Test Method for Effects of Laboratory Accelerated Weathering on Elastomeric Joint Sealants." C793.

Biel, T.D., Lee, H. (1997). "Performance study of Portland cement concrete pavement joint sealants." *Journal of Transportation Engineering,* 5 398-404.

Burke, M.P., Jr. (1998) “Pavement Pressure Generation: Neglected Aspect of Jointed Pavement Behavior.” *Transportation Research Record*, 1627, 22-28.

Burke, M.P., Jr. (2002) “The Long-Term Performance of Unsealed Jointed Concrete Pavements.” *Transportation Research Board*, National Research Council. Washington, D.C.

Cown, N. (2001). "Portland Cement Concrete Pavement Joint Study." MANH 207-1 Materials and research, Forest Park, GA

Dunn, C., Fuchs, B, Evert, K,(2009) “Practice of Unsealed Joints in New Portland Cement Concrete Pavements, Final Evaluation Report”, North Dakota.

Federal Highway Administration (FHWA). (2006a). "High Performance Concrete Pavements." Chapter 6. Illinois 2 (Route 59, Naperville).

Federal Highway Administration (FHWA). (2006b). "High Performance Concrete Pavements." Chapter 7. Illinois 3 (US 67, Jacksonville).

Federal Highway Administration (FHWA). (2006c). "High Performance Concrete Pavements." Chapter 17. Kansas 1 (Highway K-96, Haven).

Federal Highway Administration (FHWA). (2006d). "High Performance Concrete Pavements." Chapter 27. Ohio 1, 2, and 3 (US Route 50, Athens).

Findley, W., N., Lai, J., S., and Onaran, K. (1976). *Creep and Relaxation of Nonlinear Viscoelastic Materials.* North Holland Publishing Company, U.S.A. and Canada.

Florida Department of Transportation. (2007a). "Standard Specifications for Road and Bridge Construction." 413-1-413-8.

Florida Department of Transportation. (2007b). "Standard Specifications for Road and Bridge Construction." 350-12.3.

Lubliner, J. (2008). *Plasticity theory.* Dover Publication, U.S.A.

Masad, E. A. (2004). "Aggregate Imaging System (AIMS) Basics and Applications." *Rep. No. 5-1701-01-1,* .

Mindess, S., Young, J. F., and Darwin, D. (2003). *Concrete.* Pearson Education, Inc, Upper Saddle River.

Odum-Ewuakye, B., and Attoh-Okine, N. (2006). "Sealing system selection for jointed concrete pavements – A review." *Constr.Build.Mater.,* 20(8), 591-602.

Oldfield, D., Symes, T. (1996). "Long Term Natural Ageing of Silicone Elastomers." *Material Behavior,* 0142-9418/9 115-128.

Rasoulian, M., Titi, H.H., and Martinez , M. (2006). "Evaluation of Narrow Transverse Contraction Joints in Jointed Plan Concrete Pavements." *Proceedings of the International Conference on Concrete Pavements*, Colorado Springs, Co, pp. 357-371.

Shober, S.F. (1997). "The Great Unsealing, A Perspective on PCC Joint Sealing.". *Transportation Research Record* 1597, 22-33,

Smith, K.L., Pozsgay, M.A., Evans, L.D. and Romine, A.R. (1999). "LTPP Pavement Maintenance Materials: SPS-4 Supplemental Joint Seal Experiment, Final Report." *Rep. No. FHWA-RD-99-151*.

BIOGRAPHICAL SKETCH

Qiang Li was born in Jinzhou, Liaoning province, China. He received a Bachelor of Science in engineering from Dalian University of Technology in 2005.

He worked for Dalian institute of building material as a material analyst during the year 2005 to 2007. After that, he decided to cross the Pacific to pursue his Ph.D in the United States.

In August 2007, he was admitted to University of Florida and worked as a research assistant in the Department of Civil Engineering. After completing his doctoral study at University of Florida, Qiang Li intends to work in academia, government agencies, or industrial companies in civil engineering to continue his service to society.